



universität
wien

DIPLOMARBEIT

Titel der Diplomarbeit

„New RNAi vector application
and
Functional LAP2 α analysis“

Verfasser

Christian Makolm

angestrebter akademischer Grad

Magister der Naturwissenschaft (Mag. rer. nat.)

Wien, 2009

Studienkennzahl lt. Studienblatt: A 419

Studienrichtung lt. Studienblatt: Diplomstudium Chemie

Betreuer: Prof. DI Dr. Roland Foisner

Table of Contents

1. ABSTRACT	1
1.1. SUMMARY.....	1
1.2. ZUSAMMENFASSUNG	2
2. INTRODUCTION.....	3
2.1. NEW RNAI VECTOR APPLICATION	3
2.1.1. <i>RNA Interference (RNAi)</i>	3
2.1.2. <i>History of RNAi</i>	3
2.1.3. <i>Mechanisms of RNAi</i>	4
2.1.4. <i>Biological functions of RNAi</i>	7
2.1.5. <i>How to use RNAi as a tool</i>	8
2.1.5.1. Mediators of RNAi	8
2.1.5.2. Delivery of RNAi mediators into mammalian cells	8
2.1.5.3. Applications of RNAi	9
2.1.6. <i>Aim of this project</i>	10
2.2. FUNCTIONAL LAP2 α ANALYSIS.....	11
2.2.1. <i>The eukaryotic nucleus</i>	11
2.2.2. <i>The nuclear envelope</i>	11
2.2.3. <i>Nuclear Lamins</i>	12
2.2.4. <i>Integral Nuclear Membrane Proteins</i>	14
2.2.5. <i>The LAP2 family</i>	15
2.2.5.1. Lamina-associated-Polypeptide 2 alpha (LAP2 α)	17
2.2.6. <i>The nuclear envelope during mitosis</i>	18
2.2.7. <i>Functional implication of the nuclear lamina</i>	20
2.2.8. <i>Laminopathies</i>	21
2.2.9. <i>Aim of this project</i>	22
3. RESULTS.....	23
3.1. RESULTS TRIPLE RNAI.....	23
3.1.1. <i>The Triple-RNAi-Vector strategy</i>	23
3.1.2. <i>Single RNAi targeting exogenous reporters</i>	23
3.1.3. <i>Triple-RNAi-Vector</i>	26
3.2. RESULTS LAP2 α RNAI	28
3.2.1. <i>Transient approach to test the functionality of RNAi constructs</i>	28

3.2.2. <i>Conditions for stable transfection with RNAi constructs</i>	30
3.2.3 <i>Stable RNAi</i>	32
3.2.4. <i>Reduced levels of LAP2α have no influence on nuclear integrity</i>	36
3.2.5. <i>Proliferation rate is increase by reduction of LAP2α levels</i>	37
3.2.6. <i>LAP2α and lamin A/C localization during cell cycle</i>	39
3.2.6.1. <i>wt-localization of LAP2α and lamin A/C during cell cycle</i>	40
3.2.6.2. <i>Reduced levels of LAP2α does not alter its cellular localization</i>	46
3.2.6.3. <i>LAP2α RNAi does not affect lamin A/C localization</i>	47
4. DISCUSSION	55
4.1. <i>DISCUSSION OF THE TRIPLE-RNAI-VECTOR SYSTEM</i>	55
4.2. <i>DISCUSSION OF FUNCTIONAL LAP2α ANALYSIS</i>	57
5. MATERIALS AND METHODS	60
5.1. <i>CELL BIOLOGY</i>	60
5.1.1. <i>Cell Culture</i>	60
5.1.2. <i>Transfection of HeLa and HEK 293 cells with lipofectamine 2000</i>	60
5.1.3. <i>Cell lines stably expressing shRNA constructs</i>	61
5.1.4. <i>Single cell clones</i>	61
5.1.4.1. <i>Limited dilution</i>	62
5.1.4.2. <i>Isolating individual cell colonies</i>	62
5.1.5. <i>Growth rate experiments</i>	62
5.1.5.1. <i>Growth rate at full serum</i>	63
5.1.5.2. <i>Growth rate of serum starved cells</i>	63
5.2. <i>BIOCHEMISTRY AND IMMUNOLOGY</i>	63
5.2.1. <i>Preparation of total cell lysates for Western blot analyses</i>	63
5.2.2. <i>SDS PAGE and Western blot analyses</i>	64
5.2.3. <i>Immunofluorescence microscopy studies</i>	68
5.2.4. <i>Reporter assays</i>	69
5.2.4.1. <i>Preparation of cells for reporter assays</i>	70
5.2.4.2. <i>Luciferase reporter assay</i>	70
5.2.4.3. <i>β-Galactosidase reporter assay</i>	70
5.2.4.4. <i>CAT enzyme assay</i>	71
5.2.4.5. <i>Normalization, Interpretation</i>	71
5.2.5. <i>FACS (Fluorescence-activated cell sorter)</i>	72
5.3. <i>MOLECULAR BIOLOGY</i>	72
5.3.1. <i>CaCl₂ competent E.Coli</i>	72
5.3.2. <i>Transforming E.Coli</i>	72
5.3.3. <i>Glycerolstocks</i>	73

5.3.4. Expression and analysis of recombinant proteins	73
5.3.5. Miniprep DNA purification.....	74
5.3.6. Midiprep DNA purification.....	74
5.3.7. DNA restriction digest	75
5.3.8. DNA agarose gel electrophoresis	75
5.3.9. Elution of DNA fragments from agarose gel	76
5.3.10. Dephosphorylation of DNA fragments.....	76
5.3.11. Ethanol precipitation of DNA.....	76
5.3.12. DNA ligation.....	77
5.3.13. Zero Blunt TOPO PCR cloning	77
5.3.14. Poly(A ⁺) mRNA isolation.....	77
5.3.15. cDNA synthesis	78
5.3.16. RT-PCR.....	78
5.4. RNAi CLONING STRATEGY	80
5.4.1. short hairpin oligonucleotides – RNAi constructs.....	80
5.4.2. Annealing of oligonucleotides for ligation	82
5.4.3. Generation of RNAi – compatible MultiSite Gateway TM Entry vectors	82
5.4.4. PCR to clone a MultiSite Gateway TM destination vector	83
5.4.5. Gateway TM recombination reactions (Invitrogen, Carlsbad, CA, USA).....	84
5.4.5.1. LR recombination reaction.....	84
5.4.5.2. BP recombination reaction.....	85
5.4.5.3. MultiSite Gateway TM LR reaction.....	85
5.4.6. Cloning strategy for single target RNAi vectors.....	86
5.4.7. The Triple-RNAi-Vector approach	86
6. APPENDIX	88
6.1. APPENDIX A	88
6.2. APPENDIX B.....	99
6.2.1. The Gateway TM Technology.....	99
6.2.2. The MultiSite Gateway TM Technology	100
7. REFERENCES	102
8. CURRICULUM VITAE	117

1. ABSTRACT

1.1. Summary

In the first part of the thesis a new Triple RNA interference (RNAi) vector system was established. We developed an RNAi technique to simultaneously target up to three genes. For stable silencing, the MultiSite-GatewayTM system was used to shuttle up to three different cassettes, each consisting of a human U6 promoter and an oligonucleotide encoding a short hairpin RNA (shRNA), into one destination vector. The system was shown to work efficiently on three ectopically expressed proteins. Thus, this tool is applicable for analyzing proteins with redundant functions and protein hierarchies within signal transduction pathways.

In the second part of the thesis, we further analyzed the *in vivo* function of lamina-associated polypeptide 2 alpha (LAP2 α) and related proteins by RNAi. For transient and/or stable RNAi, we designed hairpin constructs targeting LAP2 α , LAP2 β , all LAP2 isoforms, A-type lamins, emerin and BAF. We were able to transiently reduce the expression of LAP2 α and all LAP2 isoforms, and created pools of cells stably expressing these functional shRNAs. Single cell clones, strongly down regulating LAP2 α , were selected and their phenotype analyzed. LAP2 α deficient HeLa cells showed increased cell proliferation rates and did not respond to serum starvation, like cells transfected with control plasmids. In contrast, HEK cells, which do not correctly process pre-lamin A, did not show any proliferation effect, underscoring the necessity of lamin A for the cell cycle control pathway. Co-localization studies by immunofluorescence indicate, that lamin A and LAP2 β localization as well as the overall integrity of the nuclear envelope was not compromised upon downregulation of LAP2 α .

In summary, RNAi mediated downregulation of LAP2 α revealed a role of LAP2 α on cell proliferation.

1.2. Zusammenfassung

Im ersten Teil der vorliegenden Diplomarbeit wird die Entwicklung einer neuen RNA Interferenz (RNAi) Anwendung, dem Triple-RNAi-Vector, beschrieben. Diese Technik erlaubt uns, zeitgleich bis zu drei Proteinexpressionen mittels RNAi zu verringern. Wir benutzten das MultiSite-GatewayTM System, um bis zu drei Kassetten, bestehend aus je einem humanen U6 Promoter und einem RNAi vermittelndem Oligonucleotid, in einem Expressionsvektor zu rekombinieren. Erste Test zeigten die effiziente Funktion des Triple-RNAi-Vektors an drei ektopisch exprimierten Reporter Enzymen in HEK 293 Zellen. Diese Technik ist konzipiert für funktionelle Proteinanalyse, speziell für funktionell redundante Proteine und für Proteine in parallelen Signalkaskaden.

Der zweite Teil der Arbeit befasst sich mit der weiterführenden Charakterisierung des Kernproteins Lamina-assoziiertes-Polypeptid 2 alpha (LAP2 α). RNAi-Konstrukte gegen LAP2 α , LAP2 β , alle LAP2 Isoformen, A-Typ Lamine, Emerin und BAF wurden in transienten Transfektionsexperimenten getestet. Funktionelle RNAi-Konstrukte gegen LAP2 α und alle LAP2 Isoformen nutzten wir um stabil transfektierte Zellpools herzustellen. Zur Charakterisierung wurden Einzelzellklone mit stark reduzierten LAP2 α Proteinniveaus in HEK und HeLa Zellen selektiert. Die HeLa Einzelzellklone zeigten stark erhöhte Zellteilungsraten verglichen mit den Kontrollzelllinien, dieser Effekt war unter Serumreduktion noch stärker ausgeprägt. Im Gegensatz dazu zeigten HEK Zellen mit reduziertem LAP2 α Proteinniveau keinen Wachstumseffekt. Da HEK Zellen kein korrekt prozessiertes Lamin A exprimieren ist dies ein weiterer Hinweis auf die Zellzyklus regulierende Funktion dieser Bindungspartner. Im Rahmen von Co-Lokalisationsstudien mittels Immunfluoreszenzen wurde gezeigt, daß ein geringes Proteinniveau von LAP2 α , keinen Einfluß auf dessen eigene, noch auf die zelluläre Lokalisation von Lamin A, oder die von LAP2 β hat. Des weiteren blieb die Integrität des Zellkerns trotz LAP2 α RNAi erhalten. Zusammenfassend konnten wir eine zellzyklusregulierende Funktion von LAP2 α durch dessen RNAi vermittelte Reduktion zeigen.

2. INTRODUCTION

2.1. New RNAi vector application

2.1.1. RNA Interference (RNAi)

RNAi is a conserved biological response of animal cells to double-stranded RNA (dsRNA), also known as post-transcriptional gene silencing (PTGS) in plants and “quelling” in fungi (reviewed in Hannon, 2002; Mittal, 2004; Hannon and Rossi, 2004; Meister and Tuschl, 2004; Matzke and Birchler, 2005). Depending on the RNA precursor and the organism, RNAi mediates a wide range of effects, such as mRNA degradation, translational repression, and epigenetic modifications to the genome.

Nowadays RNAi is used as a modern technique to knock-down target gene expression in a highly specific manner at the posttranscriptional level. RNAi became an effective method for analysis of gene function in vivo and holds the possibility of therapeutic gene silencing.

2.1.2. History of RNAi

PTGS was first discovered in plants by experiments on petunia pigmentation (Napoli et al., 1990; van der Krol et al., 1990). Years later, the phenomenon, that sense or antisense RNA molecules equally suppressed gene expression was discovered in the nematode worm *Caenorhabditis elegans* (Guo and Kemphues, 1995). RNAi itself was first described in *C. elegans* as a response to dsRNA which resulted in sequence specific gene silencing (Fire et al., 1998). Furthermore dsRNA has been found at least tenfold more effective in targeting gene silencing, than sense, or antisense RNA alone. Interestingly, systemic silencing (see 2.1.3.) in *C. elegans* could easily be reached by simply feeding dsRNA to the worms (Timmons and Fire, 1998). Subsequent studies identified short RNAs of 21-23 nucleotides as functional mediators of RNAi (Hamilton and Baulcombe, 1999; Grishok et al., 2000). The processing of long dsRNA (>50 nucleotides) to short interfering RNAs (siRNAs) has been shown in *Drosophila* (Zamore et al., 2000). RNAi, mediated by long dsRNA, was quickly adapted as tool for reverse genetics in several model organisms. However, in almost all somatic cells of higher eukaryotes (mammals), dsRNAs longer than 30 nucleotides induces a sequence independent interferon response, resulting in general inhibition of protein synthesis (Stark et al., 1998; Gil and Esteban, 2000). This problem could be circumvented experimentally by the direct use of siRNAs to target mammalian genes by RNAi (Elbashir et al., 2001; Caplen et al., 2001).

2.1.3. Mechanisms of RNAi

The short interfering RNA (siRNA) pathway:

Long, double stranded RNA (dsRNA) is cleaved preferentially by the RNase III family member Dicer, into siRNAs in an ATP - dependent manner in the cytoplasm (Figure 2-1b; Zamore et al., 2000; Bernstein et al., 2001; Ketting et al., 2001; Billy et al., 2001; Shinagawa et al., 2003). These are 21-23 nucleotide long RNA duplexes with symmetric two nucleotide, 3' hydroxylated, overhangs and are phosphorylated at their 5' ends (Figure 2-1a; Elbashir et al., 2001). The siRNAs are part of siRNA-duplex-containing ribonucleoprotein particles (siRNP), that become incorporated into the multicomponent RNA-induced silencing complex (RISC; Hammond et al., 2000) in an ATP dependent manner (Figure 2-1b; Nykänen et al., 2001; Pham et al., 2004). Most likely this energy is used to unwind the RNA duplex, leaving the single antisense strand to guide RISC to its homologous target messenger RNA (mRNA) for endonucleolytic cleavage. Each RISC contains a member of the Argonaute (Ago) family, which probably binds directly to the siRNA and to Dicer (Hammond et al., 2001; Tahbaz et al., 2004). Furthermore, crystal structure of an archaeobacterial Ago protein revealed structural homology with the RNaseH family (Song et al., 2004), whose members cleave RNA strands in RNA / DNA duplexes. So Ago proteins could also be directly involved in target messenger RNA degradation.

The micro RNA (miRNA) pathway:

Endogenous hairpin RNAs or short hairpin RNAs (shRNA) transcribed from exogenous DNA are processed to micro RNA (miRNA) precursors by Drosha in the nucleus (Lee et al., 2002; Lee et al., 2003). Subsequently the miRNA precursors are exported to the cytoplasm (Yi et al., 2003; Bohnsack et al., 2004; Lund et al., 2004), where they are further processed by Dicer to miRNAs (Figure 2-1c). In contrast to siRNAs, miRNAs encode at least one mismatch. Dicer can also cleave ~70 nucleotide long imperfectly paired hairpin RNAs, leading to double stranded, ~21 nucleotides long miRNAs. These miRNAs become also incorporated into a RISC-like complex called miRNP (miRNA-duplex-containing ribonucleoprotein particles; McManus et al., 2002; Zamore, 2002; Denli et al., 2003) and can base pair with the target mRNA and roadblock translation mostly in UTR regions by blocking elongation (Olsen et al., 1999; Pasquinelli et al., 2002). Alternatively, miRNAs can act similar to siRNAs and guide mRNA degradation (Llave et al., 2002; Kasschau et al., 2003; Boutet et al., 2003). The decision between these two possibilities seems to depend on the degree of homology between

the miRNA and the mRNA (Carrington et al., 2003). Most endogenous animal miRNAs base pair imperfectly and therefore trigger translational repression.

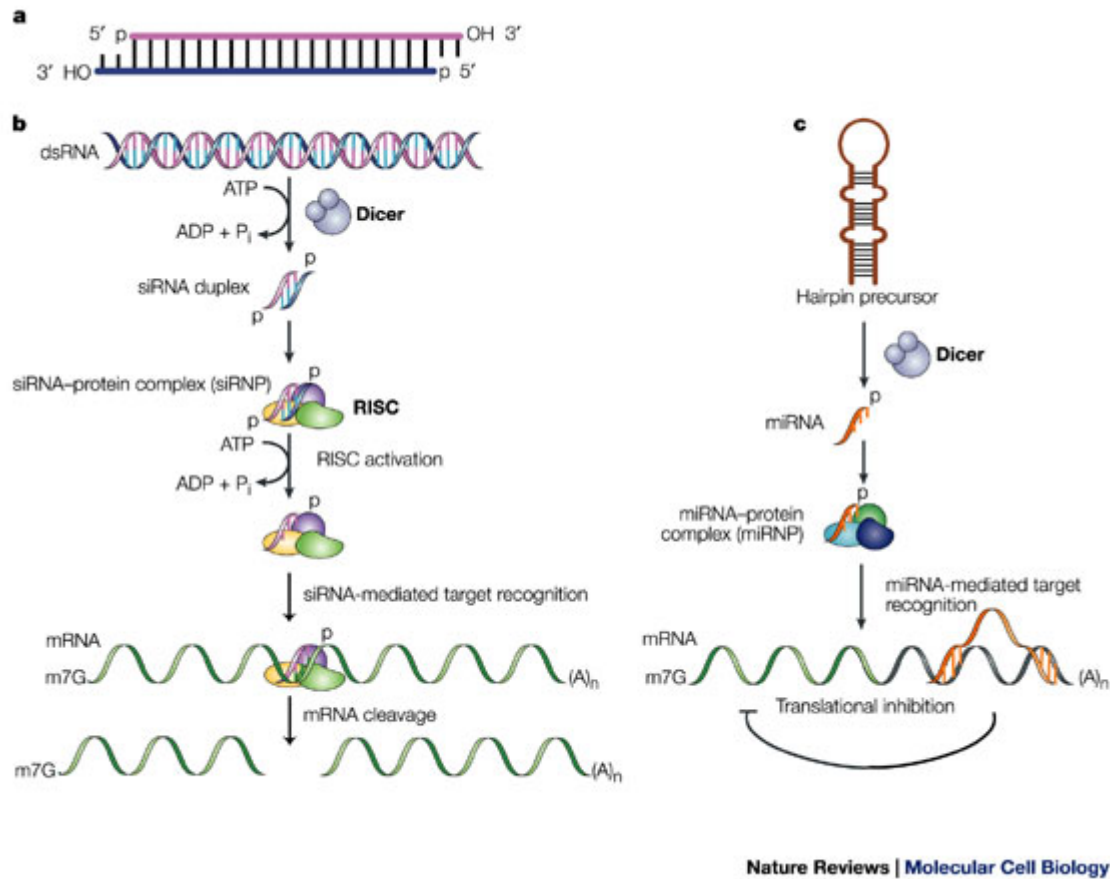


Figure 2-1: The RNA interference pathways. (a) Short interfering RNAs (siRNAs) are duplexes of 21 nucleotides length, with symmetric 2 nucleotide 3' hydroxylated overhangs and 5' phosphates. They are characteristic products of Dicer (RNase III) cleavage. (b) The siRNA pathway: Long double stranded RNA becomes cleaved by Dicer to form siRNA duplexes, which subsequently become separated and incorporated into the RNA-induced silencing complex (RISC). This multiprotein complex targets degradation of complementary mRNA. (c) The miRNA pathway: Hairpin RNAs with imperfect base pairing become first processed to micro RNAs (miRNAs) precursors by Drosha in the nucleus (not shown) by Dicer. Subsequently, they are exported to the cytoplasm, where they are cleaved to miRNAs by Dicer and incorporated into miRNPs (miRNA-duplex-containing ribonucleoprotein particles). These protein complexes are then bound to complementary mRNAs, where they block translational elongation. Modified from (Dykxhoorn et al., 2003)

RNAi - induced Heterochromatin formation:

Knockouts of essential RNAi machinery components (Argonaute, Dicer and RdRP) in fission yeast showed that RNAi is involved in heterochromatin formation (Volpe et al., 2002). It has been proposed, that transcription of centromeric regions leads to the formation of dsRNA,

which becomes processed by Dicer and amplified by RNA-directed RNA polymerase (RdRP; see 2.1.3. systemic silencing) activity. These small RNAs are thought to target H3K9 methylation (methylation of histone 3 on lysine 9), a hallmark of heterochromatin formation, to the chromosome. HP1 homologues are targeted to sites of H3K9 methylation, which results in transcriptional inhibition (Verdel et al., 2004).

RNA directed DNA methylation (RdDM):

RdDM leads to sequence specific cytosine methylation in plants (Wassenegger et al., 1994). It requires dsRNA, which becomes processed to 21-24 nucleotide RNAs (Mette et al., 2000). RNA complementary to DNA promoter regions can trigger its methylation and subsequently transcriptional gene silencing. Interestingly, two recent studies demonstrated siRNA induced promoter methylation in human cells (Kawasaki and Taira, 2004; Morris et al., 2004).

Systemic silencing:

An astonishing aspect of RNAi is systemic silencing, the ability of gene silencing to spread throughout the whole organism. It has been documented in plants (Palauqui et al., 1997; Voinnet et al., 1998) and in *C. elegans* (Timmons et al., 1998) but has not been observed in higher eukaryotes. Therefore a silencing signal, most likely siRNA, has to be amplified to move from cell to cell (see below) and induce sequence specific silencing at distant sites (Mlotshwa et al., 2002).

Amplification could occur through a phenomenon called 'transitive RNAi'. The model suggests that single stranded siRNA primes the synthesis of dsRNA along their target mRNA by RNA-directed RNA polymerase (RdRP) activity (Lipardi et al., 2001). Newly synthesized dsRNA will be processed by Dicer, thereby accumulating siRNAs complementary to regions upstream of the original targeting sequence (Sijen et al., 2001). A scenario, where these new siRNAs also silence other mRNAs can also be envisaged.

In plants siRNAs will move from cell to cell through plasmodesmata (cytoplasmic bridges between cells), but for longer range silencing they must also pass the plants vasculature (Voinnet et al., 1998). In *C. elegans* a transmembrane protein termed SID-1 has been identified as essential for systemic RNAi (Winston et al., 2002). It provides a channel system for siRNA transport.

As there are no paralogues of RdRP in *Drosophila* (Roignant et al., 2003) and vertebrates (Stein et al., 2003), they possess no mechanisms to amplify silencing signals and therefore systemic silencing has not been observed so far in these organisms.

2.1.4. Biological functions of RNAi

Most plant viruses have an RNA genome and synthesize dsRNA during their replication cycle. PTGS forms the basis for **virally induced gene silencing (VIGS)** in plants (Ruiz et al., 1998; Mourrain et al., 2000). Many plant viruses circumvent VIGS by encoding suppressors of PTGS, which are essential for pathogenesis (Hamilton et al., 2002; Mallory et al., 2002). Also in *Drosophila*, an antiviral role of RNAi has been suggested (Li et al., 2002). **Antiviral mechanisms** have also been reported in higher eukaryotes. In mammals, except in non-differentiated embryonic stem cells and erythroblasts, dsRNA longer than 30 base pairs induces a sequence independent interferon response, resulting in general inhibition of protein synthesis (Stark et al., 1998; Gil and Esteban, 2000). Long dsRNAs activate the enzymes RNaseL and RNA-dependent protein kinase (PKR) and subsequently lead to mRNA degradation and inhibition of translation.

The RNAi machinery is also involved in **transposon silencing** in *C. elegans* (Tabara et al., 1999; Ketting et al., 1999), but heterochromatic packaging of transposons has also been shown in other organisms (reviewed in Martienssen and Colot, 2001). The question whether RNAi regulates transposons through epigenetic chromatin modifications or by targeting mRNAs essential for transposition (e.g. mRNA coding for transposase) remains to be solved. Mutations in genes coding for the RNAi machinery (e.g. the Argonaute family), as well as miRNAs silencing endogenous gene expression by translational inhibition, have been linked to **developmental control** mechanisms in animals and plants (Carrington et al., 2003; Bartel et al., 2003; Hunter et al., 2003). Well studied examples are the *let-7* and *lin-4* genes in *C. elegans*. Originally termed small temporal RNAs (stRNAs) (Pasquinelli et al., 2000), these miRNAs repress regulators of developmental transition, thus control developmental timing (Banerjee et al., 2002; Carrington et al., 2003). As computational methods predict over 200 putative miRNA genes in humans (Lim et al., 2003), translational inhibition by RNAi appears to be an important regulatory mechanism and are regarded as RNA-based transcription factor equivalents.

2.1.5. How to use RNAi as a tool

There are different methods to make use of RNAi in cells or organisms as a modern molecular biological tool. The following short overview is intended to be taken as an application guide (reviewed in Hannon and Rossi, 2004; Mittal, 2004).

2.1.5.1. Mediators of RNAi

Long dsRNA, which becomes processed to several different siRNAs by Dicer, has been used to study gene function in various organisms lacking antiviral protection mechanisms, including some plants, *Drosophila*, *C. elegans*, and embryonic stem cells from mammals. This approach is limited in mammalian somatic cells, where dsRNA longer than 30 nucleotides induces a sequence independent interferon response, resulting in general inhibition of protein synthesis (Stark et al., 1998; Gil and Esteban, 2000).

Alternatively **synthetic siRNAs** can be used to mediate RNAi also in somatic cells of mammals, as these are short enough to escape from antiviral defense mechanisms (Elbashir et al., 2001). They consist of two paired, 21 nucleotide RNAs (sense and antisense) with 2 nucleotide 3' overhangs and a 3' OH for better stability. Many alternative designs, ranging from 19 to 29 nucleotides length have proven functional. Nowadays longer stems of 29 nucleotides are preferred.

Another approach to utilize RNAi in mammalian cells is to ectopically express **short hairpin RNAs (shRNAs)** by DNA vector systems. shRNAs consists of one RNA strand of base paired sense and antisense sequence, connected via a small loop structure. Alternatively, shRNAs can also be synthesized and transient transfected, as siRNAs

2.1.5.2. Delivery of RNAi mediators into mammalian cells

Basically RNAi can be applied transiently or permanently to cells. Transient RNAi can be mediated by synthetic and vector based systems, stable RNAi requires vector mediated systems in mammalian cells.

siRNAs and shRNAs can be chemically synthesized or *in vitro* transcribed. Transfection of mammalian cells with synthetic siRNAs / shRNAs can be performed by electroporation or lipophilic reagents. The efficiency of transient silencing depends on the transfection rate, on the potential of the chosen siRNA / shRNA to silence target gene expression and on the amount of siRNA / shRNA inside each transfected cell. Drawback of this system is its transient character, as mammals lack amplifying mechanisms for the silencing signal.

vector-based RNAi:

Vector systems can either be used to transcribe sense and antisense strand of siRNAs from two separate promoters (Miyagishi et al., 2002; Lee et al., 2002), or to express shRNAs (Paddison et al., 2002; Brummelkamp et al., 2002; Sui et al., 2002). Advantages of vector based systems compared to synthetic siRNA / shRNA transfection:

- shRNAs trigger RNAi more effective than siRNAs (Siolas et al, 2005).
- Transfection efficiency can be controlled by co-expressed markers as GFP.
- Co-expressed resistance genes can be used to select for transfected cells to improve RNAi efficiency read out.
- Cell lines stably expressing shRNAs can be created for long term gene silencing studies. This is especially useful to analyze functions of proteins with long half-lives.
- Transfection efficiency can be improved by viral vector systems, which also propose transfection of non-dividing cell types.
- Lower expenses

Several **RNA polymerase III promoters** (pol III) have been used, as they have a defined start site and are active in all cell types (e.g. mouse and human U6 promoter, H1 promoter). In addition RNA polymerase III recognizes a cluster of four or more T residues as a termination signal for defined transcription.

RNA polymerase II promoters have only found limited use to express shRNA in mammalian cells (Xia et al., 2002) because transcription start and stop sites are not well defined. Several groups used this promoter to express long hairpins in lower eukaryotes as *C. elegans* (Tavernarakis et al., 2000) and *Drosophila* (Kennerdell and Carthew, 2000).

Alternatively to expression plasmids, viral vectors systems can be used to express shRNAs, especially in cells that are difficult to transfect, such as primary cells, neural cells, or stem cells:

Adenoviral systems offer improved transmission rates and do not integrate into the host genome (Xia et al., 2002; Shen et al., 2003; Arts et al., 2003).

Lentiviral vectors are retroviral systems that integrate into the genome of non-proliferating cells (e.g. terminally differentiated cells) (Naldini et al., 1996; Rubinson et al., 2003; Stewart et al., 2003; Qin et al., 2003).

2.1.5.3. Applications of RNAi

Several **inducible RNAi-vectors** have been developed suitable for studies of genes essential for cell survival, cell cycle regulation and development (reviewed in Mittal, 2004). Commonly tetracycline- or doxycycline - regulated RNA pol III promoters are used for

inducible systems, as most regions in type III promoters are exchangeable (Czauderna et al., 2003; van de Wetering et al., 2003; Wiznerowicz and Trono, 2003; Matsukura et al., 2003; Chen et al., 2003). The major drawback of these systems is the relatively high background expression in an uninduced state. Recently a tightly regulated ecdysone - inducible system has been developed (Gupta et al., 2004).

First **double knock down experiments** were performed by simply co-transfecting two RNAi expression vectors (Yu et al., 2003), or by sequential transduction of cells with two retroviral vectors (Schuck et al., 2004). This latter system proposed high transduction rates and fast selection by two co-expressed resistance genes, one by each vector. The latest reports describe a more sophisticated system that proposes stable knockdowns of multiple genes by one expression vector (Jazag et al., 2005). They combine RNAi-cassettes, each encoding a human U6 promoter and a region encoding an shRNA, by a classical cloning approach and propose a hypothetical limit of >30 RNA-cassettes dependent on the saturation level of the RNAi machinery. Furthermore, the vector encodes a selection marker to create stable RNAi knock downs.

Another effort to identify gene functions are **large scale RNAi screens** (reviewed in Mittal, 2004; Hannon and Rossi, 2004). The availability of genome sequences allows the construction of either chemically synthesized siRNA- or vector-based shRNA-libraries which are used in cell based RNAi screens. This powerful tool comprises remarkable drawbacks (see discussion chapter 4.1).

2.1.6. Aim of this project

In the first part of the thesis, a new vector-based RNAi application will be presented. As many proteins are redundant in their function we wanted to establish an RNAi technique targeting several genes simultaneously. To create a cheap and versatile tool, we combined vector mediated shRNA expression with the MultiSite-GatewayTM system of Invitrogen.

This technique offers single vectors for transient RNAi and the ability to use a recombination based system for generation of Triple-RNAi-vectors. The single shRNAs can be exchanged easily and fast to target different combinations of genes, or to enhance the ability to silence one gene with three different shRNAs targeting different regions in this gene.

2.2. Functional LAP2 α analysis

2.2.1. The eukaryotic nucleus

In contrast to prokaryotes, eukaryotic cells enclose nearly their entire DNA in an internal compartment, the nucleus. The nucleus allows spatial and temporal separation of essential functions, such as DNA replication, transcription, RNA processing and ribosome assembly, from cytoplasmic protein synthesis.

Inside this largest eukaryotic organelle, a special set of structural proteins builds up a proposed nucleoskeleton, also termed nuclear matrix. This framework might be responsible for the highly organized structure of chromatin within the nucleus and for regulation of nuclear functions (reviewed in Lamond and Earnshaw 1998; Vlcek et al., 2001; Shumaker et al., 2003).

The nucleus is highly organized and includes numerous function-based foci. The most prominent of these sub-compartments is the nucleolus, where ribosomal DNA becomes transcribed and ribosomes get processed and assembled (reviewed in Taddei et al., 2004).

2.2.2. The nuclear envelope

The eukaryotic nucleus is enclosed by the nuclear envelope (NE), which is not only essential for nuclear structure but also for regulation of nuclear function (reviewed in Shumaker et al., 2003; Vlcek et al., 2001; Burke and Ellenberg 2002). The NE is formed by two concentric lipid bilayer membranes, the inner- and outer nuclear membranes (INM, ONM), and the nuclear lamina (see Figure 2-2). The ONM is continuous with the rough endoplasmatic reticulum (ER) and therefore often coated with ribosomes. The two nuclear membranes are separated by the perinuclear space (lumen) and join at sites where the nuclear pore complexes (NPC) are embedded. These numerous NPCs are large multiprotein channels, which mediate bidirectional transport of macromolecules between the cytoplasm and the nuclear interior and allow free, aqueous diffusion of ions and small molecules below a postulated size limit of 40kDa. A meshwork of proteins, termed the nuclear lamina, resides beneath the INM. The INM with its unique set of proteins is associated with the nuclear lamina via several transmembrane proteins, including the lamin B receptor (LBR) and proteins belonging to the lamina-associated-polypeptide-1 (LAP-1) and LAP-2 families.

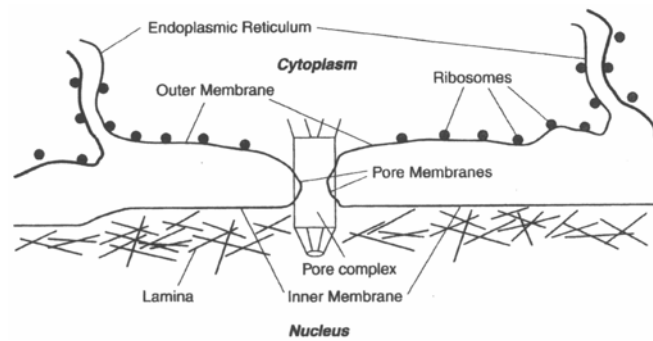


Figure 2-2: Schematic picture of a part of the nuclear envelope. The nuclear envelope is composed of the nuclear membranes, nuclear pore complexes and the nuclear lamina. The outer nuclear membrane is continuous with the rough endoplasmatic reticulum and has ribosomes on its outer surface. The inner nuclear membrane is associated with the nuclear lamina on its nuclear surface. The nuclear pore complexes allow transport of macromolecules and free, aqueous diffusion of small ions and molecules between the cytoplasm and the nucleoplasm. Modified from (Evans et al., 2004)

2.2.3. Nuclear Lamins

The nuclear lamina is a filamentous scaffold structure, positioned underneath the INM (reviewed in Gruenbaum et al., 2003; Shumaker et al., 2003). It is composed of a meshwork of type V intermediate filament proteins (IFs), the lamins, and lamina-associated proteins.

The nucleus-specific lamins classify as one out of six different types of vertebrate IFs, itself categorized on the basis of sequence homologies (reviewed in Foisner 2001, Hermann and Foisner 2003). All IF family members share a central α -helical rod domain, flanked by N- and C-terminal globular domains. Lamins differ from cytoplasmic IFs by several features (see Figure 2-3):

- short N-terminal head domains
- additional 42 amino acid residues in the central rod domain
- nuclear localization sequence in the C-terminal tail domain
- C-terminal CaaX motif (except for lamin C)

The C-terminal CaaX motif (C represents cystein, a means an amino acid with an aliphatic side chain, X is any residue) is a target site for post-translational modification, specifically farnesylation and subsequent carboxymethylation, which is important, but not sufficient, for targeting and anchoring lamins to the INM (Moir et al., 1995; Hofemeister et al., 2000). Lamins in vitro exhibit a head-to-tail association of dimeric subunits to form polar head-to-tail polymers, which can further assemble laterally (reviewed in Stuurman et al., 1998) to form a

meshwork of 10nm filaments, which has so far only been visualized in *Xenopus laevis* oocytes (Aebi et al., 1986). Lamins become phosphorylated at the onset of mitosis, leading to disassembly of the filaments, whereas dephosphorylation initiates re-assembly of the lamin meshwork after completion of mitosis. (Collas et al., 1990).

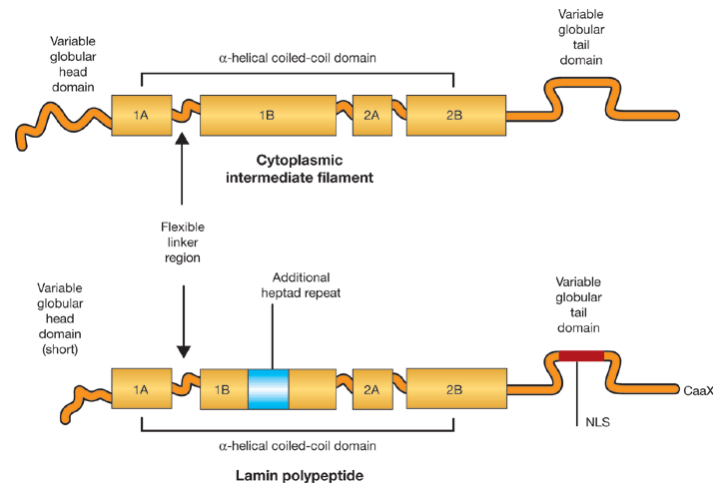


Figure 2-3: Generalized structure of cytoplasmic intermediate-filament proteins compared to lamins. Intermediate-filament proteins have a conserved domain structure consisting of a variable globular head domain, a central α -helical coiled-coil dimerization domain (rod domain) and a variable globular tail domain. The major differences between lamins and vertebrate cytoplasmic intermediate filaments are: first, the head domains are very short (about 33 amino acids); second, a six-heptad extension in the central rod domain (blue), and third, the globular tail domain is usually characterized by the presence of a nuclear localization signal (NLS) sequence and a site for farnesylation, carboxymethylation and proteolytic cleavage (CaaX). Modified from (Huthison and Worman 2004)

Lamins are grouped into two classes (A- and B-type) based on their biochemical and structural properties. In mammals, three genes (*LMNA*, *LMNB1* and *LMNB2*) give rise to seven different proteins and splice variants (Cohen et al., 2001). The *LMNA*-encoded proteins lamin A and the smaller splice variant lamin C are expressed in most terminally differentiated somatic cells but are not essential for embryonic development. Lamins B1 and B2, encoded by *LMNB1* and *LMNB2*, respectively, are constitutively expressed throughout development and cell differentiation. All somatic cells express at least one B-type lamin.

In contrast to B-type lamins, immature pre-lamin A loses its post-translational modification at its C-terminal CaaX motif due to proteolytic cleavage, leading to mature lamin A (Lutz et al., 1992). These differences in post-translational modifications of A- and B-type lamins are the reason for their different behaviour throughout the cell cycle (see 2.2.7.). In addition to their presence at the nuclear periphery, A-type lamins are also found inside the cell nucleus of

interphase cells. These structures appear as discrete foci and filamentous structures (Goldman et al. 1992, Bridger et al. 1993, Jagatheesan et al. 1999). A-type lamins become soluble and dispersed throughout the cytoplasm during mitosis, whereas B-type lamins preferentially remain associated with membrane vesicles (reviewed in Sturman et al., 1998).

2.2.4. Integral Nuclear Membrane Proteins

Most integral proteins of the inner nuclear membrane interact either directly or indirectly with lamins and are considered to be part of the nuclear lamina (reviewed in Ye et al. 1998; Gotzmann and Foisner 1999; Holmer and Worman 2001; Gruenbaum et al. 2003). Therefore, they can serve as adaptor proteins that link the INM to the lamina filaments and/or chromatin, as many lamin-binding proteins were also shown to interact with DNA or chromosomal proteins. Binding to the nuclear lamina provides a mechanism for the appropriate localization of these integral membrane proteins on the basis of selective retention within the nucleus (reviewed in Burke and Ellenberg 2002). According to this model, all proteins that are mobile within the ER can access the INM, but only those proteins that specifically interact with lamins or chromatin are retained and concentrated in the INM. Therefore, the INM can be seen as a specialized domain of the ER with a distinct composition of integral and peripheral proteins.

The first INM proteins were identified by their ability to bind to lamins, like lamin B receptor, lamina-associated polypeptide-1, or lamina-associated polypeptide-2 (LAP2). Since then, several additional proteins have been identified, including MAN-1, emerin, otefin, nurim, ringfinger binding protein (RFBP), nesprin and several others (see Figure 2-4; Mattout-Drubezki and Gruenbaum, 2003; Gruenbaum, 2005). Recently, a lot of new INM proteins have been classified (Schirmer et al., 2005), but so far not verified or characterized.

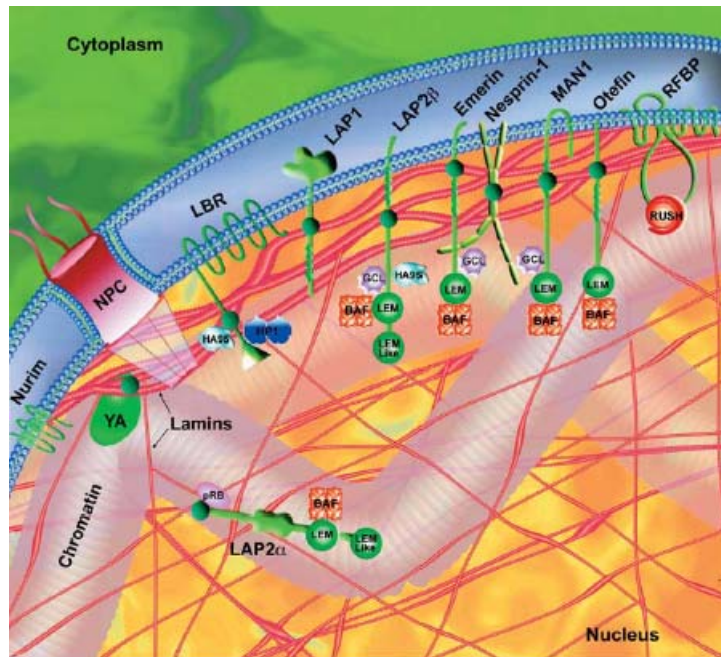


Figure 2-4: Schematic view of the nuclear envelope, including selected interactions between the lamina and chromatin. The inner and outer nuclear membranes join at the nuclear pore complexes (NPC) and are separated by the nuclear lumen (blue). Lamins (both A- and B-types) are shown as thicker filaments at the nuclear periphery and as thinner filaments in the nucleoplasm (red). Also shown are selected proteins of the inner nuclear membrane and proteins that interact with lamins in the nuclear interior (green). The green dots represent interactions with lamins. Especially indicated are the LEM domain and the LEM-like domain (see 2.2.4.). Chromatin at the nuclear periphery is structurally condensed, since it is mostly transcriptionally silent. Modified from (Mattout-Drubezki and Gruenbaum, 2003)

2.2.5. The LAP2 family

The lamina-associated polypeptide 2 (LAP2) family consists of six alternatively spliced isoforms (LAP2 α , β , γ , δ , ϵ and ζ) in mammalian cells (see figure 2-5) (Foisner and Gerace 1993; Furukawa et al., 1995; reviewed in Dechat et al., 2000). They share a common N-terminal domain (aa1-187), including a LEM-like and a LEM domain (Cai et al., 2001). The ~40 amino acids long LEM domain was first identified as a common structural motif in lamina associated polypeptide2, emerin and MAN1 (Lin et al., 2000). It mediates chromatin interaction via the small DNA bridging molecule barrier-to-autointegration-factor (BAF) (Furukawa 1999, Shumaker et al., 2001), dimers of which link double-stranded DNA in a sequence-independent manner. Additionally, the very N-terminal LEM-like motif may also permit direct binding to DNA (Cai et al., 2001).

LAP2 β is the largest isoform integrated into the membrane. Beside its N-terminal nucleoplasmic domain it consists of a single transmembrane region and a short C-terminus,

located in the lumen. The three smaller spliced isoforms LAP2 γ , δ and ϵ differ only little from LAP2 β . Compared to LAP2 β they lack regions of 40, 72 and 109 amino acids respectively, in their nucleoplasmic N-termini (see figure 2-5). These four LAP2 isoforms are type II integral membrane proteins of the inner nuclear membrane. LAP2 ζ corresponds to the first 219 N-terminal residues of LAP2 β , has five additional C-terminal amino acids and lacks a transmembrane domain. LAP2 α only shares the N-terminal common domain (first 187aa) with the other LAP2 isoforms and its 506 amino acid C-terminus is unique.

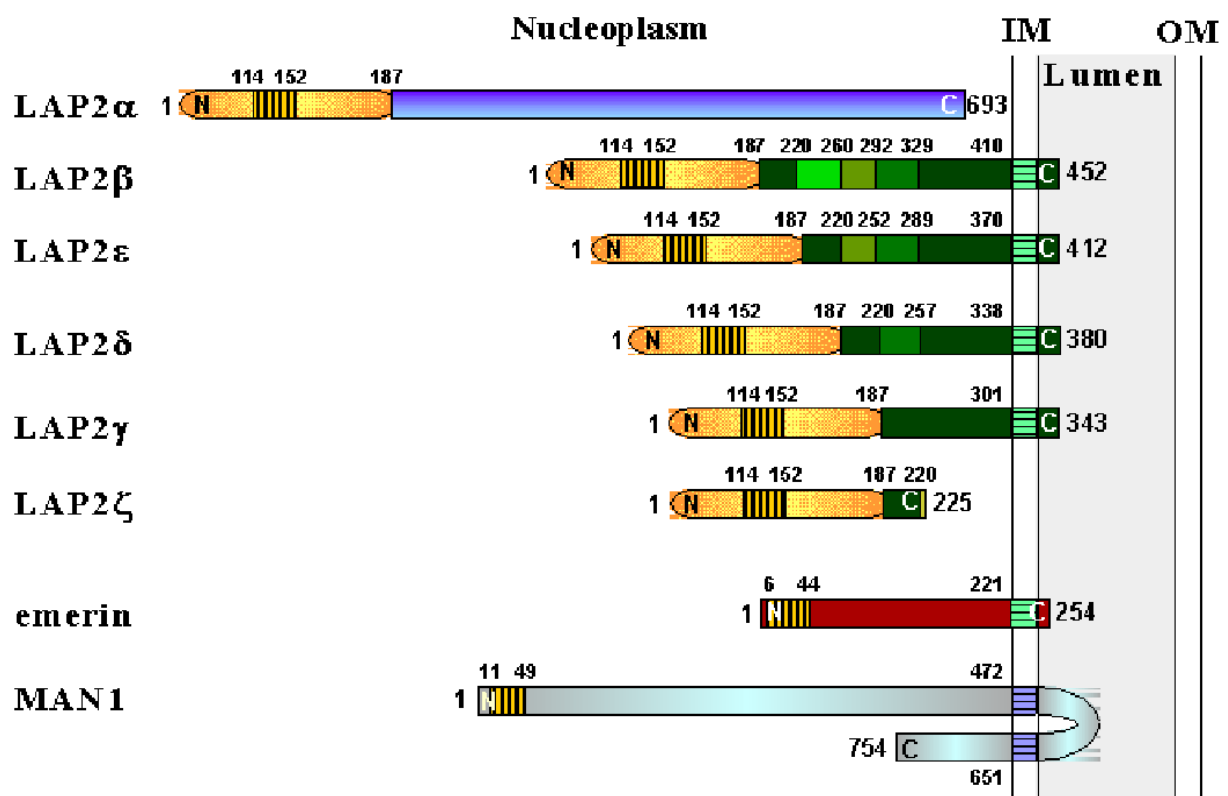


Figure 2-5: LAP2 isoforms and related LEM protein family. The six alternatively spliced isoforms of the LAP2 family share the common LEM protein motif (hatched box) with the LEM family, named after lamina associated polypeptide 2, emerlin and MAN1. The LEM domain mediates binding to BAF, a DNA-bridging protein. The LAP2 family shares the N-terminal common domain (yellow) encoding the LEM and a DNA binding LEM-like domain (at the very N-terminus). Most of the isoforms are C-terminally membrane bound and structurally related. They differ only by small insertions in the nucleoplasmic domain (differently shaded green boxes). In contrast LAP2 α has a unique C-terminus (blue) without a putative transmembrane region.

LAP2 β is restricted to the nuclear envelope, where it interacts with B-type lamins (Foisner and Gerace, 1993), chromatin (Dechat et al., 2000) and germ-cell-less (*gcl*) (Nili et al., 2001). Both, LAP2 β and *gcl* are able to repress E2F-dependent gene transcription. However, full repression requires both proteins, suggesting that these repressors act cooperatively. Together

with HA95, LAP2 β is involved in regulation of DNA replication (Martins et al., 2003). Disruption of this association does not interfere with elongation, but stops initialization of DNA replication.

2.2.5.1. Lamina-associated-Polypeptide 2 alpha (LAP2 α)

In contrast to LAP2 β , γ , δ , ϵ (see 2.2.5.), LAP2 α has no putative transmembrane region and is therefore distributed throughout the nucleus except for nucleoli. The N-terminal LAP2 common domain encodes the DNA binding LEM-like domain and the LEM domain, which interacts with chromatin via BAF (see Figure 2-6). The LAP2 α -specific C-terminus contains a stretch of basic residues forming a putative nuclear localization signal. Furthermore, the unique C-terminus mediates chromosome association and binds to lamin A/C and to tumor suppressor retinoblastoma protein (pRb) (Dechat et al., 1998; Vlcek et al., 1999; Dechat et al., 2000; Markiewicz et al., 2002).

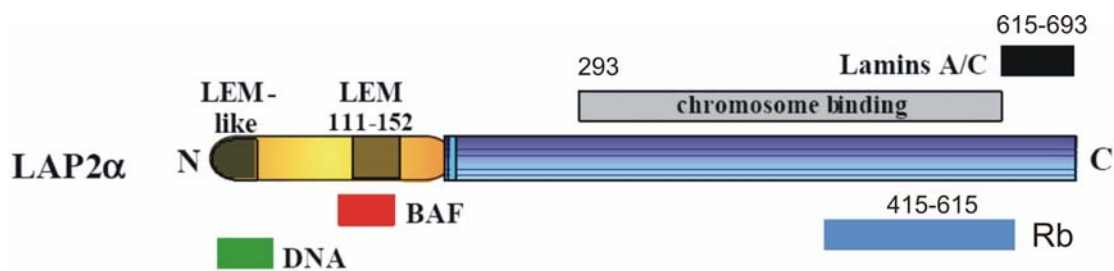


Figure 2-6: Schematic representation of LAP2 α protein regions, found to contain specific interaction sites. The LAP2 α constant N-terminus (yellow) contains the LEM domain binding to BAF (red) and the LEM-like domain binding to DNA (green). The unique C-terminus (blue) has a nuclear localization signal (light blue box), a chromosome binding domain (grey) and is capable of interacting with lamin A/C (black) and Rb.

Considering their intranuclear localization, it is likely that LAP2 α and A-type lamins help to organize chromatin structure all over the nuclear interior. Interactions of LAP2 α with chromatin and DNA via the LEM motif and the LEM-like motif, respectively, support this idea. During mitosis LAP2 α becomes cytoplasmic in a phosphorylation dependant manner (Gajewski et al., 2004) and relocates to the Chromosomes during late anaphase in a characteristic way (see 2.2.6.). Moreover it has been shown that LAP2 α is essential for nuclear reassembly after mitosis (Vlcek et al., 2002). Additionally, LAP2 α and A-type lamins were found to exist in a complex with hypophosphorylated pRb implicating a role in cell

cycle regulation (see 2.2.7.). Recent data implicated a very C-terminal mutation in LAP2 α with Dilated Cardiomyopathy (Taylor et al., 2005).

2.2.6. The nuclear envelope during mitosis

In vertebrates the NE completely disassembles during mitosis (reviewed in Burke and Ellenberg 2002; Foisner 2003; Margalit et al., 2005). This nuclear envelope breakdown (NEBD) defines the transition between prophase and prometaphase stages of mitosis. The models suggest that NEBD is initiated by phosphorylation of nucleoporins, lamins and lamin associated proteins (Heald and Mckeon, 1990; Foisner and Gerace, 1993 Stuurman et al., 1998). The resulting disassembly weakens nuclear structure and enables chromatin condensation. Further on, the disassembling NE is torn apart by microtubule guided motor proteins (Beaudouin et al., 2002; Salina et al., 2002). However, this microtubule-dependent rupture seems to facilitate NEBD, but is not essential for this process, as nuclear disassembly can also occur in the absence of microtubule induced mechanical stress (Georgatos et al., 1997) but not without phosphatase Cdk1 (Laronne et al., 2003).

Two exclusive theories try to describe the fate of nuclear membranes and their integral proteins during mitosis:

The first model suggests that nuclear membranes become fused to the endoplasmatic reticulum (ER) after NEBD (Ellenberg et al., 1997; Yang et al., 1997). According to this model, integral membrane proteins of the INM are re-distributed to the endoplasmatic reticulum of mitotic cells.

The second hypothesis predicts domain specific vascularization of the nuclear membrane into different populations of vesicles containing different sets of integral membrane proteins. In support of this model, two vesicle populations containing specific protein markers, different from the endoplasmatic reticulum, have been found in *Xenopus* oocytes (Vigers and Lohka, 1992; Drummond et al., 1999).

Non-membrane bound proteins like lamin A or LAP2 α become dispersed in the cytoplasm by NEBD.

During anaphase and telophase NE reassembly takes place in a temporally and spatially highly regulated manner.

- (1) Targeting of individual nucleoskeletal proteins to the chromosomal surface
- (2) Membrane recruitment and fusion
- (3) Assembly of NPCs
- (4) Transport of lamins into the nucleus

(5) Formation of the nuclear lamina

The exact chronological order of reassembly of lamina associated proteins and INM proteins has not been determined so far. Lamin B receptor (LBR) was detectable associated with anaphase chromatin slightly before LAP2 α , followed by LAP2 β (see figure 2-7) (Dechat et al., 2004). However, both LAP2 β and LBR first localize to more peripheral sites of the chromatin bulk, whereas LAP2 α first accumulates on telomeric regions of lagging chromosomes, followed by concentration into two ‘core’ structures adjacent to the mid-spindle and spindle pole area, respectively. These data indicate different chromosome binding properties of LAP2 isoforms during nuclear reassembly (Vlcek et al., 2002). In this context, it has been shown that the initial association of LAP2 α with chromatin required its unique C-terminal chromosome binding region, while the N-terminal LEM and LEM-like domains were dispensable at these stages.

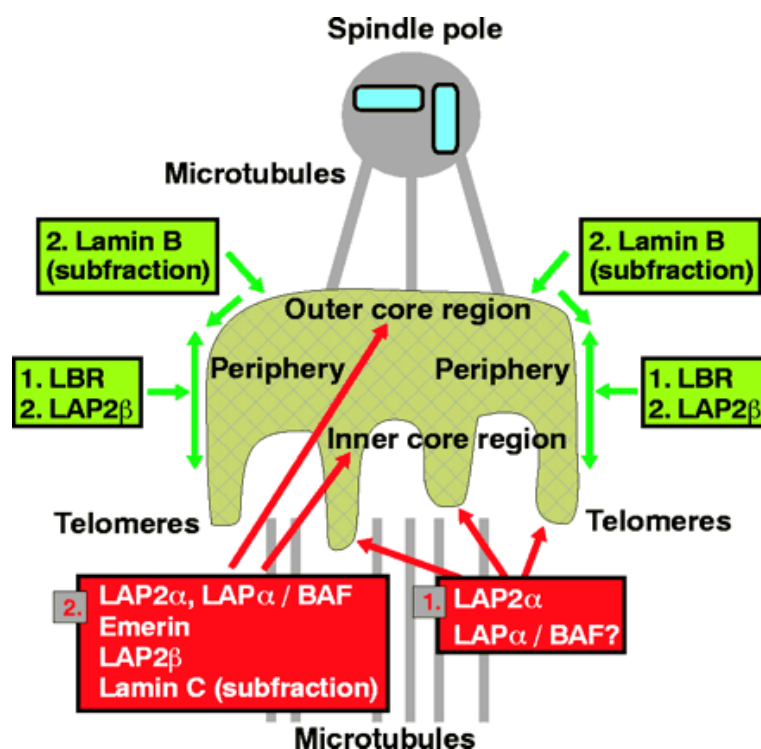


Figure 2-7: Model depicting the observed chronological order (numbers) of lamina protein relocation to the chromatin during nuclear reassembly. Colors distinguish the two pools of proteins which either initially associate with telomeres and core regions (red), or with more peripheral regions of the chromatin (green). Modified from (Dechat et al., 2004)

Interestingly, a large fraction of BAF colocalized with LAP2 α at telomeres and core structures (Haragutchi et al., 2001), to form a stable complex at early stages of nuclear reassembly (Dechat et al., 2004; Shimi et al., 2004). The LAP2 α /BAF complex is suggested

to trigger changes in chromatin structure, to provide binding sites for other NE proteins, such as proteins of the LEM-domain family.

Like lamina binding proteins differently localizing at the chromosomes, A- and B-type lamins also seem to assemble by different pathways. During chromosome separation B-type lamins are associated with disassembled “nuclear” membrane structures. B-type lamins could target membrane structures to the peripheral chromosome regions by interaction with LBR and LAP2 β . In contrast, A-type lamins are evenly distributed in the cytoplasm and only a small subfraction of lamin C colocalized with LAP2 α core structures but the majority of lamin C was translocated to the nuclear interior at later stages (Dechat et al., 2004).

After these crucial events in nuclear reassembly, membranes accumulate and fuse. The main fraction of lamins is imported through newly formed NPC and polymerizes to a filament network. Further nuclear proteins are imported and the nucleus grows in size.

2.2.7. Functional implication of the nuclear lamina

The nuclear lamina with its diverse composition of lamins and lamina associated proteins fulfills a wide range of functions. Similar to cytoplasmic IF networks, the nuclear lamina seems to serve as structural backbone for the nucleus defining its shape (reviewed in Wilson 2000; Hutchison et al., 2001; Wilson et al., 2001). Lamins are also thought to play an important role in higher order chromatin organization and regulation of gene expression via several binding partners (reviewed in Mattout-Drubezki and Gruenbaum 2003). In general, heterochromatin, including centromeres, telomeres and repetitive DNA, is preferentially positioned near the nuclear envelope. It was also shown that human gene-rich and transcriptionally highly active chromosomes are often found more centrally in the nucleus, whereas gene-poor chromosomes are localized at the periphery (Boyle et al., 2001). Moreover, it has been shown that the nuclear lamina affects transcription not only by interaction with chromatin, but also with the RNA polymerase II based transcription machinery and more specifically with individual transcription factors (reviewed in Mattout-Drubezki and Gruenbaum 2003). Lamins might also be involved in DNA replication (reviewed in Goldman et al., 2002; Gruenbaum et al., 2003) and proper execution of apoptosis (Rao et al., 1996; Ruchaud et al., 2002).

Finally, lamin A/C binds to pocket C of hypophosphorylated pRb (Ozaki et al., 1994; Mancini et al., 1994) and both are tightly bound by LAP2 α , as shown by blot overlay and coimmunoprecipitations assays (Markiewicz et al., 2002). Expression of a dominant negative lamin A/C mutant resulted in mislocalization of lamin A/C, LAP2 α and partly pRb,

suggesting that hypophosphorylated pRb is anchored in the nucleus by this trimeric complex. Furthermore, hypophosphorylated Rb is not anchored in the nucleus in the absence of LAP2 α , when cells reenter G1 phase from a quiescent state, induced by serum starvation (Markiewicz et al., 2002). According to these findings, pRb is mislocalized in *Lmna*^{-/-} cells and in cells with reduced lamin A/C expression (Johnson et al., 2004). In addition, proteasomal degradation of pRb was increased in these two cell systems. Both phenotypes, Rb localization and proteasomal degradation, could be rescued by reintroduction of GFP-lamin A into *Lmna*^{-/-} cells.

These findings propose a complex of lamin A/C, LAP2 α and hypophosphorylated pRb. pRb is known to regulate cell cycle progression via binding to members of the E2F transcription factor family in a phosphorylation dependent manner and by recruiting histone deacetylase complexes (Kaelin, 1999). Conclusively, the nuclear lamina might actively participate in the regulatory circuits of cell cycle control.

2.2.8. Laminopathies

Laminopathies are a group of diverse inherited diseases that were found to arise from mutations in genes that code for A-type lamins and lamina-associated proteins (reviewed in Gotzmann and Foisner, 2005). Laminopathies affect different tissues, giving rise to muscular dystrophy, cardiomyopathy, lipodystrophy, neuropathies, dermatopathies and premature aging syndromes. Most of these diseases arise from single point mutations in *LMNA*, despite this relation, the symptoms vary over a wide range. For example, two mutations in the C-terminus, causing Hutchinson Gilford Progeria (De Sandre-Giovannoli et al., 2003; Erikson et al., 2003) and restrictive dermopathy (Navarro et al., 2004), respectively, lead to accumulation of a shortened form of pre-lamin A, which misses the C-terminal proteolytic cleaving site and therefore remains farnesylated.

So far, five different not exclusive models have been postulated to explain the phenotypes which arise from mutations in *LMNA*:

- 1) The structural model: It predicts nuclear fragility or problems during nuclear assembly and / or during nuclear growth due to lamina instability. Preferentially muscle tissues are affected due to mechanical stress.
- 2) The ER-retention model: Mutations in lamin A cause misslocalization of emerin to the ER (Di Blasi et al., 2000). This correlates with the nuclear retention model (see 2.2.3.).

- 3) The gene expression model: Lamin A has been linked to chromatin organization, mutations could change gene expression by altering binding properties of lamin A to transcription factors, such as pRb, germ-cell-less (gcl), or SREBP-1.
- 4) The cell cycle model: Mutations in lamin A could influence cell cycle control by deregulating pRb function, as lamin A is essential for pRb localization and stability.
- 5) The regeneration model: This very recent hypothesis supposes that lamin A mutations affect plasticity or self-renewal potential of mesenchymal stem cells. This would explain the late onset of nearly all laminopathic phenotypes during childhood or puberty.

Most likely the different laminopathic diseases are based on different combinations of these five hypotheses.

2.2.9. Aim of this project

In this project we wanted to further characterize LAP2 α 's in vivo function by RNAi. Therefore, we designed sh-oligonucleotides targeting LAP2 α , LAP2 isoforms and other NE proteins. First we transiently tested the functionality of the RNAi constructs, than we selected stable cell lines and single cell clones. These were used to analyze the proposed role of LAP2 α in cell cycle regulation, as it has previously been shown to anchor hypophosphorylated pRb to the nucleus together with lamin A/C. Additionally, we were especially interested in potential changes in the localization of LAP2 α binding partners upon LAP2 α downregulation.

3. RESULTS

3.1. Results Triple RNAi

3.1.1. The Triple-RNAi-Vector strategy

The goal was to establish an RNAi vector, which allows to simultaneously knock down up to three target mRNAs. Cloning and flexibility of the system was facilitated using the MultiSite Gateway™ technology (see appendix B).

First we designed three pairs of primers with appropriate *attB* overhangs for recombination into donor vectors (according to Invitrogen's manual) and amplified three individual RNAi-cassettes by PCR using pSHAG as a template (see 5.4.3.; pSHAG provided by Greg Hannon, Cold Spring Harbor Laboratories). Each RNAi-cassette is flanked by Gateway™ recombination sites, and composed of a human U6 promoter, followed by BseRI and BamHI restriction sites for insertion of sh-oligonucleotides. The three PCR-products contained suitable recombination sites for three separate BP recombination reactions (see 5.4.5.2.) into the respective Donor vectors (see Appendix A). The resulting Entry vectors pMU6-A, pMU6-B and pMU6-C were sequenced with M13 forward and M13 reverse primers by VBC-Genomics (Vienna, Austria), to confirm the integrity of the recombination sites and the RNAi-cassettes.

Entry vectors could then be shuttled into a single Destination vector by Invitrogen's MultiSite Gateway™ Technology to form a Triple-RNAi-Vector. The MultiSite Gateway™ LR reaction (see 5.4.5.3.) was tested to construct control vector pJG100, encoding three empty RNAi-cassettes, each lacking sh-oligonucleotides.

3.1.2. Single RNAi targeting exogenous reporters

Single RNAi-Entry vectors were now tested for functionality in transient RNAi-assays (see 5.2.4.). sh-oligonucleotides (see 5.4.1.), designed to target exogenous reporter mRNAs for Firefly Luciferase, Renilla Luciferase and β -Galactosidase, were ligated (see 5.3.12.) each into the three different pMU6 Entry vectors (see Table 3-1).

The resulting vectors were tested by co-transfection of shRNA and reporter gene-expressing vectors. Substrate-dependent interference was ruled out by testing different combinations of reporter constructs and measuring respective enzyme activities in the absence/presence of the others (Figure 3-1).

RNAi Entry vector	sh-oligo / RNAi target	Empty Entry vector / pMU6-X
pJG177a+b	Firefly Luciferase	pMU6-A
pJG178	Renilla Luciferase	pMU6-B
pJG179	β -Galactosidase 1	pMU6-C
pCM4	β -Galactosidase 2	pMU6-C
pCM5	β -Galactosidase 3	pMU6-C
pCM6	β -Galactosidase 3	pMU6-A
pCM7	β -Galactosidase 2	pMU6-B
pJG173	SUN1	pMU6-A

Table 3-1: Overview of the used Entry vectors listed with their corresponding sh-oligonucleotides.

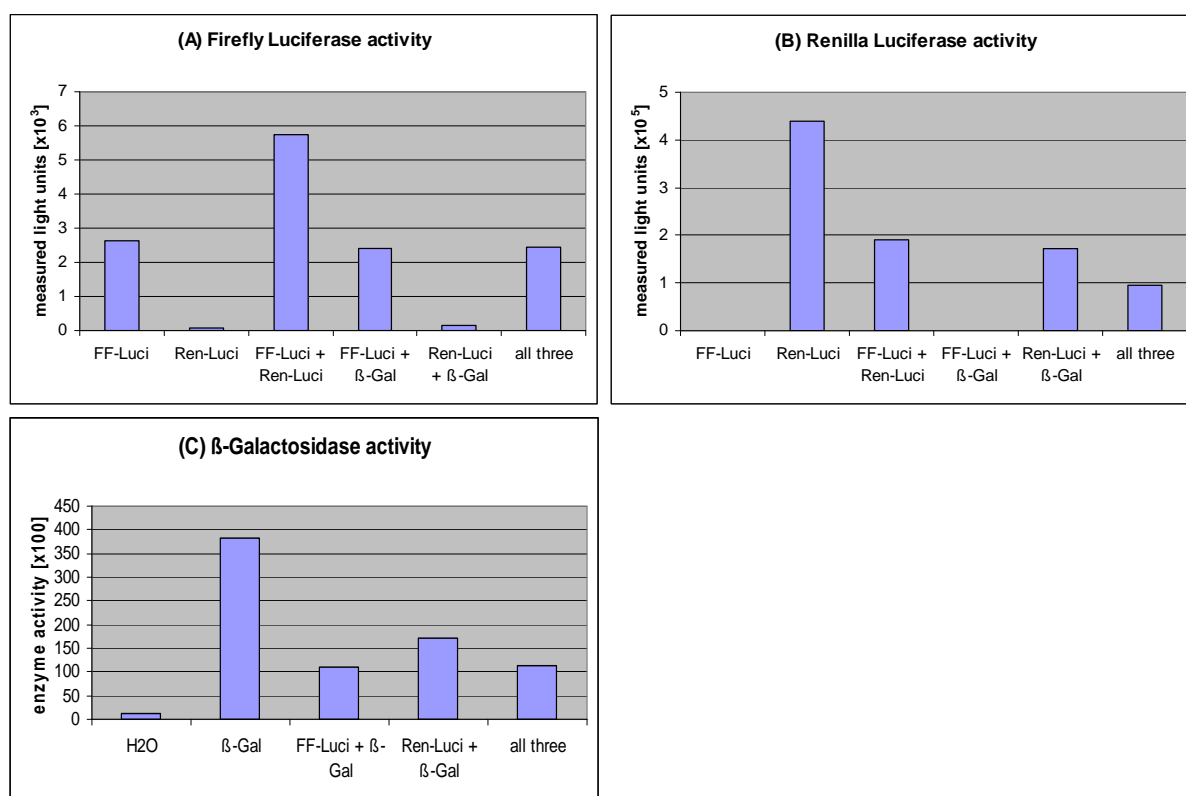


Figure 3-1: There is no substrate-dependent interference between the respective reporter enzymes. Single reporter activity was measured ((A) Firefly Luciferase (FF-Luci), (B) Renilla Luciferase (Ren-Luci), (C) β -Galactosidase (β -Gal)) in several single, double and triple reporter plasmid transfections of HEK 293 cells. X-axis indicate the reporter enzymes expressed by the cells, Y-axis indicate the measured enzyme activity. The amount of each plasmid used for transfection depended on the number of plasmids per transfection, therefore the measured enzyme activities vary a lot.

Single RNAi Entry vectors were transfected into HEK 293 cells together with two reporter plasmids. The pMU6 vector pJG173 containing an RNAi construct targeting SUN1, a nuclear

envelope protein, served as control. Two days after transfection, we measured the reporter enzyme activities. The RNAi efficiency was calculated by normalizing for transfection efficiencies with a second reporter enzyme. Each result was determined by at least two independent transfection experiments. The RNAi constructs reaching the highest efficiencies are shown in Figure 3-2.

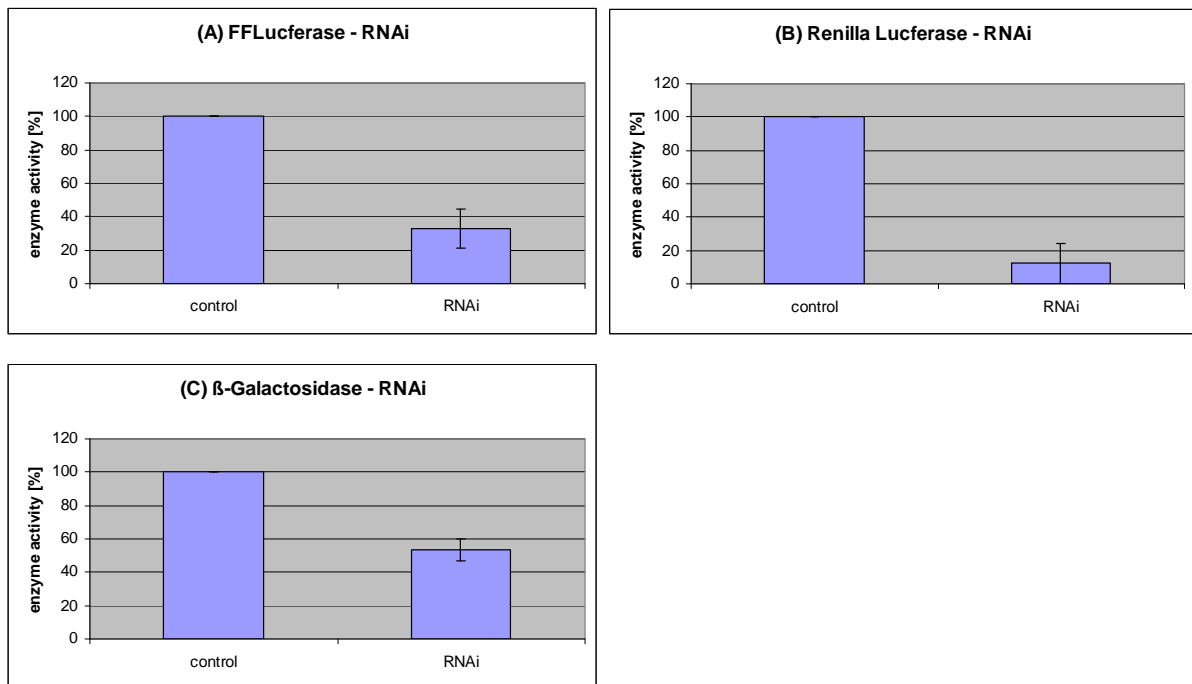


Figure 3-2: Efficiencies of RNAi mediated reduction of target gene protein levels were determined by quantitative enzyme activity assays. HEK 293 cells were transfected with two reporter plasmids (out of pGL3, phRL and pSVβ-Gal) and one RNAi vector (out of pJG177b (A), pJG178 (B) or pCM4 (C)). Co-transfections with pJG173 in all assays served as a control. One reporter was used for normalization of different transfections, the other was targeted by RNAi. Efficiencies of RNAi constructs are given as percent enzyme activity relative to the level of control transfections. Standard deviations were determined between results of independent transfection experiments.

Firefly Luciferase activity could be reduced by $67 \pm 12\%$ using pJG177b. pJG178 was even more effective reducing Renilla Luciferase reporter activity by $88 \pm 12\%$. For β-Galactosidase we achieved a maximal reduction of $46 \pm 7\%$ using pCM4. The other β-Gal constructs (see Table 3-1) were rather ineffective. Since all single RNAi vectors worked in our assay, we started creating a Triple-RNAi-Vector targeting all three exogenous reporters.

3.1.3. Triple-RNAi-Vector

MultiSite Gateway™ LR reactions were performed to obtain pCM3 and pCM8 (see 5.4.5.3.). Both plasmids encode three independent human U6 promoters, driving transcription of shRNA targeting Firefly Luciferase, Renilla Luciferase and β -Galactosidase (Figure 3-3), respectively. The two Triple-RNAi-Vectors are different only in the target sequences for β -Galactosidase (see Table 3-1 and Table 5-5). The functionality of the system was tested using a co-transfection setup, as follows: We transfected HEK 293 cells with four reporter plasmids (pGL3, phRL, pSV- β Gal and pCAT3) and one Triple-RNAi-Vector. Setups containing varying amounts of plasmids were used to find the conditions optimized for RNAi-efficiency. Plasmids were finally used in rates: 50% RNAi vector; 4x12.5% different reporter plasmids, to obtain highest RNAi efficiencies. The cells were lysed 48 hours after transfection and enzyme activities were measured.

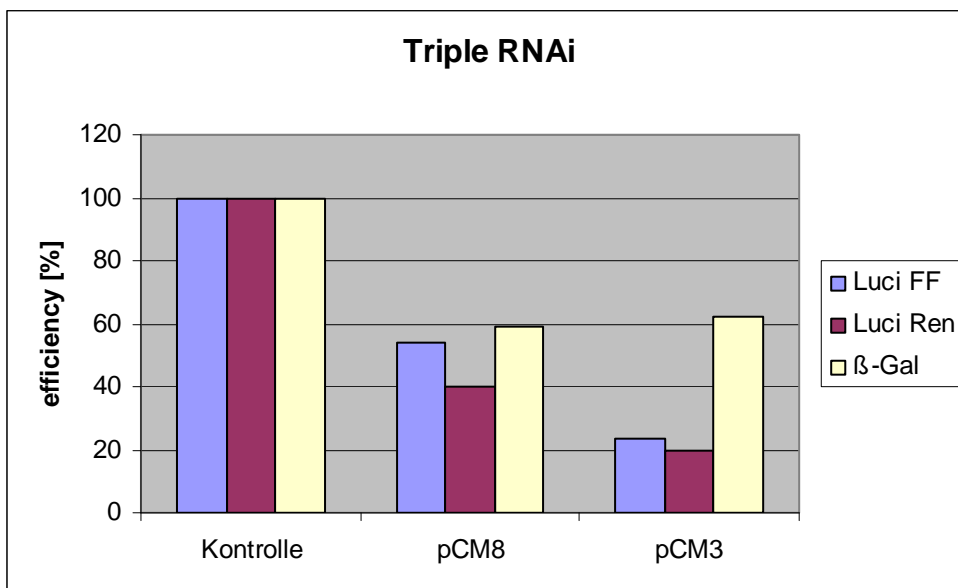


Figure 3-3: RNAi mediated reduction of enzyme activity levels of Firefly Luciferase, Renilla Luciferase and β -Galactosidase by the Triple-RNAi-Vectors pCM8 and pCM3, respectively. HEK 293 cells were transfected with the reporter plasmids pGL3, phRL, pSV- β gal, with pCAT3 for normalization) and with a triple RNAi vector (pCM3, or pCM8). The control vector (pJG100; see 3.1.1.) served as RNAi-control.

The measured enzyme activities of all lysates of different transfections were normalized by their chloramphenicol acetyltransferase activities and compared with the ones of the control transfection (pJG100 was used as triple RNAi vector in control transfections.). The results of the two Triple-RNAi-Vectors (Figure 3-3) and the ones of the single RNAi tests (Figure 3-2) are summarised in Table 3-2.

	pCM3	pCM8	single RNAi tests
Firefly Luciferase	-77%	-46%	-67 ±12%
Renilla Luciferase	-80%	-60%	-88 ±12%
β-Galactosidase	-38%	-41%	-46 ±7%

Table 3-2: RNAi results of Triple-RNAi-Vectors compared to single RNAi tests. The reduction in reporter enzyme activity compared to control is indicated.

Both Triple-RNAi-Vectors resulted in a significant reduction of all three enzyme activities. In two cases pCM3 was even more effective than the same RNAi constructs in single RNAi tests, but all results of pCM3 were within the range of standard deviation. Luciferase activity results using pCM8 showed higher variation compared to the other construct. There are several possible explanations for this result.

To summarize, both Triple-RNAi-Vectors showed clear knockdowns of all three targets. Thus, the system works efficiently on three ectopically expressed targets. Two questions remain to be answered:

1. Is the RNAi effect additive in a setup, where one gene is targeted by three different shRNAs.
2. Does the system work also on endogenous genes?

3.2. RESULTS LAP2 α RNAi

Lamina-associated polypeptide (LAP) 2 α belongs to the LEM-domain protein family. It has been described as a multifunctional, intranuclear protein, binding to BAF (Cai et al., 2001), lamins A/C, Rb (Markiewicz et al., 2002) and chromosomes (Vlcek et al., 1999). During mitosis, LAP2 α was shown to associate with telomeres and to form core structures adjacent to the spindle in telophase (Dechat et al., 2004). These data suggest, that LAP2 α is involved in chromatin reorganization during early stages of nuclear reassembly. Additionally, over expression studies (Andreas Gajewski, unpublished data) revealed that LAP2 α delays cell cycle progression.

To get a deeper insight to nuclear reassembly after mitosis and to confirm a proposed cell cycle regulatory role of LAP2 α , we decided to reduce LAP2 α expression levels by RNAi.

3.2.1. Transient approach to test the functionality of RNAi constructs

First, we designed RNAi short hairpin oligonucleotides (sh-oligonucleotides) targeting human LAP2 α , LAP2 β , all LAP2 isoforms, Lamin A, emerin, BAF and Lco1 using a software applicable for the BseR1/BamH1 strategy (see 5.4.1.). The RNAi targets and the corresponding plasmids are listed in Table 3-3, the targeting regions on LAP2 isoforms are shown in Figure 3-4.

RNAi target	pSHAG (transient RNAi)	pTRACER (trans.+stable RNAi)
all LAP2 isoforms	pJG101a	pJG111a
LAP2 β , γ , δ	pJG102a	pJG112a
Emerin	pJG103a	pJG113a
all LAP2 isoforms	pJG104a	pJG114a
BAF	pJG105a+b	pJG115a+b
LAP2 α	pJG106a	pJG116a
Lco1	pJG107a+b+c	pJG117a+b+c
LAP2 α	pJG108a+b	pJG118a+b
LAP2 α	pJG109a+b	pJG119a+b
Lamin A	pJG120a+b	pJG120a+b
Firefly Luciferase (control)	pSHAG-FF	pJG121

Table 3-3: RNAi targets listed with their corresponding plasmids. a and b are indicating different bacterial clones. For sh-oligonucleotide sequences and more detailed information see 5.4.1..

Molecular Target Overview:

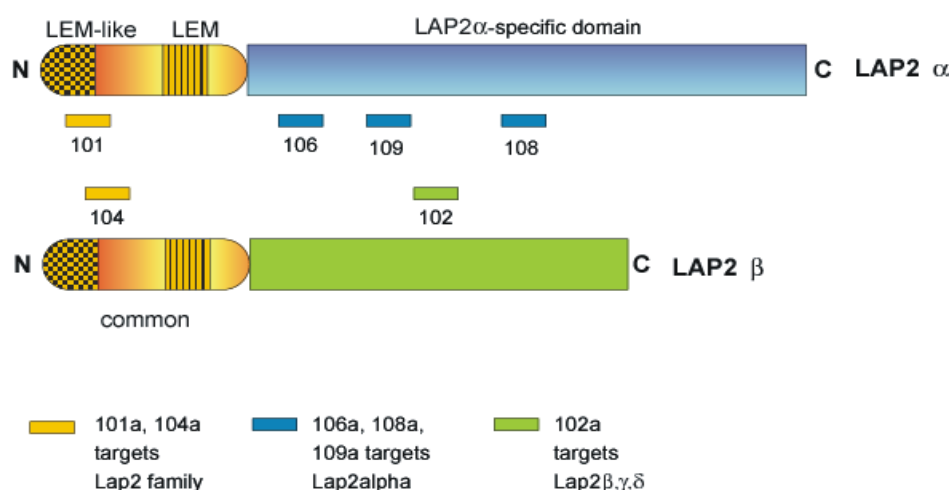


Figure 3-4: Molecular target-sequence localization of siRNAs on LAP2 isoforms, here represented by LAP2 α and LAP2 β . Two constructs were used to knock-down all LAP isoforms, three siRNAs were LAP2 α – specific, whereas one plasmid should interfere with the expression of LAP2 isoforms β , γ and δ . The RNAi constructs are indicated by the number of the respective pSHAG -based pJGx- plasmids (see Table 3-3).

The sh-oligonucleotides were annealed (see 5.4.2.) and ligated (see 5.3.12.) into a BseR1/BamH1 digested pSHAG vector, which contains a human U6 promoter driving transcription of a hairpin RNA and can be used to analyze RNAi-efficiencies in a transient manner. The RNAi cassette is enclosed by GatewayTM (Invitrogen) recombination sites to easily shuttle the RNAi-cassette between different GatewayTM-compatible vectors (see appendix B). First, we tested the efficiency of the new LAP2 α -targeting RNAi hairpin constructs by western blot analysis of HeLa cell lysates, processed 48 hours after transfection (Figure 3-5).

The target protein levels were compared to the ones of control transfections (pSHAG-FF and pTRACER) and of untransfected HeLa cells. Out of three constructs targeting different regions within the LAP2 α specific domain (see Figure 3-4) only vectors pJG108a and b proved functional in reducing LAP2 α protein levels significantly. A potential down regulation of LAP2 protein levels using vector pJG101a was also indicated in the blot. Similarly, Western blots were performed with cells following treatment with the RNAi constructs targeting lamin A and emerin (see Table 3-3) but in both cases there was no significant reduction in protein levels.

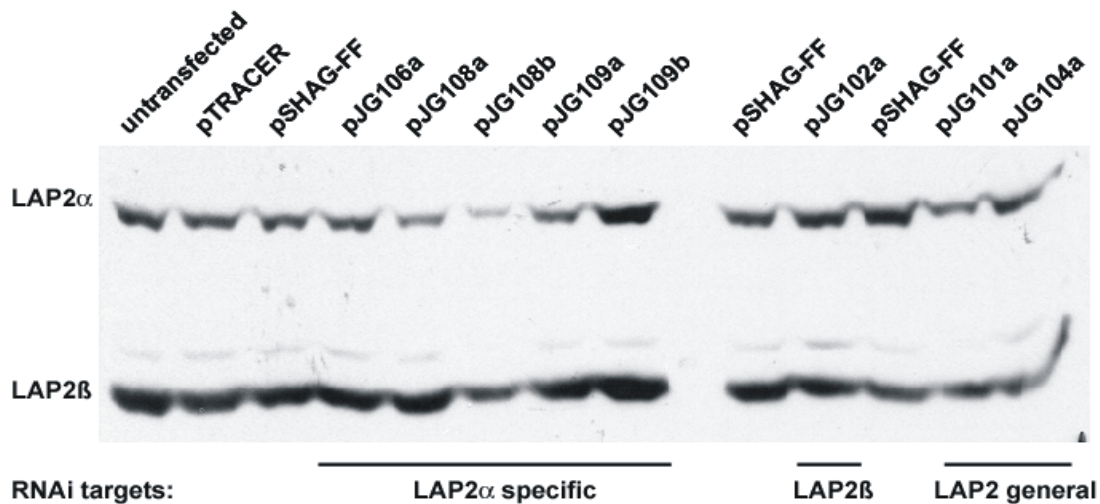


Figure 3-5: Western blot analysis of HeLa cells, transiently transfected with RNAi mediating pSHAG vectors (pJG101a, pJG102a, pJG104a, pJG106a, pJG108a+b, pJG109a+b). As control we used a pSHAG vector with a hairpin construct against Firefly Luciferase (pSHAG-FF), a pTracer vector and untransfected cells. 48h after transfection the cells were lysed and equal amounts of protein were probed for LAP2 isoforms using mAb12.

3.2.2. Conditions for stable transfection with RNAi constructs

We next shuttled the RNAi-cassettes into a GatewayTM-compatible pTracer plasmid (see appendix B). The pTracer vector is suitable for transient and stable transfection in eukaryotic cells (see 5.1.2., 5.1.3.), as it enables selection on Blasticidin by a co-expressed (CMV – driven) GFP-Blasticidin resistance fusion protein. We made use of the GFP-based fluorescence not only to determine transfection efficiencies but also to clearly distinguish transfected from non-transfected cells. Later the blasticidin resistance was exploited to select for cells stably expressing a functional RNAi-cassette (see 3.2.3.).

To test the vector system in transient assays, HEK 293 cells were grown on polylysine coated coverslips and transfected with the plasmids pJG111a, pJG112a, pJG114a, pJG116a, pJG118a+b, pJG119a+b and pJG120a+b. 48 hours after transfection the cells were processed for immunofluorescence (see figure 3-6).

Two independent transfections with pJG111a targeting all LAP2 isoforms (upper and lower panels) are shown. We compared LAP2 protein levels of transfected and untransfected HEK cells, which were distinguished by co-expressed GFP (left panels). Monoclonal ab12 was used to stain all LAP2 isoforms. This antibody preferentially decorates the NE, where all LAP2 isoforms except LAP2 α and - ϵ are located. Therefore, untransfected cells show a clear rim-staining, whereas transfected cells show only weak and diffuse background staining.

These results show a clear down regulation of LAP2 by pJG111a, which was also demonstrated using pJG118a+b (data not shown and see 3.2.3).

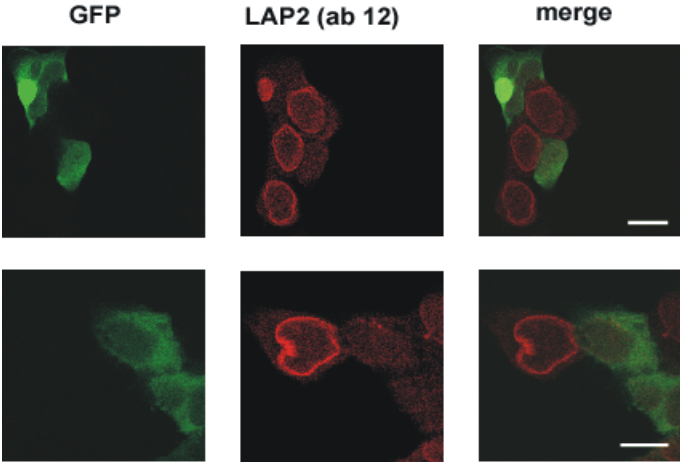


Figure 3-6: Confocal immunofluorescence images of HEK 293 cells, transiently transfected with pJG111a, expressing a shRNA targeting all LAP2 isoforms. GFP indicates the transfected cells (green), ab12 and Texas Red conjugated secondary antibody was used to stain all LAP2 isoforms (red). Bars, 10µm.

Thus, the system and some of the RNAi constructs worked efficiently. We next wanted to confirm these data by Western blot analysis of cell lines stably expressing these RNAi-cassettes.

To create stable cell lines, we first determined the blasticidin concentration necessary for selection on transfected cells. Therefore we studied its dose dependency on the viability of HEK 293 and HeLa cells (Figure 3-7).

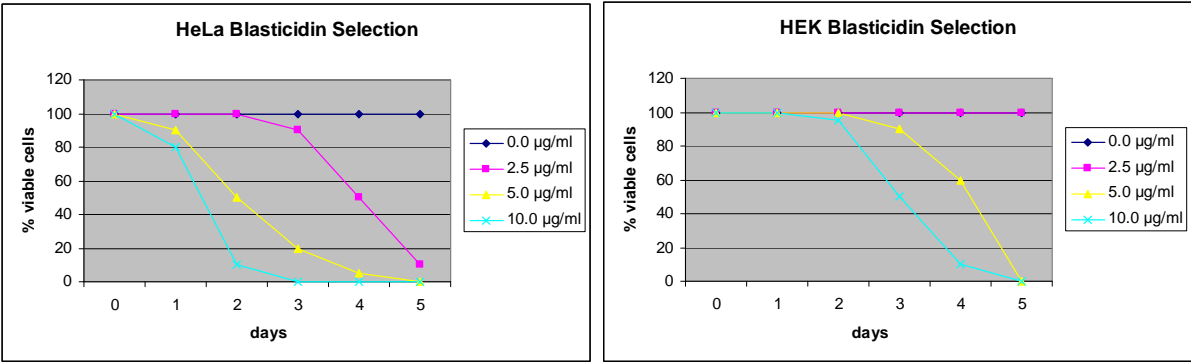


Figure 3-7: Influence of different Blasticidin concentrations on the viability of HeLa and HEK 293 cells, respectively. Cells of cultures with 80% confluency were exposed to culture medium substituted with different concentrations of blasticidin [0, 2.5, 5, 10µg/ml]. The amount of viable cells on the culture dish was estimated by visual screening of cultures under the light microscope.

The cells were grown to a confluence of about 80% before they were exposed to culture medium supplemented with blasticidin concentrations ranging from 0 to 10µg/ml. Every other day the medium was exchanged for two reasons:

- a) to remove dead cells and cellular degradation products
- b) to ensure an effective blasticidin concentration

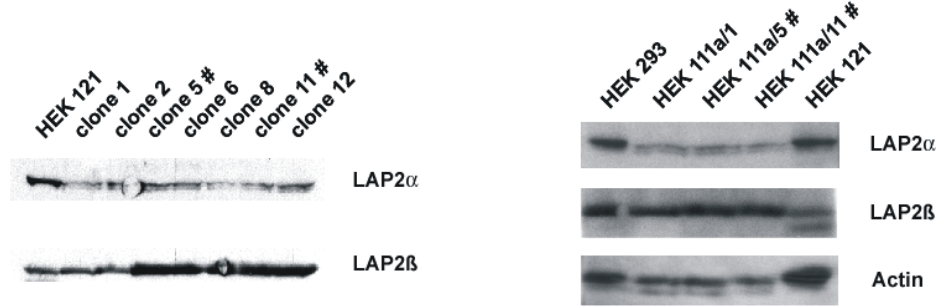
This experiment showed strong variation of blasticidin resistance between these two cell lines. HeLa cells reacted more sensitively and started to die after 24 hours, when exposed to blasticidin concentrations >2.5µg/ml. After five days of treatment no viable HeLa cells were detectable. On the other hand, HEK 293 cells sustained Blasticidin concentration of 2.5µg/ml and proliferated like untreated cells. Nonetheless, HEK cells proved sensitive to higher concentrations (>2.5µg/ml) of blasticidin and efficiently died within 4-5 days.

As HEK 293 cells were able to grow at low blasticidin concentration, we first started selection for stable transfected cell lines at 15 µg/ml blasticidin in culture medium. In later experiments we raised the concentration up to 25µg/ml which turned out to be adequate to achieve fast and highly efficient selection.

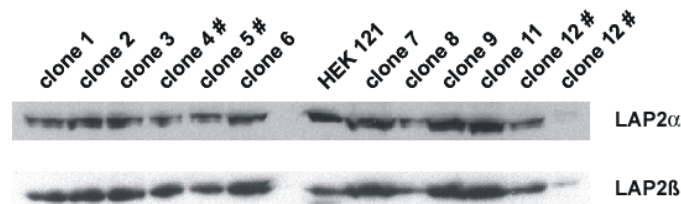
3.2.3 Stable RNAi

With this basic knowledge, we started to select for pools of cells stably expressing either pJG111a, pJG112a, pJG113a, pJG114a, pJG116a, pJG118a+b, pJG119a+b, pJG120a+b or pJG121 (Table 3-3) in HEK 293 cells. These pools were examined for the expression levels of targeted proteins, by Western blot analysis of cell lysates. As controls, we used pools of HEK 293 cells, stably transfected with pJG121, targeting Firefly Luciferase (HEK 121). RNAi constructs encoded by plasmids pJG118a+b showed very high efficiency in knocking down LAP2α, which was also successfully targeted by pJG116a and pJG111a. As the knock-down effect varied significantly within these pools we decided to select for single HEK cell clones expressing plasmids pJG111a, pJG116a and pJG118a. We also generated stable transfected cell pools and single cell clones of HeLa cells expressing pJG118a, pJG113a and pJG121 (HeLa 121) for control purpose. The selected single cell clones were again tested by Western blot analysis of total cell lysates (Figure 3-8).

(a) HEK 293, transfected with pJG111a (RNAi targeting Lap2 common domain):



(b) HEK 293, transfected with pJG116a (RNAi targeting Lap2 α):



(c) HEK 293 and HeLa, transfected with pJG118a (RNAi targeting Lap2 α):

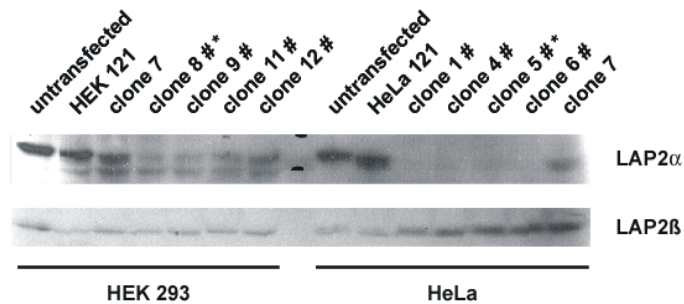


Figure 3-8: Stable RNAi single cell clones tested by Western blot. To obtain single cell clones, we first selected on transfected cells with Blasticidin to generate stable cell pools. Afterwards, we either picked single clones (HeLa), or achieved them by limited dilution (HEK). Protein levels of whole cell lysates of the single cell clones were compared with stable cell pools transfected with pJG121. Aliquots of cells marked with # were stored in liquid nitrogen. (a) HEK cells transfected with pJG111a targeting LAP2 common domain. Either LAP2 α and LAP2 β were stained with ab12 (left panels), or LAP2 α was stained with ab15/2, LAP2 β with ab16 and actin as loading control (right panels). (b) HEK cells transfected with pJG116a targeting LAP2 α , which was stained with ab12, which also stained LAP2 β , shown as loading control. (c) Single cell clones of HEK 293 and HeLa cells transfected with pJG118a, targeting LAP2 α , which was stained with ab 15/2. LAP2 β was used as loading control and was stained with ab 16.

Clones indicated with an asterisk were used for further investigations.

Several single cell clones expressing plasmid pJG111a were tested for LAP2 α protein levels (Figure 3-8 (a), left panels). All clones showed reduced LAP2 α levels compared to the control (HEK 121), whereas the amount of LAP2 β remained constant. As pJG111a targets the LAP2

common domain we made further immunoblots of clones 1, 5 and 11 with specific antibodies to LAP2 α , LAP2 β and actin as loading control (Figure 3-8 (a) right panels). All three single cell clones displayed reduced LAP2 α protein levels. Considering the different amounts of loaded protein (compare actin lanes, right lower panel), LAP2 β was moderately affected by RNAi.

Only some of the single cell clones expressing pJG116a functionally reduced LAP2 α protein level (Figure 3-8 (b)).

The most efficient RNAi effect was achieved by expressing pJG118a (Figure 3-8 (c)). In several single cell clones LAP2 α protein levels were hardly detectable.

For further experiments, we chose single cell clones of plasmid pJG118a, notably clone 5 in HeLa cells (HeLa 118a/5) and clone 8 in HEK 293 cells (HEK 118a/8). HEK 293 and HeLa cell pools stably transfected with pJG121 (HEK 121 and HeLa 121), respectively, served as controls. First, the strong RNAi effect on LAP2 α , shown by Western blot analyzes (Figure 3-8 (c)), was confirmed by immunofluorescence (Figure 3-9).

Four cell lines were separately plated on coverslips and processed for immunofluorescence. Confocal images showed a strong decrease in LAP2 α fluorescence intensity in LAP2 α RNAi clones versus control cells (Figure 3-9 (a)). For better demonstration of the silencing effect, we also co-cultivated HeLa 118a/5 with HeLa 121 control cells (Figure 3-9 (b)). A clear difference in the amount of LAP2 α (left panel) became obvious between the LAP2 α -RNAi cells (right side) and the control cells (left side). To test whether the residual LAP2 α is distributed normally, we analyzed the same cells at higher detector sensitivity levels to make little protein levels detectable (right panel). Neither the shape of the nucleus nor the localization of remnant LAP2 α seemed to be altered.

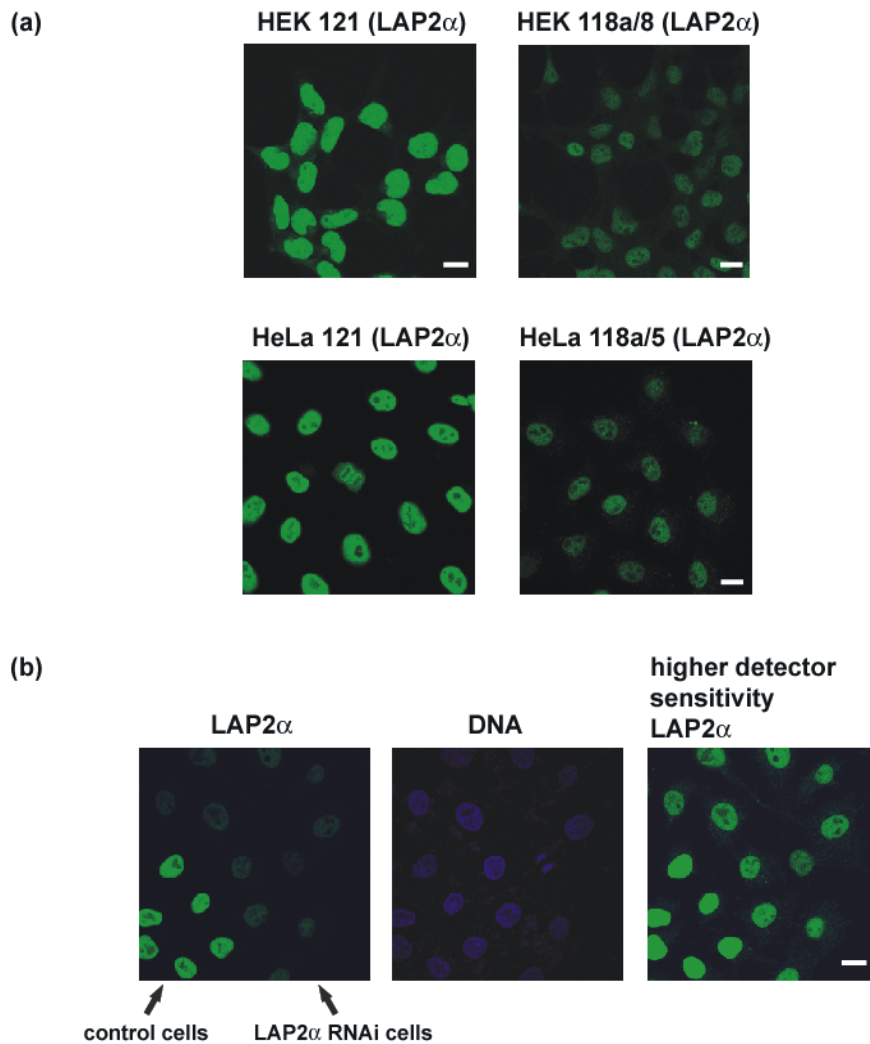


Figure 3-9: Confocal immunofluorescence images of LAP2 α RNAi single cell clones stained for LAP2 α compared to control cell lines. The cells were grown on polylysine coated coverslips and processed for immunofluorescence microscopy. LAP2 α was stained with ab 245-2, DNA by Hoechst dye. (a) Single cell clones HEK 118a/8 and HeLa 118a/5 compared to HEK 121 and HeLa 121 control cell lines (b) LAP2 α RNAi single cell clone HeLa 118a/5 co-cultivated with control cell line HeLa 121. The LAP2 α image was made twice with altered detector sensitivity. Bars, 10 μ m.

As we were able to generate single cell clones with strong downregulation of LAP2 α , we were interested to determine the cellular phenotype. We analyzed nuclear integrity, cell cycle behaviour and the localization of LAP2 α 's intranuclear binding partner lamin A/C in LAP2 α deficient cells.

3.2.4. Reduced levels of LAP2 α have no influence on nuclear integrity

LAP2 α has been described as a multifunctional protein, binding to BAF, DNA (Cai, M. et al., 2001), lamins A/C, Rb (Markiewicz et al., 2002) and chromosomes (Vlcek et al., 1999). We wanted to see, if low levels of LAP2 α might influence nuclear shape.

We co-cultivated single cell clone HEK 118a/8 with mock transfected HEK 293 cells and performed immunofluorescence co-stainings for LAP2 α , and an unaffected protein, the nuclear pore protein 62 (NUPp62), scaffold attachment factor SAF-A and LAP2 β (Figure 3-10).

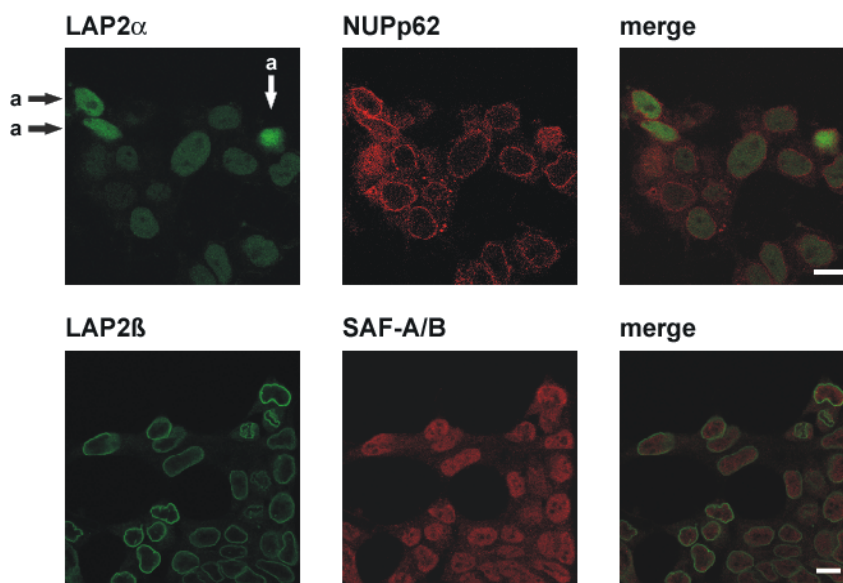


Figure 3-10: The nuclear integrity is not affected by LAP2 α RNAi. HEK 118a/8 and mock transfected HEK cells were co-cultivated for two days and processed for immunofluorescence with ab 245-2 to stain LAP2 α , ab NUP p62 for nuclearpore protein 62 (NUP p62), ab 16 for LAP2 β and ab K371 to stain scaffold attachment factor A (SAF-A). Confocal images are shown. Bars, 10 μ m.

To distinguish HEK 118a/8 from mock transfected cells, we made use of GFP, which was only expressed by HEK 118a/8 (not shown). For better illustration, stainings were pseudocoloured. The three mock transfected cells (a) in the upper panel show normal LAP2 α expression. In contrast, LAP2 α was nearly absent in HEK 118a/8 cells (all the other cells). Nevertheless, localization and distribution of nuclear pore complexes remained unaffected, as can be seen by the rim staining of nuclear pore protein p62. Also LAP2 β and SAF-A were unaffected. Similar stainings were performed for lamin A and emerin all revealing no irregularities of interphase nuclei with respect to shape and size. Moreover, the localization of

all tested proteins remained normal. Thus, the nuclear integrity seems unaffected by loss of LAP2 α .

3.2.5. Proliferation rate is increased by reduction of LAP2 α levels

Preliminary data indicated an involvement of LAP2 α in cell cycle regulation: It has previously been shown that LAP2 α -lamin A/C form a complex with the retinoblastoma protein (Rb) (Markiewicz et al., 2002), which regulates cell cycle progression in G1 phase. HeLa cells over-expressing LAP2 α showed reduced cell proliferation compared to control cells (Dorner et al., 2006). To verify these data, we performed comparable growth rate experiments with the LAP2 α RNAi single cell clones HeLa 118a/5 and HEK 118a/8 in comparison to the control cell lines HeLa 121 and HEK 121 (Figure 3-11).

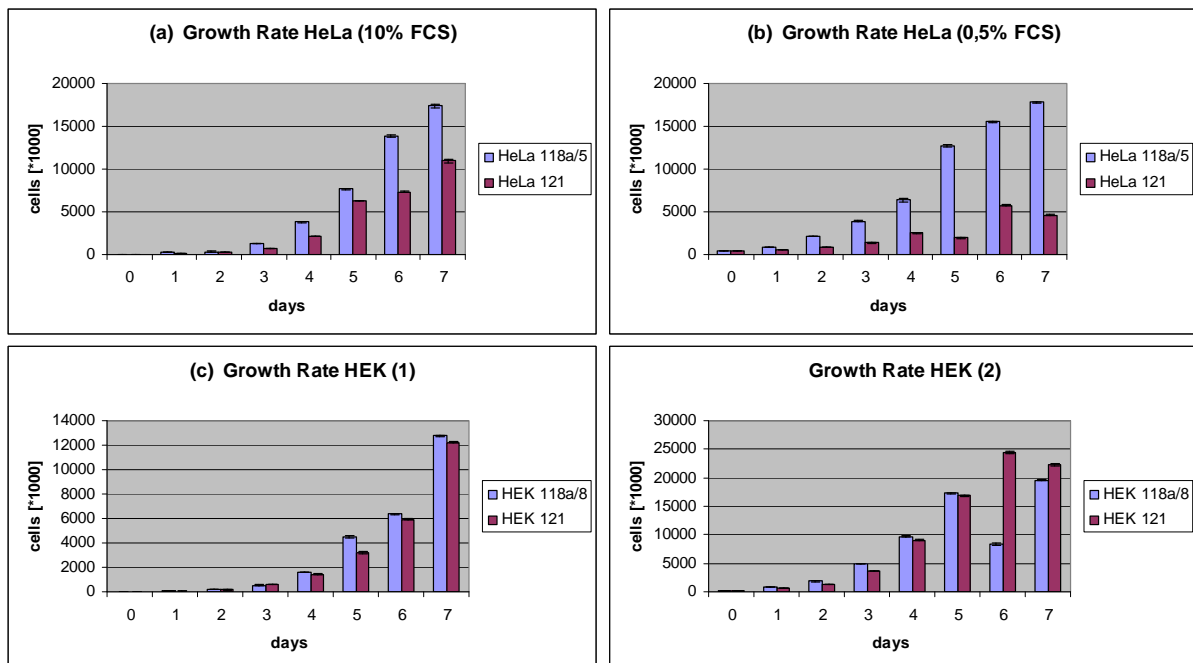


Figure 3-11: Cumulative cell number of LAP2 α RNAi cells compared to control cells. Identical numbers of cells of each type were seeded into 14 individual dishes and were grown in semi-conditioned medium for up to 7 days. Each day the cells of two dishes were counted to determine cell numbers. [(a) 5×10^4 HeLa 118a/5 and HeLa 121 cells were grown in complete medium (10% FCS). (b) HeLa 118a/5 and HeLa 121 cells were stepwise adapted to low serum (0,5% FCS) conditions. Then an experiment as shown in (a) was started with 5×10^5 cells per plate. (c) Growth curves of HEK 118a/8 and HEK 121 in complete medium (10% FCS) were done. One experiment was started with 5×10^4 cells per plate (left panel), the other started with 2×10^5 cells per plate (right panel).]

In brief, we plated identical numbers of cells on 14 dishes per cell type and grew them in semi-conditioned medium. Each day the cells of two plates were counted to obtain

proliferation kinetics over a period of seven days. HeLa cells with reduced LAP2 α expression were growing faster than the control cells at normal serum conditions (Figure 3-11 (a)). The effect was even more pronounced under serum starvation (Figure 3-11 (b)). Interestingly, there was no proliferation effect in HEK cells cultivated in full serum (Figure 3-11 (c)). The reason for the absence of a proliferation effect could be the lack of mature lamin A/C in HEK cells (Figure 3-12).

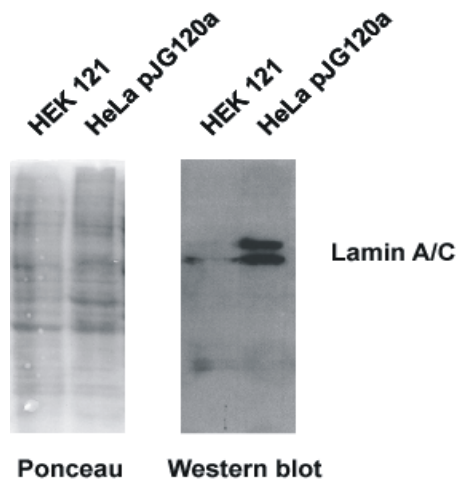


Figure 3-12: HEK 293 cells lack mature lamins A/C expression. Ponceau stain after PAGE and Western blot of HEK 121 control cell line and HeLa cells stable transfected with pJG120a. Lamin A/C was stained with McKeon antibody.

Total cell lysates of HEK 121 and HeLa cells stably transfected with pJG120a were used for immunoblotting. The Ponceau stain of the blot membrane indicated that similar protein amounts were loaded, but Western blot showed strong lamin A/C bands only in HeLa cell lysates, while no lamin A and hardly any lamin C were detected in HEK 121 cell lysates.

To analyze the cell cycle phenotype in more detail, we performed DNA FACS analysis of the four cell lines (Figure 3-13). Reduced levels of LAP2 α however, did not result in clear changes in the number of G1 and S-phase cells.

To sum up, these experiments confirmed the involvement of LAP2 α - lamin A/C complexes in cell cycle regulation. Finally, we investigated the influence of reduced LAP2 α protein levels on lamin A/C localization during the cell cycle or on nuclear envelope reassembly.

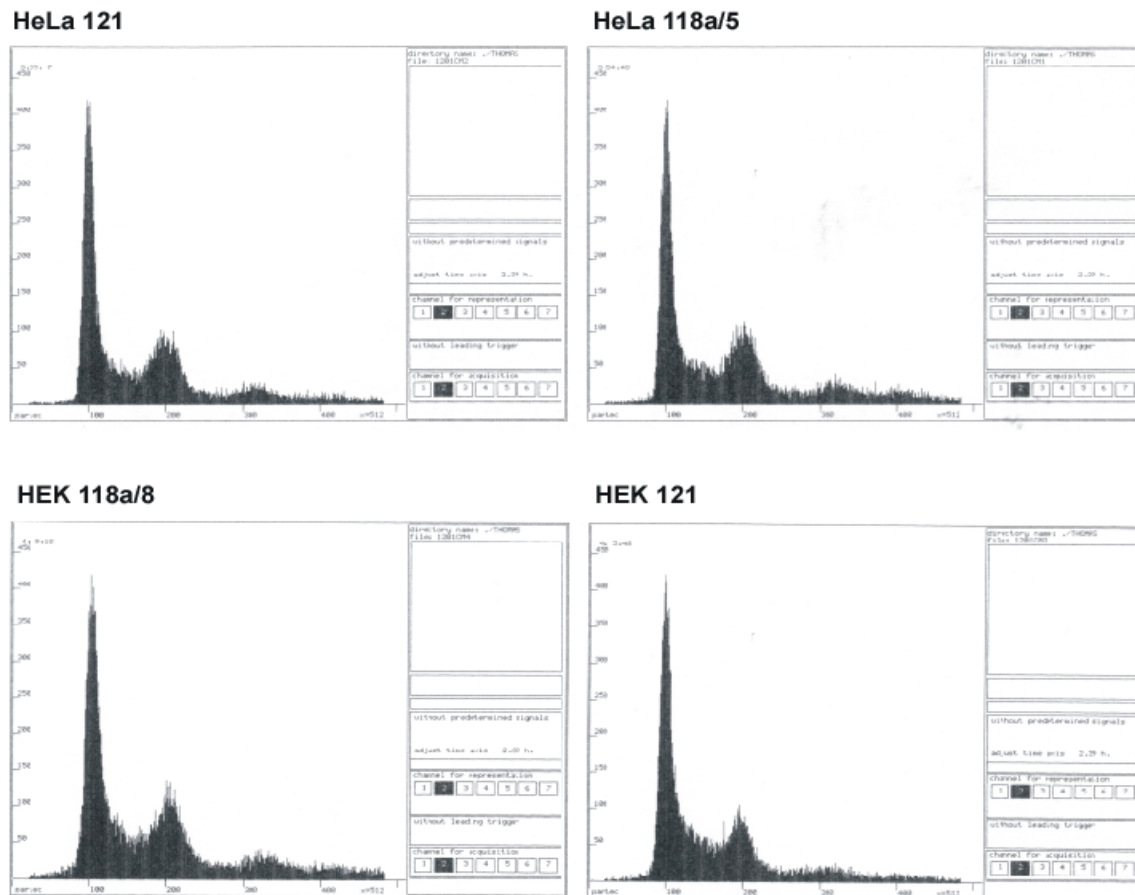


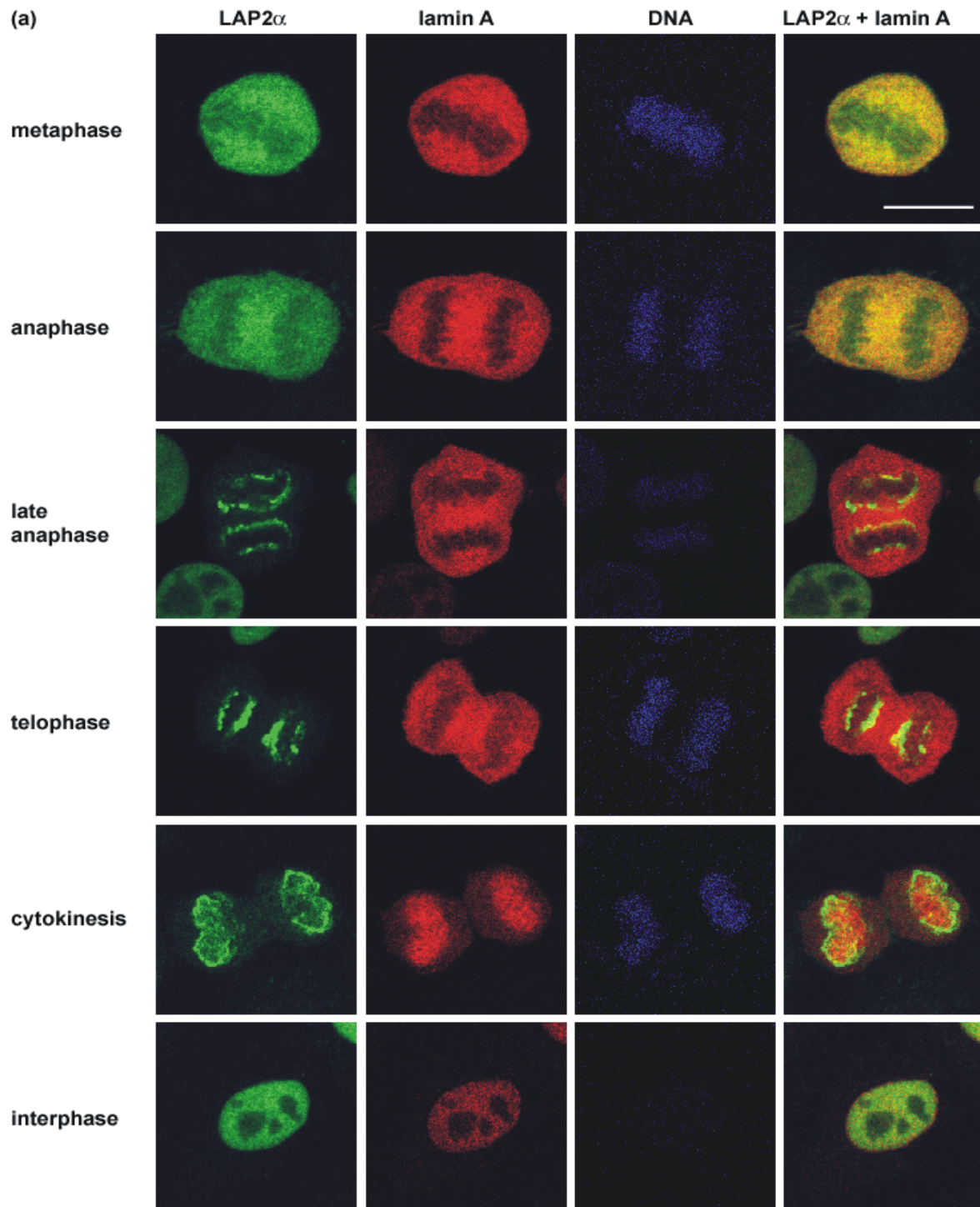
Figure 3-13: FACS analysis of HeLa 118a/5, HeLa 121, HEK 118a/8 and HEK 121.

3.2.6. LAP2 α and lamin A/C localization during cell cycle

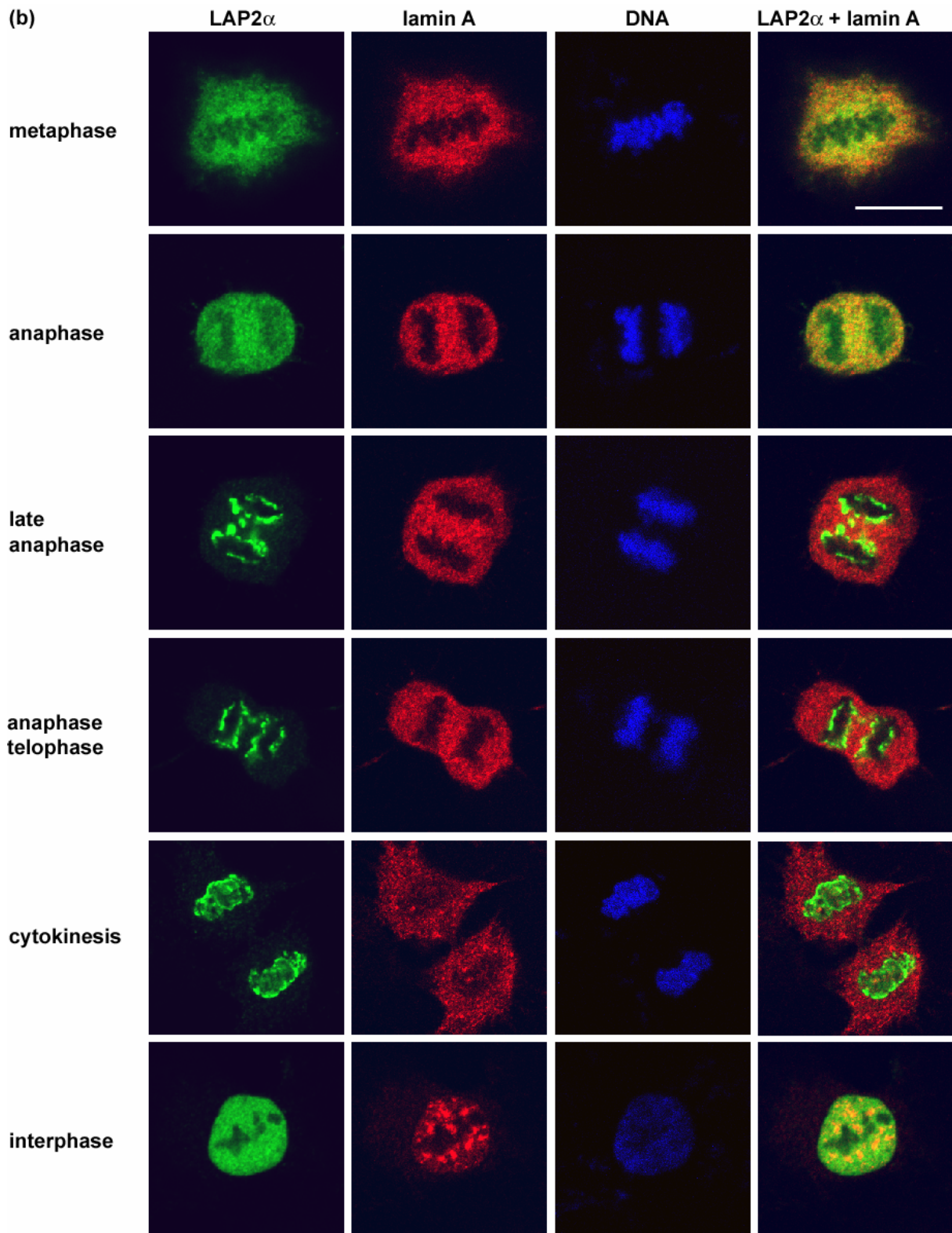
LAP2 α was shown to dissociate from chromatin during NEBD and to relocalize to chromosomes during early stages of nuclear reassembly in late anaphase, before other nuclear envelope proteins like LAP2 β , emerin or lamins accumulate around decondensing chromatin (Dechat et al., 2004). Therefore, LAP2 α seems to be one of the first nucleoskeletal proteins, which associates with chromosomes during nuclear envelope reassembly. These findings suggest a pivotal role of LAP2 α during very early stages of post-mitotic nuclear envelope reassembly. Furthermore, LAP2 α is part of a complex with lamin A/C and Rb (Markiewicz et al., 2002). We wanted to see if markedly reduced amounts of LAP2 α due to RNAi exert an influence on nuclear envelope reformation, or cellular distribution of lamin A/C.

3.2.6.1. wt-localization of LAP2 α and lamin A/C during cell cycle

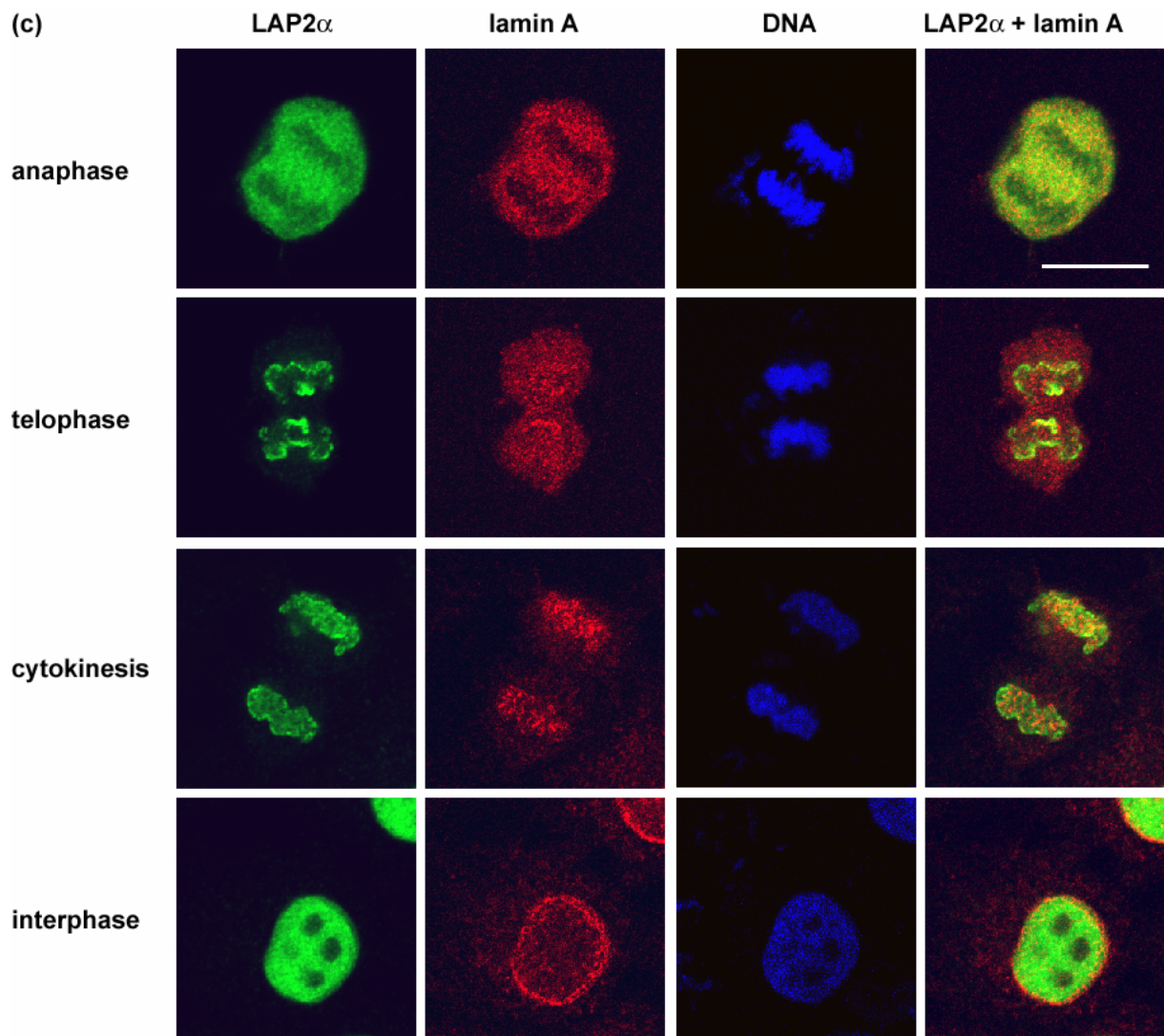
The wt-situation was illustrated by analyzing HeLa 121 control cells at different cell cycle stages in confocal immunofluorescence microscopy. We could confirm the typical LAP2 α localization in this cell line throughout the whole cell cycle (Figure 3-14 (a-e)).



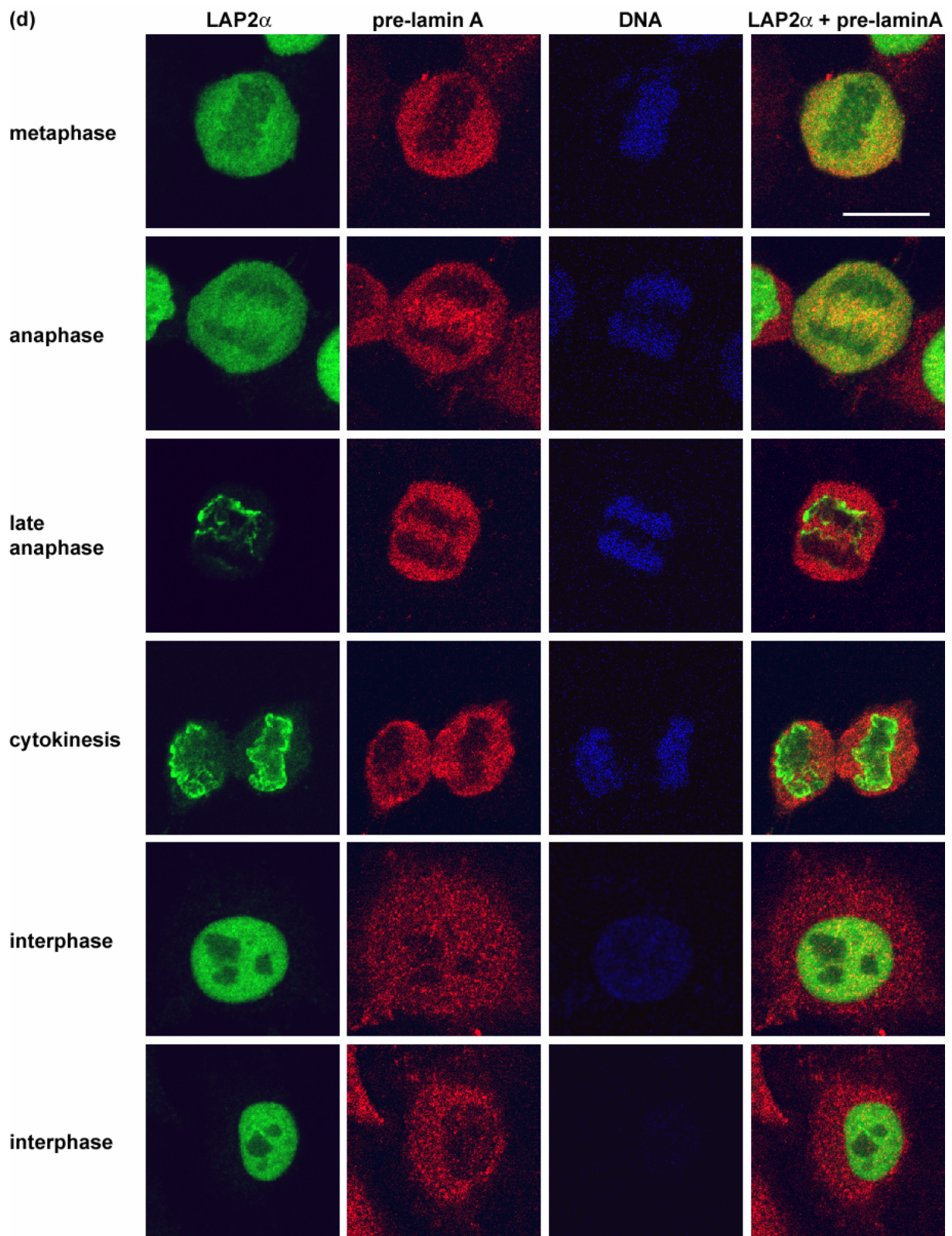
HeLa 121; antibody McKeon to lamin A/C



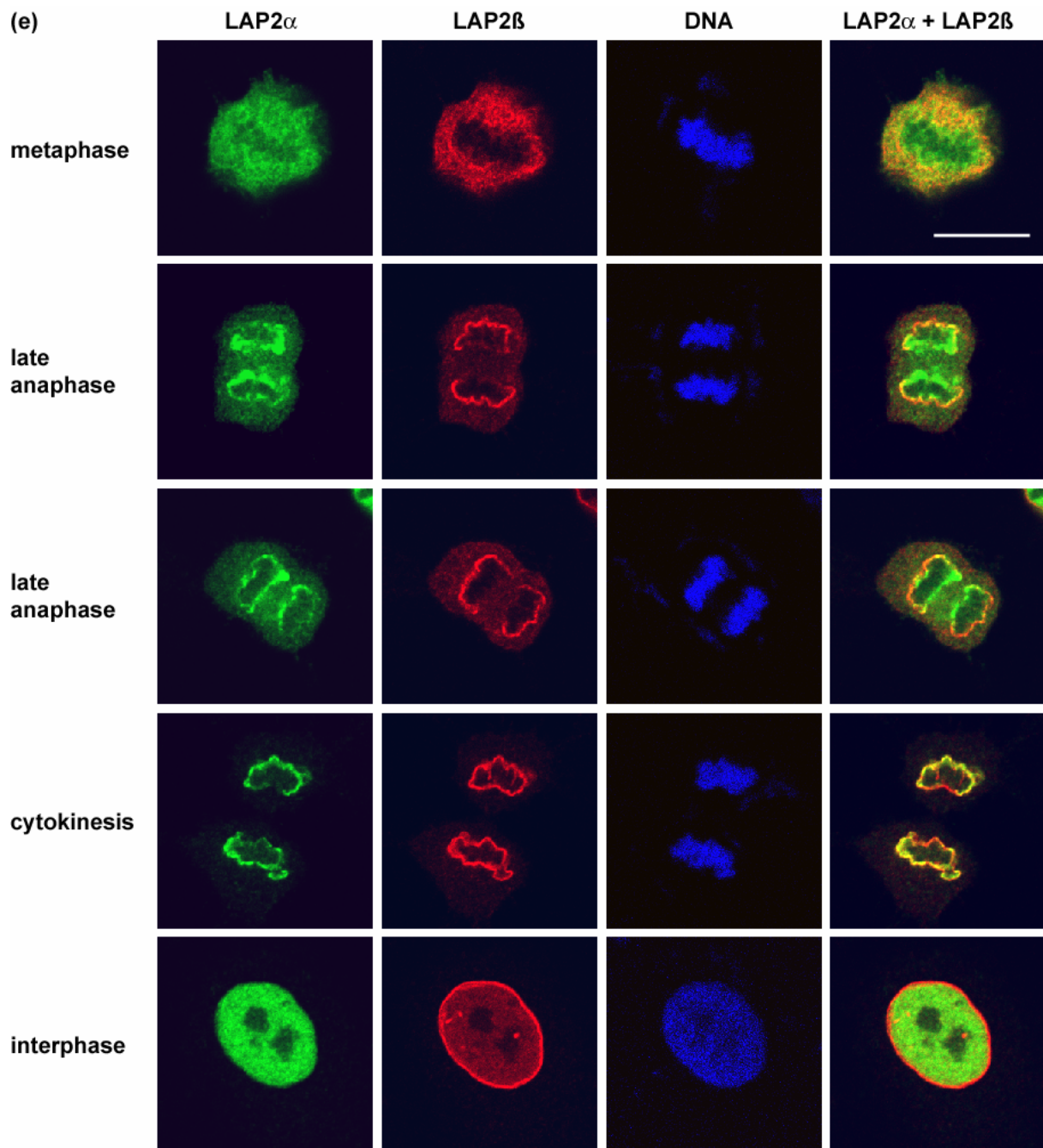
HeLa 121; antibody 2H10 to lamin A/C



HeLa 121; antibody 133A2 to lamin A



HeLa 121; antibody C-20 to pre-lamin A



HeLa 121; antibody 16 to LAP2 β

Figure 3-14: LAP2 α , lamin A/C and LAP2 β localization throughout cell cycle in HeLa 121 control cells. The cells expressing shRNA targeting Firefly Luciferase, were processed for immunofluorescence microscopy using antibody 245-2 to LAP2 and Hoechst dye to stain DNA. The co-stainings were done with: (a) McKeon antibody to lamin A/C, (b) lamin A/C antibody 2H10, (c) lamin A antibody 133A2 (d) pre-lamin A antibody C20 (e) Antibody 16 to stain LAP2 β . Confocal images are shown. Bars, 10 μ m.

During interphase LAP2 α is nucleoplasmic excluding the nucleoli. In metaphase most of it becomes cytoplasmic, excluding condensing chromosomes (Dechat et al., 2004). Interestingly LAP2 α starts to associate with telomeres in anaphase, followed by its accumulation in two

‘core’ structures on chromatin adjacent to the spindle in telophase. During cytokinesis, LAP2 α started to accumulate in the nucleoplasm, where it remained throughout interphase.

As lamins A/C are binding partners of LAP2 α (Dechat et al., 2000), we analyzed their localization during mitosis and post-mitotic nuclear reassembly by immunofluorescence microscopy. Different mitotic stages were identified by LAP2 α localization, which was identical in HeLa 121 and wt cells. Thus, we compared immunofluorescence images using different antibodies to decorate either lamin A/C (McKeon, 2H10), exclusively lamin A (133A2), or pre-lamin A. LAP2 β was used as a control to stain the NE (Figure 3-14). Since the antibodies to lamins A/C stained differently, a reference picture for the respective antibodies was generated in HeLa 121 control cells:

- McKeon antibody stains nucleoplasmic lamins A/C in interphase in proliferating cells (Figure 3-14 (a)). Similar to LAP2 α the nucleoli were excluded, but in the merged image of LAP2 α and lamin A/C, a narrow rim staining became visible, suggesting that this antibody also decorates lamin A/C underneath the inner nuclear membrane. In meta- and anaphase lamin A/C was cytoplasmic, excluding the condensed chromosomes and only partial spatial overlap with core structures was detected. At the end of telophase or during cytokinesis, lamin A/C was translocated to the nuclear interior.
- Antibody 2H10 to lamin A/C labelled large intranuclear speckles or foci in interphase cells (Figure 3-14 (b)). These speckles have been shown to colocalize with RNA splicing factors (Jagatheesan et al., 1999). During meta- and anaphase ab 2H10 also showed a cytoplasmic localization of lamins A/C excluding the condensed chromosomes. Surprisingly this ab showed only weak nucleoplasmic staining of lamins A/C at the end of cytokinesis and still strong cytoplasmic localization. Drawback of ab 2H10 is that it is not exclusively decorating lamins A/C but also other nuclear proteins that have not been identified yet (Vecerova et al., 2004).
- Antibody 133A2 stained a rim at the nuclear periphery in interphase cells (Figure 3-14 (c)). As suspected this antibody recognized lamin A in the cytoplasm during anaphase, excluding the condensed chromosomes. Lamin A stained by 133A2 started to concentrate on the chromosomes during early telophase.
- The last lamin antibody we tested was C20, labeling pre-lamin A (Figure 3-14 (d)). We observed two different stainings in interphase cells: An exclusively diffuse cytoplasmic staining was detectable as well as cells which displayed a significant

- Finally, we performed co-stainings of LAP2 α and LAP2 β (Figure 3-14 (e)). As LAP2 β is anchored within the inner nuclear membrane, we observed a pronounced rim pattern in interphase cells, together with a weak intranuclear staining. In metaphase, LAP2 β was cytoplasmic, excluding the condensing chromosomes. During late anaphase, LAP2 α first locates to the telomeres, before it forms core structures, whereas LAP2 β lines up at the periphery and the outer core region of the chromatin (Dechat et al., 2004). At this stage labelling of the two proteins showed a partial overlap at the outer core region and the periphery. In late telophase and during cytokinesis, both isoforms LAP2 α and LAP2 β enclosed decondensing chromatin.

To summarize, we tested three lamin A antibodies in immunofluorescence and observed three different inner nuclear stainings in interphase cells. An even nucleoplasmic distribution of lamin A/C detected with McKeon antibody, a characteristic speckled pattern of lamin A/C by antibody 2H10, or a rim staining of the nuclear lamina underlying the inner nuclear membrane by lamin A antibody 133A2. During meta- and anaphase they all showed cytoplasmic localization of lamin A, excluding the condensed chromosomes, but they stained different structures of lamin A in reassembling nuclei.

These extensive localization studies in HeLa 121 control cells confirmed former results of LAP2 α , lamin A/C and LAP2 β and interesting antibody-specific differences became evident.

3.2.6.2. Reduced levels of LAP2 α does not alter its cellular localization

We next investigated the distribution of remnant LAP2 α in HeLa 118a/5 cells during the cell cycle (Figure 3-15). For better visualisation of low levels of LAP2 α , laser excitation energy and detector sensitivity were increased. Thus, we got strong cytoplasmic background during nuclear reassembly, which was not seen under normal conditions.

There was no obvious difference to LAP2 α stainings in control cells. The protein was cytoplasmic until anaphase, when it started to translocate to the tips of chromosome ends and the inner core region, directly followed by additional localization to the outer core structure. While wt-HeLa interphase cells showed uniform diffuse distribution of LAP2 α throughout the nucleoplasm, in HeLa 118a/5 LAP2 α appeared in a grainy, spotted staining pattern.

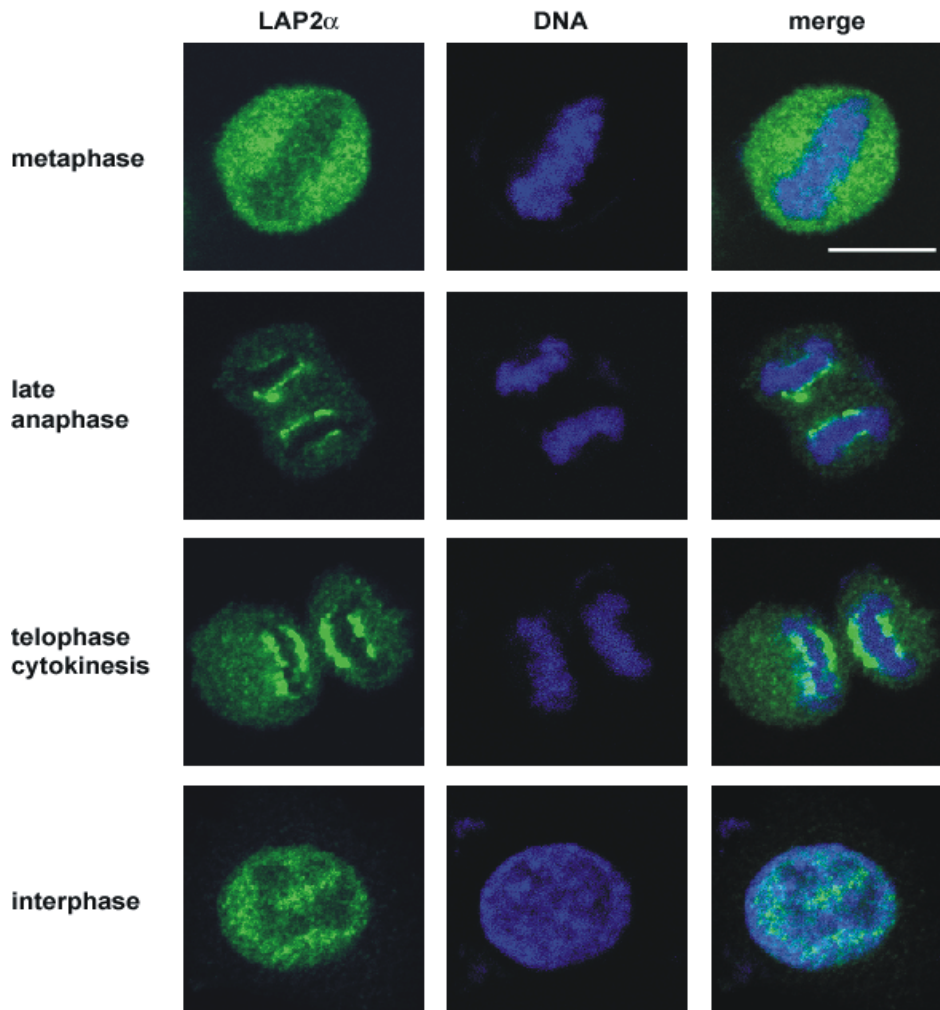


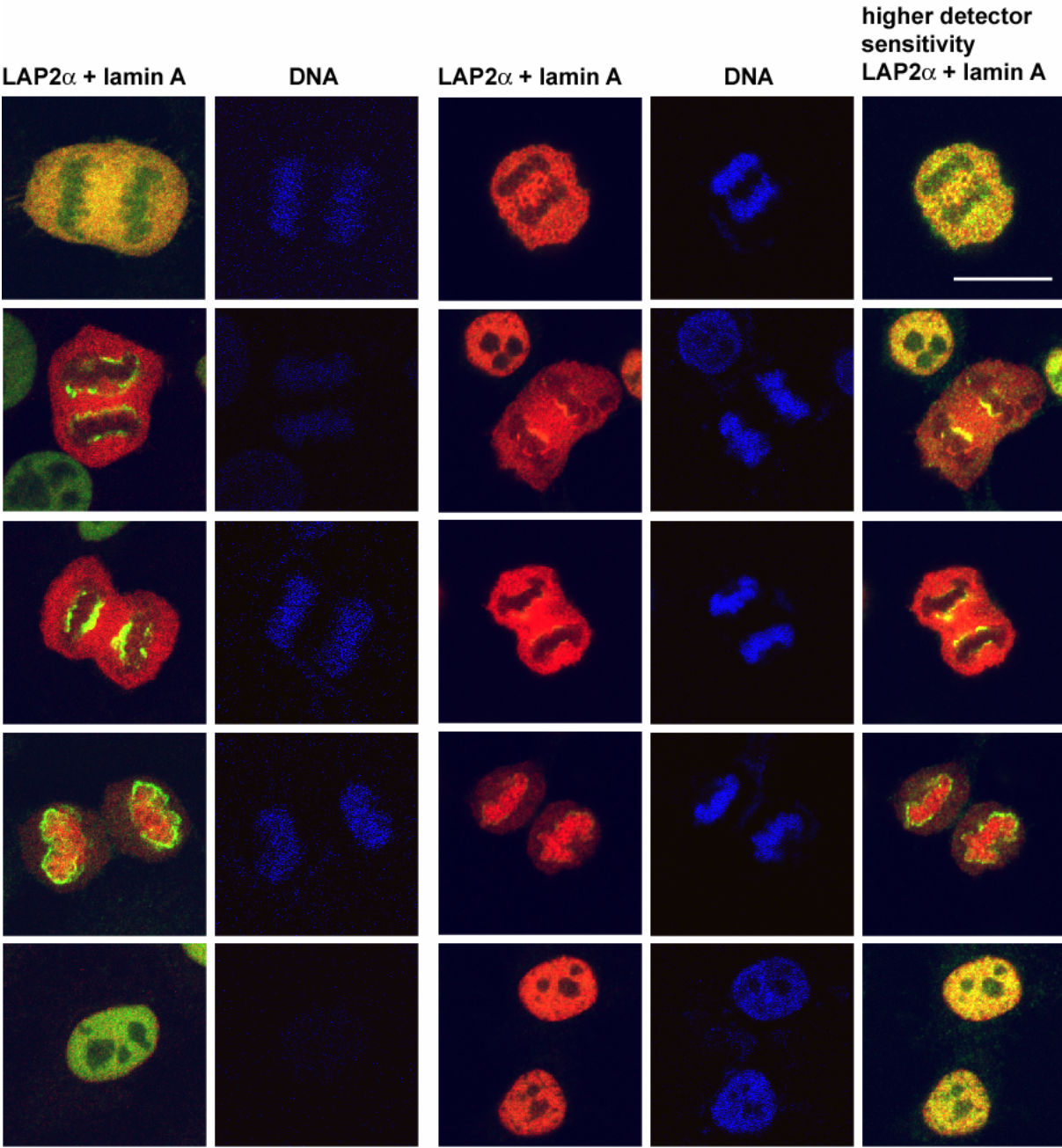
Figure 3-15: LAP2 α distribution during cell cycle in HeLa 118a/5 LAP2 α RNAi cells. Cells were processed for immunofluorescence with ab 245-2 to LAP2 α and Hoechst dye to stain DNA. Confocal images are shown. Bar, 10 μ m. Note that LAP2 α RNAi immunofluorescence images were overexposed to detect the fluorescence signal.

3.2.6.3. LAP2 α RNAi does not affect lamin A/C localization

LAP2 α is thought to cooperate with lamin A/C in anchoring Rb within the nucleus (Markiewicz et al., 2002). We analyzed possible implications of LAP2 α RNAi on lamin A/C localization. We compared LAP2 α / lamin A/C confocal immunofluorescence co-stainings in HeLa 121 and HeLa 118a/5 cells (Figure 3-16).

(a) HeLa 121 (control)

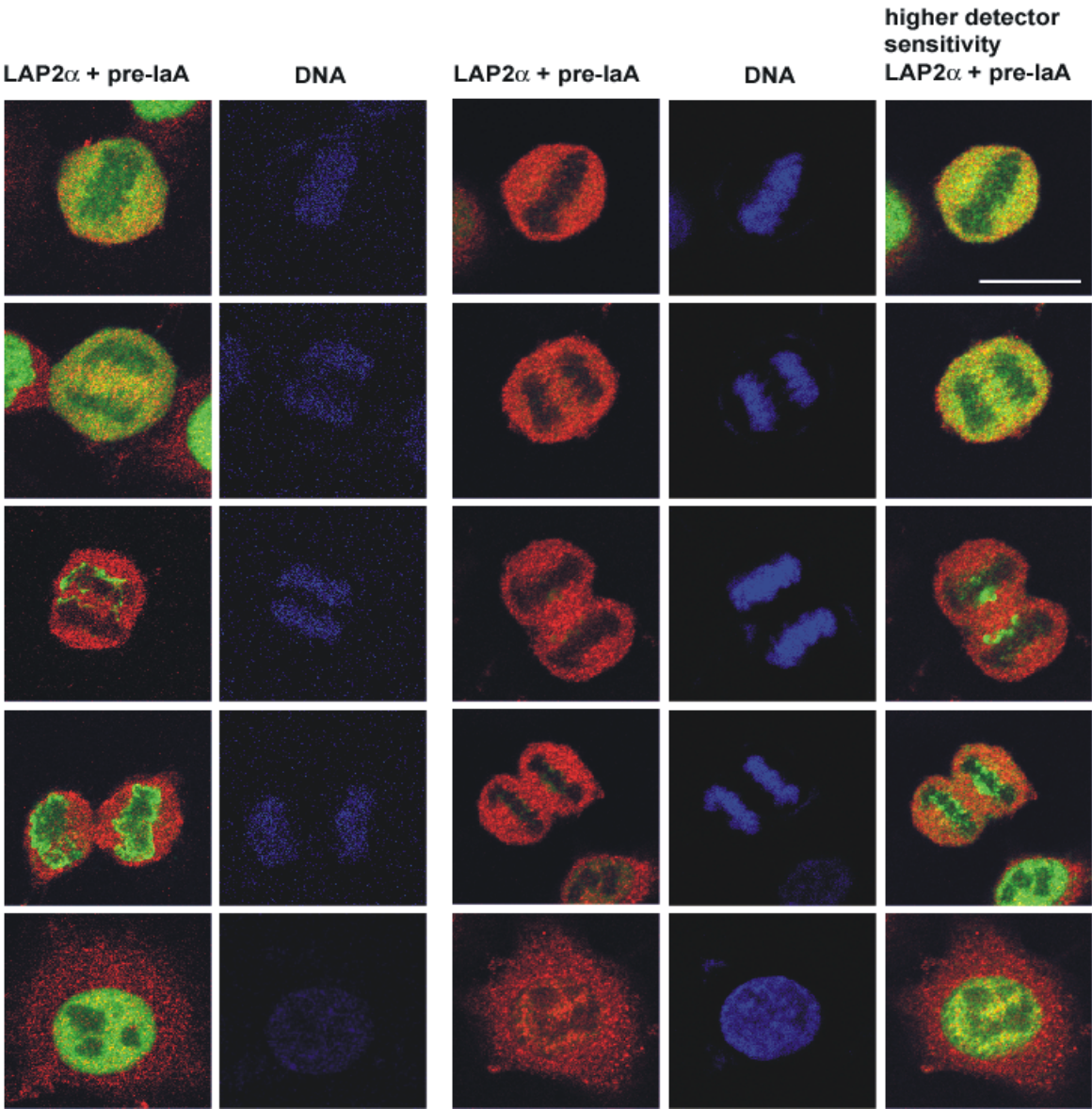
HeLa 118a/5 (LAP2 α RNAi)



Antibodies McKeon to lamin A/C (red) and 245-2 to LAP2 α (green)

(b) HeLa 121 (control)

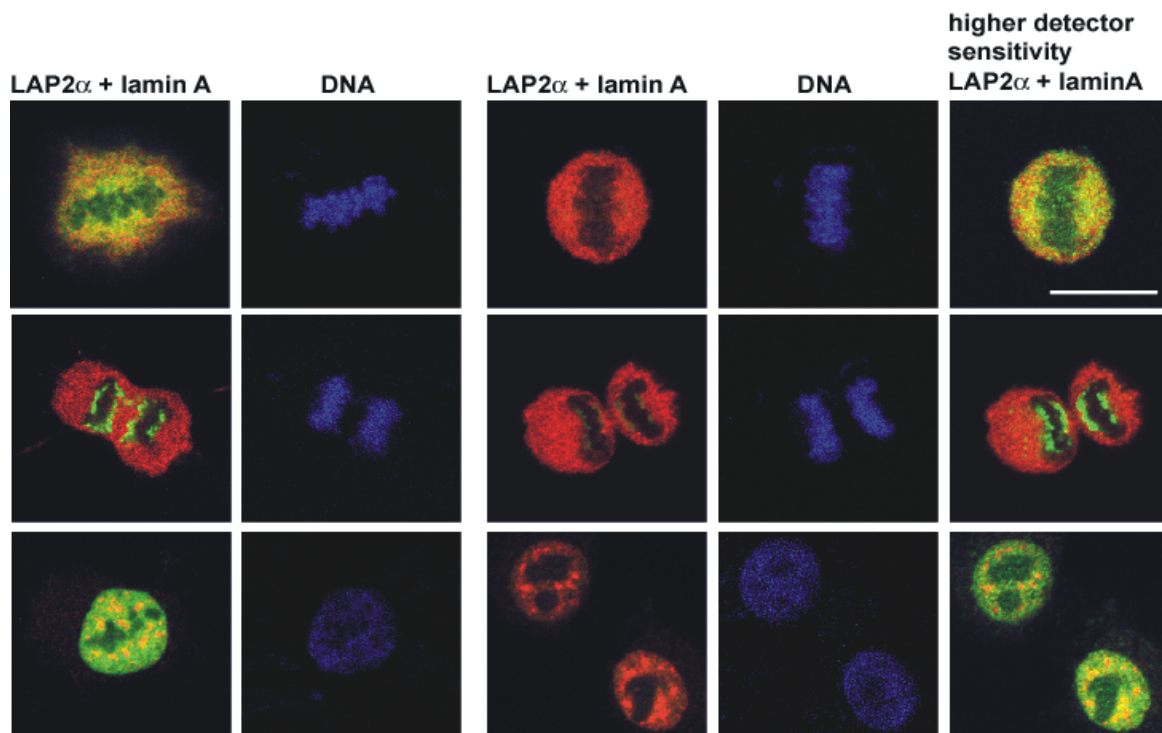
HeLa 118a/5 (LAP2 α RNAi)



Antibodies C-20 to pre-lamin A (red) and 245-2 to LAP2 α (green)

(c) HeLa 121 (control)

HeLa 118a/5 (LAP2 α RNAi)



Antibodies 2H10 to lamin A/C (red) and 245-2 to LAP2 α (green)

Figure 3-16: Comparison of LAP2 α (green) and lamin A (red) localization of HeLa 118a/5 and HeLa 121 cells during cell cycle. Cells were processed for immunofluorescence with ab 245-2 to LAP2 α , McKeon ab to lamins A/C (a), pre-lamin A ab C20 (b), lamins A/C ab 2H10 (c) and Hoechst dye to stain DNA. Confocal images are shown with two detector sensitivities for LAP2 α RNAi cells. Bars, 10 μ m.

As shown before, HeLa 121 and HeLa 118a/5 cells showed normal LAP2 α stainings, which we used for the identification of the different cell cycle stages.

- McKeon antibody yielded a uniform intranuclear lamin A/C pattern in HeLa 118a/5 interphase cells, as well as a lamin A/C redistribution during cell division indistinguishable of control cells (Figure 3-16 (a)).
- Pre-lamin A was cytoplasmic from metaphase to cytokinesis and partially nucleoplasmic in interphase cells, like in the control (Figure 3-16 (b)).
- Similarly, lamin A/C antibody 2H10 labeled large intranuclear speckles in interphase cells and the typical mitotic staining pattern seen in control (Figure 3-16 (c)).

Thus, neither in interphase, nor in mitotic stages, we were able to detect any difference of lamin A localization between HeLa 118a/5 and HeLa 121 cell lines. Therefore, we focused on a short time period after M-phase, to determine whether reduced levels of LAP2 α influence lamin A/C relocation to the nucleus. Three different lamin A/C antibodies (stainings a, b, c)

were used to co-stain lamin A/C and LAP2 α at three time points with defined LAP2 α distribution in HeLa 121 control cells (Figure 3-17).

- The first time point (Figure 3-17 left panel column) shows a strong rim staining of LAP2 α , during early redistribution to the nuclear interior.
- The second time point (Figure 3-17 middle panel column) depicts LAP2 α nearly completely translocated to the nucleoplasm, with only a weak rim staining remaining at the reassembling nuclear envelope.
- The third time point (Figure 3-17 right panel column) indicates even distribution of LAP2 α in the nucleoplasm during interphase.

Lamin A staining of these cells with the three different antibodies revealed the following.

a) Antibody 2H10 (Figure 3-17 (a)), showed lamin A/C relocation to the nucleus after cytokinesis, shortly after LAP2 α started to dissociate from the rim to the nuclear interior. As soon as subfractions of lamin A/C were detectable in the nucleoplasm, they concentrated to speckles, characteristic for this antibody in interphase.

b) In the case of McKeon antibody (Figure 3-17 (b)), we were not able to detect initial stages of lamin A/C relocation. Most lamin A/C was already redistributed to the nuclear interior, when LAP2 α was only partially translocated from the rim into the nucleus.

c) Antibody 133A2 (Figure 3-17 (c)), revealed lamin A evenly distributed throughout the cell, when LAP2 α started to relocate from the rim to the nucleus. We observed a dispersed nuclear staining of lamin A, when LAP2 α was nearly completely translocated to the nuclear interior, but the rim staining, typical for lamin A antibody 133A2 in interphase cells, had not formed yet.

Thus the three antibodies (2H10, McKeon, 133A2) detect different lamin A pools, which varied not only in their localization during interphase but showed also different redistribution kinetics to the nuclear interior during cytokinesis.

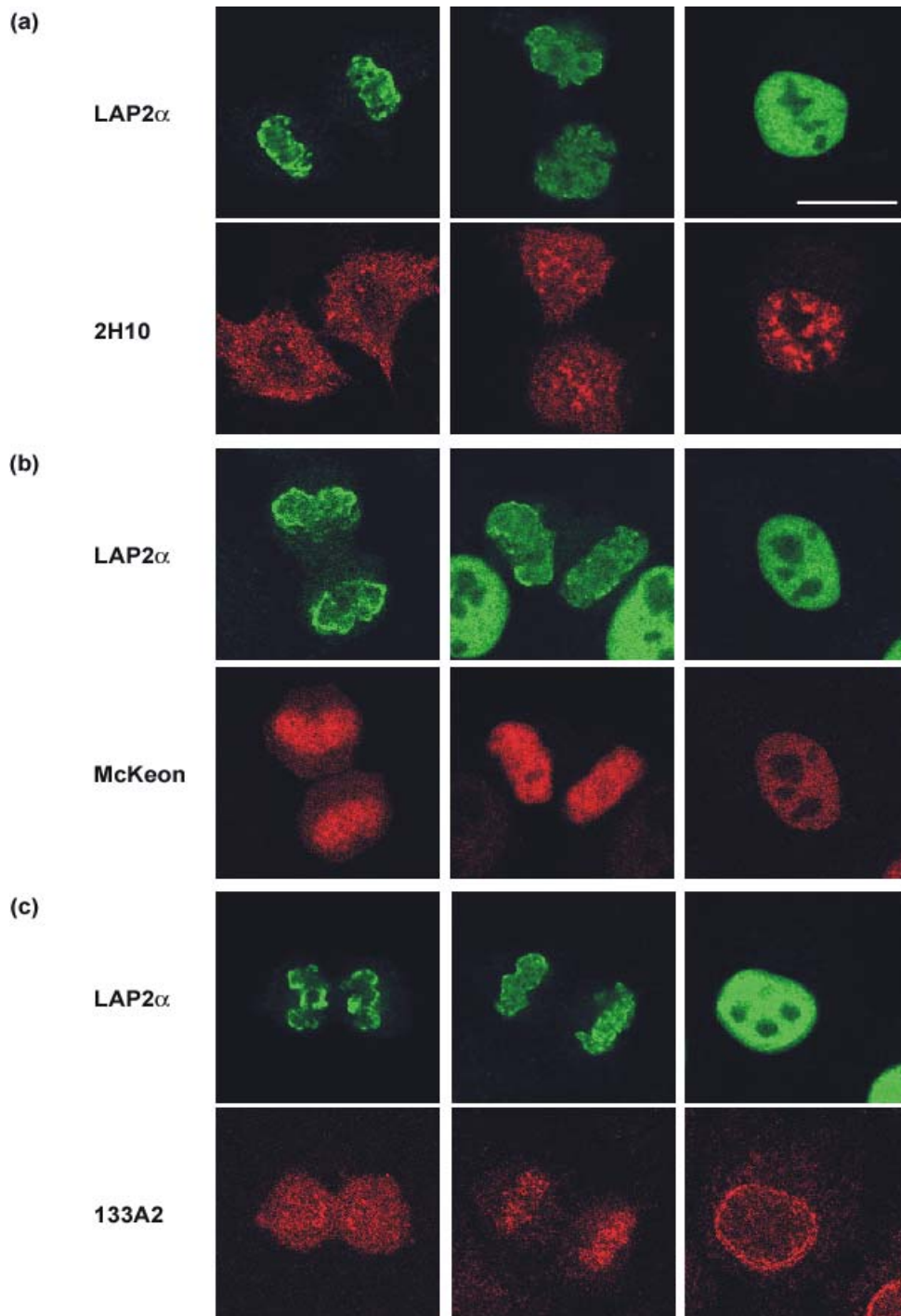


Figure 3-17: Lamin A during the formation of the nuclear envelope in HeLa 121 control cells. Cells were processed for immunofluorescence with ab 245-2 to LAP2 α , lamin A ab 2H10 (a), McKeon ab to lamin A (b) and lamin A antibody 133A2 (c). Confocal images are shown. Bar, 10 μ m.

We next took a closer look at LAP2 α / lamin A/C redistribution from telophase to interphase in LAP2 α -deficient HeLa 118a/5 cells (labeled with McKeon antibody to lamin A/C) (Figure 3-18).

While LAP2 α localized to chromosome tips and core structures during telophase, lamin A/C was still evenly distributed in the cytoplasm (upper panels). When cytokinesis had already started (second row of panels), lamin A/C was still exclusively cytoplasmic. However, at the end of cytokinesis, most of lamin A/C was concentrated inside the reassembling nucleus (panels of row 3 and 4). The lowest panels show lamin A/C completely inside the nucleus, even before LAP2 α was totally translocated to the nucleoplasm.

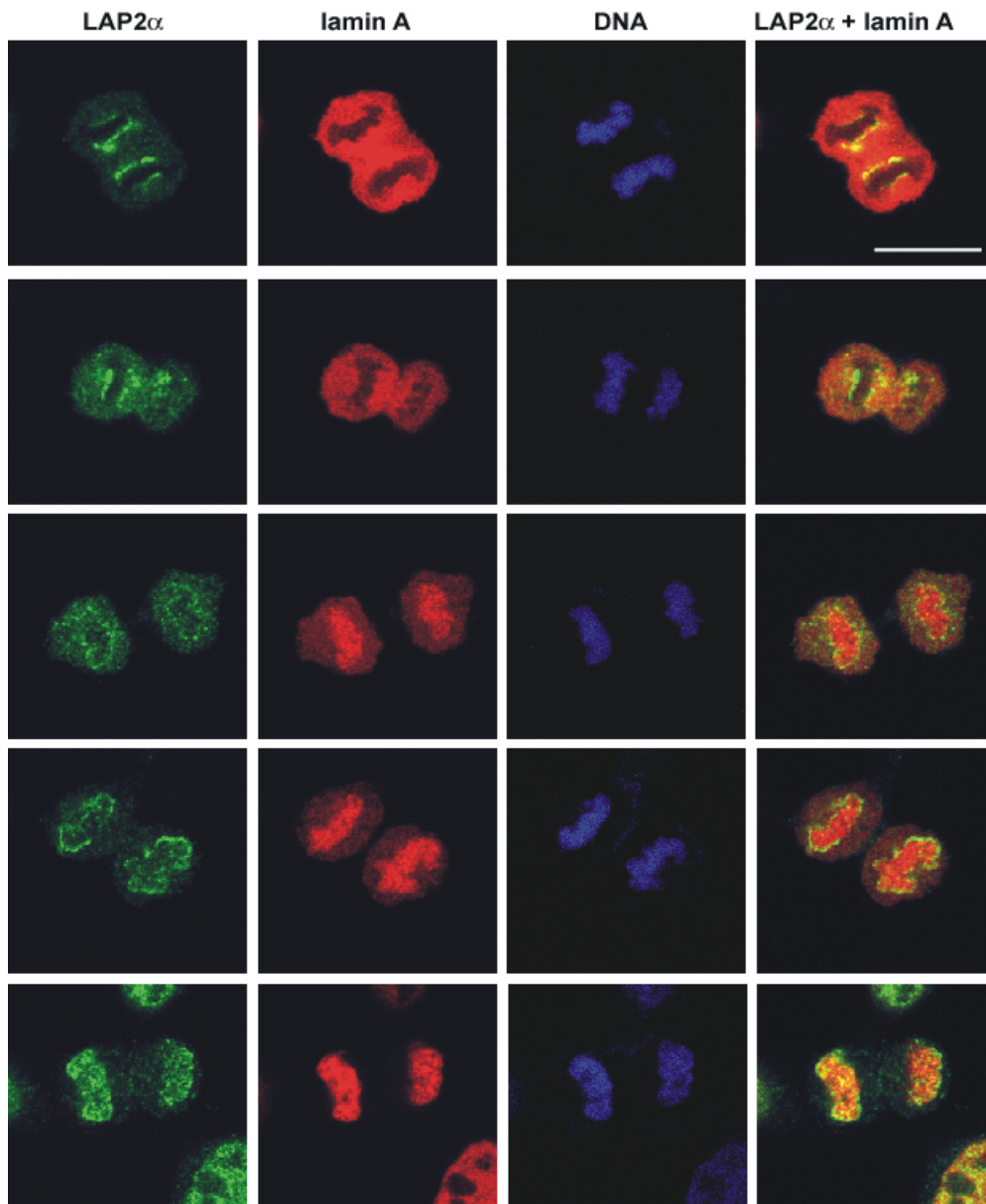


Figure 3-18: LAP2 α and lamin A during formation of the nuclear envelope in HeLa 118a/5 RNAi cells. LAP2 α RNAi cells were processed for immunofluorescence with ab 245-2 to LAP2 α , McKeon ab to lamin A and Hoechst dye to stain DNA. Confocal images are shown. Bar, 10 μ m. Note that LAP2 α RNAi immunofluorescence images were overexposed to detect fluorescence signals.

Since the kinetics of lamin A redistribution during mitosis did not significantly change upon LAP2 α downregulation, we have to conclude that LAP2 α is not required for lamin A localization (as suggested previously) or that the remaining LAP2 α in LAP2 α -downregulated cells is sufficient to regulate lamin A kinetics.

4. DISCUSSION

4.1. Discussion of the Triple-RNAi-Vector system

RNAi based gene silencing has revolutionized biological research as it is an efficient tool for functional protein analysis. The advantages of RNAi are that it is a fast, cheap and also versatile technique, as it can be used in several cell types as well as in vivo. Therefore RNAi can be a competing alternative to transgenic or knock out mice. One problem of functional protein studies in general is the functional redundancy of different groups of proteins, or the existence of alternative pathways transducing the same extracellular signal. As a result, revealing the function of a protein may require inhibition of several proteins activities. Therefore, an important potential application for RNAi is the simultaneous inhibition of multiple genes. In this study we established a vector based RNAi system, which allows to simultaneously knock down up to three target mRNAs to meet this challenge. So far the system proved highly efficient on three ectopically expressed reporters in HEK 293 cells.

The latest effort to knock down multiple genes at once is based on combining RNAi-cassettes, each consisting of a human U6 promoter and encoding an shRNA, by classical cloning. (Jazag et al., 2005). This system proposed a hypothetical limit of >30 RNA-cassettes dependent on the saturation level of the RNAi machinery and stable transfection via a co-expressed selection marker. Compared to the presented Triple-RNAi-Vector, this system proposes an optional number of RNAi constructs within one vector combined with higher labour efforts and less variability in expression vector properties.

Genome-wide loss-of-function analysis (reviewed in Mittal, 2004; Hannon and Rossi, 2004) by RNAi libraries are a powerful technology especially for easily detectable phenotypes, such as apoptosis. Nonetheless this technique bears several limitations: First, insufficient silencing creates false negative results of for example 10-30% in *C. elegans* (Simmer et al., 2003). Second, experimental variability in the efficiency of RNAi makes detailed functionally analysis difficult. We realised these differences for example between pCM3 and pCM8. Both encode the same RNAi constructs against Firefly and Renilla Luciferases, but the efficiency of silencing varied noticeably. Third, unspecific side effects due to high siRNA concentrations could cause false phenotypes.

The Triple-RNAi-Vector system is based on human U6 promoter driven shRNA expression in mammalian cells. It makes use of the MultiSite GatewayTM technology which allows fast shuttling of three RNAi-cassettes from respective Entry vectors into one Destination vector.

This feature makes the Triple-RNAi-Vector highly flexible in combining two or three arbitrary RNAi-cassettes within one plasmid. Furthermore, the properties of the expression vector are variable by making the plasmid of choice as a MultiSite GatewayTM Destination vector. To summarise, the Triple-RNAi-Vector system provides highly flexible, fast and cheap knockdown of up to three genes in mammalian cells and is therefore an ideal tool for detailed functional analysis of proteins and protein complexes.

Future prospects

Which type of endogenous proteins are potential targets?

General considerations on attributes of potential target proteins lead to the conclusion that their half-lives should not be too long. This is because our vector mediates transient gene silencing, which is most pronounced from second to fourth day post transfection. A long half-life of target proteins would weaken the observed silencing effect, because already existing proteins are not affected by RNAi. Furthermore, the lifespan of the two, or three targeted proteins should be about the same length, to obtain the silencing effect at the same time. Proteins with longer half-lives can be silenced by stable transfection, therefore another MultiSite GatewayTM compatible Destination vector encoding a selection marker has to be chosen.

What will happen, if one targets three RNAi constructs at one gene?

This interesting question remains to be answered. Several possibilities are supposable: First, the RNAi induced silencing effect could be additive and thereby especially effective. Second, the RISC complexes could sterically inhibit each other if the target sequences were chosen to near to each other, so that no increased silencing will be observed compared to only one RNAi construct targeting the same gene. Third, the capacity of the RNAi machinery could be saturated and for this reason lose efficiency. Contrary evidence for this hypothesis comes from our preliminary data, that the efficiency of the Triple-RNAi-Vector pCM3 was not affected. Other studies using multiple knockdowns also did not reach the limits of the cellular RNAi machinery (Yu et al., 2003; Jazag et al., 2005). Furthermore, overloading the RNAi machinery may compromise the regulatory function of cellular miRNAs, leading to unspecific side effects. Finally, working at high enzyme (RISC) to substrate (mRNA) ratios is likely to affect the enzyme's specificity and could not only increase silencing of the targeted gene but also result in unspecific silencing (Bridge et al., 2003; Hannon and Rossi, 2004). Rescue experiments can be used to ensure the specificity of an observed effect.

4.2. Discussion of functional LAP2 α analysis

In this study we wanted to reveal a functional implication of LAP2 α on cell cycle control and post-mitotic nuclear reassembly. Therefore, we transiently and stably knocked down LAP2 α by RNAi. Reduced levels of LAP2 α increased cell proliferation in HeLa cells especially under serum starvation conditions, an effect we could not observe in HEK cells. Furthermore, we could not make out an effect of decreased LAP2 α levels on nuclear reassembly.

What are the advantages of stable versus transient RNAi?

To determine whether our RNAi constructs were functional or not we tested several constructs by transient transfection of mammalian cells. 48h after transfection we performed immunoblots of total cell lysates and monitored differences in target protein level. In most cases we were not able to realise a clear decrease in protein quantity. In cell lysates of stably transfected cells the knockdown effect of RNAi was obviously more pronounced. There are three reasons for this effect:

- transfection efficiency
- RNAi efficiency
- protein stability

For example, a transfection efficiency of 40% paired with 50% of RNAi efficiency ended up in a reduction of only 20% of target protein level in total cell lysates of transient transfections. Proteins with long half lives are even less affected. In stably transfected cells, the effect of transfection efficiency is excluded and the variability of RNAi efficiency can be eliminated by single cell cloning. Consequently, RNAi efficiency depends on protein stability, if only threshold levels of target protein remain due to single cell cloning.

How does LAP2 α influence cell cycle control?

It has been shown that LAP2 α together with lamin A/C plays an important role in nuclear anchorage of hypophosphorylated retinoblastoma protein (pRb) (Markiewicz et al., 2002). One function of pRb is to control cell cycle progression in G1-S phase transition by negatively regulating the transcription factor E2F in a phosphorylation dependent manner (Chellappan et al., 1991, Classon and Harlow, 2002). Our data of increased cell proliferation due to decreased LAP2 α levels fit to the hypothesis that LAP2 α influences cell cycle control via E2F activity in an Rb mediated manner. Furthermore, over-expression studies of LAP2 α caused a reduction of cell proliferation in HeLa cells (unpublished data, Andreas Gajewski).

An explanation for the even more increased cell proliferation rate under serum starvation conditions in HeLa cells is that LAP2 α is downregulated when nutrients become scarce in HeLa cells (unpublished data, Nana Naetar). These observations suggest that LAP2 α protein levels in LAP2 α RNAi single cell clones could be further reduced upon serum starvation and thereby pronounce the effect of increased proliferation rates. In line with this suggestion, it has been shown that hypophosphorylated Rb is not anchored in the nucleus in primary skin fibroblasts due to reduced levels of LAP2 α under shortage of nutrients (Markiewicz et al., 2002)

LAP2 α RNAi did not cause a cell cycle effect in HEK cells. We propose that a complex of LAP2 α , lamin A/C and Rb is required for inhibiting E2F activity. Lamins A/C are expressed in a differentiation dependent manner. We found that both are expressed at the mRNA level in HEK cells, but only lamin C seems to get correctly processed to mature proteins. This implies that the proposed hetero-trimeric complex is not functional in HEK cells. Supporting this idea, co-expression of lamin A and LAP2 α in HEK cells reduced endogenous E2F activity by 20-30% (unpublished data, Daniela Dorner).

Furthermore it has been shown that lamins A/C are essential for proper pRb localization (Marciewicz et al., 2002; Johnson et al., 2004) and proteasomal degradation of pRb was found increased in *Lmna*^{-/-} cells (Johnson et al., 2004).

Based on the data known so far, we suggest that nucleoplasmic complexes of LAP2 α and lamins A/C anchor hypophosphorylated pRb to the nucleus in a phosphorylation dependent manner, where it represses E2F activity.

What is the role of LAP2 α in post-mitotic nuclear reassembly?

Previous results indicated that LAP2 α is among the first lamina proteins in post-mitotic nuclear reassembly (Dechat et al., 2004). The unique C-terminus is essential and sufficient for early association of LAP2 α on telomeres of lagging chromosomes during anaphase, followed by further concentration to core structures adjacent to the midspindle and spindle poles (Vlcek et al., 1999; Dechat et al., 2004). Interestingly, BAF, which localizes to the entire chromatin and to the cytoplasm in metaphase, also localizes to telomeric structures before it accumulates at core structures together with LAP2 α . Slightly afterwards a small subfraction of lamin C, emerin and a small amount of LAP2 β relocalize to the core region (Dechat et al., 2004). In vitro nuclear assembly studies have previously shown that C-terminal LAP2 α fragments bind to chromatin, but not to BAF, and inhibit chromatin decondensation as well as assembly of

nuclear membranes and lamin A/C around chromatin (Vlcek et al., 2002). These data indicate an important role of LAP2 α in post-mitotic nuclear reassembly. On the one hand LAP2 α together with BAF may be involved in chromatin organization during decondensation. On the other hand LAP2 α could target other lamina proteins to the chromatin, or directly interact with DNA via its LEM-like domain. As lamins A/C are important nuclear binding partners of LAP2 α , we wanted to determine a potential role of LAP2 α in targeting lamins A/C to the nucleus during early stages of nuclear reassembly. Therefore, we performed co-localization studies of these two proteins in LAP2 α RNAi cells. Our data show that reduced levels of LAP2 α were sufficient for proper post-mitotic nuclear reassembly and had no obvious effect on nuclear shape or lamin A/C localization. According to these results overexpression of the clinical relevant mutated LAP2 α , which showed less binding affinity to lamins A/C *in vitro* (Tayler et al., 2005), did not alter lamin A/C localization. Either low levels of LAP2 α are sufficient to target lamin A/C to the post-mitotic nucleus, or this is the function of another binding partner of lamin A/C.

Conclusively, very small amounts of LAP2 α are essential and sufficient for its role in nuclear reassembly. Perhaps LAP2 α together with an N-terminal binding partner, evidence for this comes from ectopic expression of LAP2 α fragments (Vlcek et al., 2002), fulfills the function, which still has to be determined, during nuclear reassembly.

5. MATERIALS AND METHODS

5.1. Cell biology

5.1.1. Cell Culture

In the present study the human epithelial cervix carcinoma cell line HeLa, the human embryonic kidney cell line HEK 293 and the mouse fibroblast cell line 3T3 F442A were used. Cells were routinely maintained in DMEM (Dulbecco's modified Eagle's Medium) supplemented with 10% fetal calf serum (FCS), 2mM glutamine, 50U/ml penicillin and 50µg/ml streptomycin (all from Gibco-Invitrogen, Carlsbad, CA, USA) at 37°C in a humidified atmosphere containing 8.5% CO₂. Confluent cells were split according to the following protocol: Cells were washed once with PBS, pH 7.4, (Gibco-Invitrogen, Carlsbad, CA, USA) and incubated with 0.5ml trypsin-EDTA / 10cm dish (Nunc, Roskilde, Denmark) (0.25% trypsin + 0.5M EDTA in PBS) for 1-5 minutes at 37°C to detach cells from the plastic surfaces. The cell suspension was resuspended in 4.5ml of culture medium and the respective volume of cell suspension (split ratio 1:3 - 1: 20) was seeded into new cell culture dishes containing culture medium (e.g. 10ml for 10cm dishes).

For freezing, the trypsinized cells were supplemented with 9.5ml culture medium and centrifuged for 3 minutes at 110g (800rpm) in a Heraeus centrifuge (Megafuge 1.0). The cell pellet was resuspended in FCS containing 10% dimethylsulfoxide (DMSO; Fluka, Buchs, Switzerland). Cells were transferred to a cryo tube (Nunc, Roskilde, Denmark) and were slowly cooled down to -80°C in a polystyrene box. For long-term storage cells were transferred to liquid nitrogen containers.

For thawing, frozen cells were incubated at 37°C in a water bath. Thawed cells were transferred to a Falcon tube containing 10ml of culture medium and centrifuged for 3 minutes at 110g (800rpm) to remove residual DMSO followed by resuspension in 5-10ml of fresh culture medium to remove residual DMSO. The cell suspension was transferred to a new 6cm or 10cm cell culture dish and incubated at 37°C.

5.1.2. Transfection of HeLa and HEK 293 cells with lipofectamine 2000

For transfection, HeLa cells or HEK 293 cells were seeded in culture medium without antibiotics and grown to a confluency of 90-95%. In the case of 6-well plates, in total 4µg of plasmid DNA were diluted in 250µl of Opti-MEM medium (Gibco-Invitrogen, Carlsbad, CA, USA). If the cells were transfected with more than one plasmid, the amount of DNA was

distributed asymmetrically (e.g. 2µg RNAi vector; 4x0.5µg different reporter plasmids). In addition, 10µl of lipofectamine 2000 (Invitrogen, Carlsbad, CA, USA) were diluted in 250µl of Opti-MEM medium and incubated for 5 minutes at room temperature. The two dilutions were combined, mixed gently and incubated for 20 minutes at room temperature. Cells were washed once with PBS and covered with 2ml of antibiotic-free culture medium, containing 2% FCS. The lipofectamine-DNA mix was added to the cells while rocking them gently back and forth for mixing. After 3-5h incubation at 37°C, transfection medium was replaced by fresh antibiotic-free culture medium containing 10% FCS. After incubating the cells for 15-24h at 37°C they reached confluency and were replated into larger culture dishes. For immunofluorescence microscopy (see 5.2.3.) the cells were initially seeded on poly-L-lysine (Sigma-Aldrich, St. Louis, Mo, USA) coated glass coverslips (Christine Gröpl, Tulln, Austria) prior transfection. 48h after transfection, the samples were either processed for biochemical protein analyses (Western blot (see 5.2.2.), reporter assays (see 5.2.4.)) or immunofluorescence microscopy (see 5.2.3.).

5.1.3. Cell lines stably expressing shRNA constructs

The plasmids pJG111, pJG112, pJG113, pJG114, pJG116, pJG118, pJG119, pJG120 and pJG121 (see Table 5-5 for sh-oligonucleotides or 5.4.6. for cloning strategy) were chosen for stable expression of shRNA constructs in HEK 293 and HeLa cells. As control we used the pRi 6-1 plasmid, a pTracer with a human U6 promoter, but without an RNAi construct. These vectors express a GFP-Blasticidin resistance chimera gene for selection purpose.

One day after transfection (see 5.1.2.), the cells were split and seeded at about 10% confluency in DMEM selection medium (+ 10% FCS, + 25µg/ml Blasticidin; Invitrogen, Carlsbad, CA, USA). At least half of the medium was exchanged every second day during selection. To passage the stably transfected cells, a Blasticidin concentration of 10µg/ml has proven to be sufficient.

5.1.4. Single cell clones

Stably transfected cell pools (see 5.1.3) were tested by Western Blot (see 5.2.2). Single cell clones were generated out of those cell pools (see below), which showed a strong RNAi effect. The single cell clones were named by the cell type, the number of the plasmid with which the cells were transfected and the number of the obtained clone (e.g. HeLa 118/5).

5.1.4.1. Limited dilution

HEK 293 cells of stable transfected cell pools (see 5.1.2.), expressing one of the following plasmids - pJG111, pJG116, pJG118 - were chosen to obtain single cell clones by limited dilution.

The cells were trypsinized (see 5.1.1.) and two aliquots per plate were counted three times each with a Coulter Counter Z2. In several steps we diluted the cell suspension to two different concentrations of 1 cell/ml and 2.5 cells/ml DMEM supplemented with 10 μ g/ml Blasticidin (Invitrogen, Carlsbad, CA, USA) and 10% FCS. These suspensions were transferred to 96-well plates, 200 μ l per well, by the means of a multichannel pipette (Eppendorf Research pro). After 7 – 10 days the single cell clones were transferred to larger dishes and tested by Western blot (see 5.2.2.).

5.1.4.2. Isolating individual cell colonies

Single cell clones can also be obtained by isolating individual cell colonies. This technique was performed with HeLa cells, expressing either pJG113 or pJG118.

During the selection period for stable transfected cells (see 5.1.3.), resistant cells grew in small colonies, could be isolated with the help of cloning cylinders. First we selected colonies under the microscope and marked their positions on the culture dish. The cloning cylinders were placed on the nearly dry culture dish, surrounding the marked cells colonies. These were detached with 10 μ l of trypsin-EDTA inside the cylinders and resuspended in additional 30 μ l of culture medium, supplemented with 10 μ g/ml Blasticidin (Invitrogen, Carlsbad, CA, USA). 5 μ l of these cell suspensions were diluted into 100 μ l of medium per 96-well. After several days the cell clones were transferred to larger dishes and tested by Western blot (see 5.2.2.).

5.1.5. Growth rate experiments

LAP2 α overexpression experiments showed an inhibitory influence of LAP2 α on cell cycle. To affirm these results, we performed growth rate experiments with LAP2 α RNAi single cell clones (HeLa 118/5 and HEK 118/8; see 5.1.4). As control, we used cell pools of the same cell type, stably transfected with pJG121 (see 5.1.3).

5.1.5.1. Growth rate at full serum

On day zero 5×10^4 HEK 293 or HeLa cells were seeded on each of the fourteen 10cm culture dishes per experiment. Every 24h the cells of two dishes were trypsinized (see 5.1.1.) and the cell number was determined by counting two aliquots per plate, three times each, with a Coulter Z2. Throughout the experiment cells were grown in semi-conditioned medium, which was adjusted every day.

5.1.5.2. Growth rate of serum starved cells

Using a step by step procedure HeLa cells were adapted to low serum growth conditions by reducing FCS down to 2% over a period of two days, followed by reduction to 0.5% FCS for another 20h. 5×10^5 of these cells were seeded on each of the fourteen 10cm dishes. The following seven days cells were counted and culture medium supplemented with 0.5% FCS was adjusted as described above (see 5.1.5.1).

5.2. Biochemistry and Immunology

5.2.1. Preparation of total cell lysates for Western blot analyses

To prepare total cell lysates, proliferating cells were trypsinized (see 5.1.1.) and supplemented with culture medium, followed by 3 minutes of centrifugation at 110g (800rpm) in a Heraeus centrifuge (Megafuge 1.0). The pellet was washed twice in PBS with additional 0.5mM $MgCl_2$ and 0.1mM $CaCl_2$. The pellet was resuspended in a small volume of ice-cold hypotonic buffer ($10\mu l / 10^5$ cells) and incubated for 10 minutes on ice. Subsequently the same volume of 3x SDS PAGE sample buffer was added and the lysate was heated for 5 minutes at $95^\circ C$. The samples were frozen in liquid nitrogen and stored at $-20^\circ C$.

Solutions:	Hypotonic buffer	10mM HEPES pH 7.4 10mM NaCl 5mM $MgCl_2$ 1x Complete EDTA-free protease inhibitor cocktail (added freshly; Roche, Basel, Switzerland)
	3x SDS PAGE sample buffer	186mM Tris-HCl pH 6.8 30% Glycerol

6% SDS
 300mM DTT
 0.1% Bromphenol blue

5.2.2. SDS PAGE and Western blot analyses

For electrophoretic separation of proteins on SDS polyacrylamide gels, the discontinuous buffer system (Laemmli 1970) was used. According to the size of the proteins, resolving gels with different concentrations of acrylamide/bisacrylamide were prepared and overlaid with 4% stacking gels (see Table 5-1).

<i>Concentration of monomer</i>	Resolving gel (4 gels)					Stacking gel (4 gels)
	6.25%	7.5%	10%	12.5%	15%	4%
acrylamide/bisacrylamide	3.75ml	4.5ml	6ml	7.5ml	9ml	1ml
dH ₂ O	9.75ml	9ml	7.5ml	6ml	4.5ml	4ml
Resolving gel buffer	4.5ml	4.5ml	4.5ml	4.5ml	4.5ml	--
Stacking gel buffer	--	--	--	--	--	1.67ml
10% Ammonium persulfate	120μl	120μl	120μl	120μl	120μl	47μl
TEMED	12μl	12μl	12μl	12μl	12μl	8μl

Table 5-1: Composition of resolving and stacking gels for SDS PAGE

Solutions:	Acrylamide/ Bisacrylamide	Acrylamide M-Bis 30% Stock solution for 3% crosslinked acrylamide gels
	Resolving gel buffer	1.5M Tris-HCl pH 8.8 0.4% SDS
	Stacking gel buffer	0.5M Tris-HCl pH 6.8 0.4% SDS

Protein samples in 1x SDS PAGE sample buffer were incubated at 95°C for 5 minutes and 5-15μl were loaded on the gels. For exact size calculation 3-10μl of precision plus protein standard (all blue or unstained; Bio-Rad, Hercules, CA, USA) were loaded in a separate lane. Electrophoretic separation of proteins was performed at 12-30mA per gel in 1xSDS PAGE buffer using the Mini Protean III gel electrophoresis system (Bio-Rad, Hercules, CA, USA). After separation of proteins, gels were either directly stained in Coomassie solution for 1h,

washed with dH₂O, destained in 10% acetic acid over night and again washed with dH₂O or were used for immunoblot analysis.

For immunoblot analysis, proteins were blotted at 400mA for 1h onto a nitrocellulose membrane (pore size 0.2µm; Schleicher&Schuell, Dassel, Germany) in 1x blot buffer using the Mini Trans-blot electrophoretic transfer system from Bio-Rad (Hercules, CA, USA). A positive replica for better evaluation was prepared according to Gotzmann and Gerner, 2000. Membranes were shortly incubated in ponceau solution to stain the protein bands. The background was cleared by washing in dH₂O. A positive replica of the Ponceau stained nitrocellulose was created by simply placing it protein-side up on a sheet of already fixed and developed photo paper. Subsequently the membrane was destained in dH₂O with some drops of NaOH. To prevent unspecific binding of antibodies, membranes were blocked in 5% gelatine in TBS (at least 10ml per blot) for 1h at room temperature or over night at 4°C. After washing twice with TBS, membranes were incubated for one hour at room temperature or over night at 4°C with primary antibodies or antisera diluted in PBST (for dilutions see Table 5-2). Membranes were washed with TBS, TBS high salt and TBS, followed by incubation for one hour at room temperature with either alkaline phosphatase (AP)- or horseradish peroxidase (HRP)-coupled secondary antibodies (for dilution see Table 5-3). After washing 3 times with TBS or TBS high salt, membranes were incubated in AP staining solution until appearance of bands or in case of HRP-coupled secondary antibodies in lumino enhancer/peroxidase solution (1:1) using the SuperSignal ECL detection system (Pierce, Rockford, IL, USA). The membranes were exposed to X-ray films (Kodak X-omat LS or BioMax MR / Light; Kodak, Rochester, NY, USA) for suitable times until the detection of bands.

Solutions:	3x SDS PAGE sample buffer	186mM Tris-HCl pH 6.8 30% Glycerol 6% SDS 300mM DTT 0.1% Bromphenol blue
	1x SDS PAGE buffer	25mM Tris-HCl pH 8.3 192mM Glycin 0.1% SDS
	Coomassie solution	45% Methanol 10% Acetic acid 0.4% Coomassie B-brilliant blue R250
	1x Blot buffer	48mM Tris-HCl pH 9.1 40mM Glycin

Ponceau solution	0.2% Ponceau-S 3% Trichloroacetic acid
TBS	20mM Tris 150mM NaCl
TBS high salt	20mM Tris 500mM NaCl
PBST	0.05% Tween in PBS
AP staining solution	100mM Tris-HCl pH 9.5 100mM NaCl 50mM MgCl ₂ 0.033% Nitroblue tetrazolium (66µl of 50mg/ml NBT in 70% dimethylformamide per 10ml solution) 0.0165% Bromo-chloro-indolylphosphate (33µl of 50mg/ml BCIP in 70% dimethylformamide per 10ml solution)

<i>Antibody</i>	<i>WB dilution</i>	<i>IF dilution</i>	<i>characterization</i>
11/2	---	undiluted	monoclonal mouse antibody to LAP2α , hybridoma supernatant (Dechat et al., 1998)
12	1:1-1:10 in PBST	undiluted	monoclonal mouse antibody to LAP2 , hybridoma supernatant (Dechat et al., 1998)
15-2	1:2 in PBST	undiluted	monoclonal mouse antibody to LAP2α , hybridoma supernatant (Dechat et al., 1998)
245-2	---	1:500 in PBS	polyclonal rabbit antiserum to LAP2α (Vlcek et al., 2002)
16	undiluted	undiluted	monoclonal mouse antibody to LAP2β , hybridoma supernatant (Dechat et al., 1998)
17	---	undiluted	monoclonal mouse antibody to LAP2β , hybridoma supernatant (Dechat et al., 1998)
133A2	1:5000 in PBST	1:100 in PBS	monoclonal mouse antibody to lamin A (Hozak et al., 1995)
McKeon	1:1000 in PBST	1:100 in PBS	monoclonal mouse antibody to lamin A/C , (Loewinger and McKeon 1988)
LA-2H10	---	1:10 in PBS	monoclonal mouse ab to lamin A/C , hybridoma supernatant (Jagatheesan et al. 1999)
C-20	---	1:10 in PBS	polyclonal goat antibody to pre-lamin A (Santa Cruz, Santa Cruz, CA, USA)
MANEM5	1:100 in PBST	1:30 in PBS	monoclonal mouse antibody to emerin (Glenn Morris; North East Wales Institute of Higher Education)
MANEM15	1:50 in PBST	---	monoclonal mouse antibody to emerin (Glenn Morris; North East Wales Institute of Higher Education)
MAN1	1:250 in	---	polyclonal goat antibody to MAN-1

	PBST		(Santa Cruz, Santa Cruz, CA, USA)
Nucleoporin 62	---	1:150 in PBS	monoclonal mouse antibody to Nuclear Pore Complex protein p62 (BD Pharmingen, San Jose, CA, USA)
K371	---	1:100 in PBS	polyclonal rabbit antiserum to SAF-A/B (Romig et al., 1992)
Anti-Luciferase pAb	1:1000 in PBST	1:100 in PBS	polyclonal goat antibody to Firefly Luciferase (Promega, Madison, WI, USA)
Firefly Luciferase	1:1000 in PBST	---	polyclonal rabbit antibody to Firefly Luciferase (Sigma, St. Louis, MO, USA)
Renilla Luciferase	1:1000 in PBST	1:200 in PBS	monoclonal mouse antibody to Renilla Luciferase (Chemicon, Temecula, CA, USA)
β -Galactosidase	1:1000 in PBST	1:1000 in PBS	monoclonal mouse antibody to β-Galactosidase (Promega, Madison, WI, USA)
β -Galactosidase	1:1000 in PBST	---	polyclonal rabbit antibody to β-Galactosidase (Molecular Probes-Invitrogen, Carlsbad, CA, USA)
Anti-GFP	1:2000 in PBST	---	monoclonal mouse antibody to GFP (Roche, Basel, Switzerland)
Anti-Actin	1:200 PBST	---	polyclonal rabbit antibody to actin (Sigma, St. Louis, MO, USA)

Table 5-2: Primary antibodies used for Western blotting and immunofluorescence microscopy

<i>Antibody</i>	<i>Dilution</i>	<i>Characterization</i>
AP anti-rabbit	1:10.000 in PBST	AffiniPure goat anti-rabbit IgG (H+L) AP conjugate (Jackson IR Laboratories, West Grove, PA, USA)
AP anti-mouse	1:5000 in PBST	AffiniPure goat anti-mouse IgG (H+L) AP conjugate (Jackson IR Laboratories, West Grove, PA, USA)
HRP anti-rabbit	1:40.000 in PBST	AffiniPure goat anti-rabbit IgG (H+L) HRP conjugate (Jackson IR Laboratories, West Grove, PA, USA)
HRP anti-mouse	1:10.000 in PBST	AffiniPure goat anti-mouse IgG (H+L) HRP conjugate (Jackson IR Laboratories, West Grove, PA, USA)
HRP anti-goat	1:10.000 in PBST	AffiniPure donkey anti-goat IgG (H+L) HRP conjugate (Jackson IR Laboratories, West Grove, PA, USA)

Table 5-3: Secondary antibodies used for Western blotting

5.2.3. Immunofluorescence microscopy studies

HeLa or HEK 293 cells grown on poly-L-lysine coated glass coverslips (see 5.1.2.) to 70% confluency were washed once with PBS and fixed with 3.7% formaldehyde or 2% p-formaldehyde in PBS for 20 minutes at room temperature. Cells were washed twice with PBS, and incubated in 50mM NH₄Cl in PBS for 5 minutes at room temperature. After two washes with PBS, cells were permeabilized in 0.1% Triton X-100 in PBS for 5 minutes at room temperature. The coverslips were washed twice with PBS and blocked with 0.2% gelatine in PBS for 30-60 minutes at room temperature, followed by incubation with primary antibodies (see Table 5-2) in a humidified chamber for 60 minutes at room temperature. After three washing steps in PBS, the coverslips were incubated with secondary antibodies in PBS (see Table 5-4) likewise. Coverslips were again washed 3 times in PBS and incubated in Hoechst solution (1µg/ml in PBS) for 10 minutes at room temperature to counterstain for DNA. After washing twice with dH₂O and air-drying, coverslips were mounted on microscope slides (Menzel Gläser, Braunschweig, Germany) in Mowiol, dried over night and stored at 4°C in the dark. Confocal images of stained cells were obtained using a ZEISS Axiovert 200M microscope equipped with a ZEISS LSM 510 confocal laser scanning unit.

Solutions:	Mowiol	2.4g Mowiol 4-88 (Hoechst, Frankfurt, Germany) 6g Glycerol 6ml dH ₂ O Incubation for 2h at room temperature Addition of 12ml 0.2M Tris-HCl pH 8.5 Stirring for 10 minutes Heating to 50°C for 10 minutes Centrifugation at 5000xg for 15 minutes Aliquoting of supernatant and storage at -20°C
	Phosphate buffered saline (PBS)	137mM NaCl 2.6mM KCl 8mM Na ₂ HPO ₄ 1.5mM KH ₂ PO ₄ pH 7.4

<i>Antibody</i>	<i>Dilution</i>	<i>Characterization</i>
Texas Red anti-mouse	1:200 in PBS	AffiniPure goat anti-mouse IgG (H+L) TexasRed dye conjugate (Jackson IR Laboratories, West Grove, PA, USA)
Texas Red anti-rabbit	1:200 in PBS	AffiniPure goat anti-rabbit IgG (H+L) TexasRed dye conjugate (Jackson IR Laboratories, West Grove, PA, USA)
Texas Red anti-goat	1:200 in PBS	AffiniPure donkey anti-goat IgG (H+L) TexasRed dye conjugate (Jackson IR Laboratories, West Grove, PA, USA)
Alexa 488 anti-mouse	1:1000 in PBS	goat anti-mouse IgG (H+L) Alexa fluor 488 conjugate (Molecular Probes, Invitrogen, Carlsbad, CA, USA)
Alexa 488 anti-rabbit	1:1000 in PBS	donkey anti-rabbit IgG (H+L) Alexa fluor 488 conjugate (Molecular Probes, Invitrogen, Carlsbad, CA, USA)
Cy3 anti-mouse	1:150 in PBS	donkey anti-mouse Cy3 conjugate
Cy3 anti-goat	1:200 in PBS	donkey anti-goat Cy3 conjugate
Cy5 anti-mouse	1:150 in PBS	donkey anti-mouse Cy5 conjugate
Cy5 anti-rabbit	1:150 in PBS	donkey anti-rabbit Cy5 conjugate

Table 5-4: Secondary antibodies used for immunofluorescence microscopy

5.2.4. Reporter assays

HEK 293 cells were transfected (see 5.1.2.) with a combination of reporter plasmids and corresponding RNAi vectors, to first test the RNAi constructs and then establish the Triple-RNAi-Vector. The following reporter plasmids (Promega, Madison, WI, USA) were used (vector maps see appendix A):

pGL3 for SV40 promoter driven Firefly Luciferase expression

phRL for Thymidine kinase promoter driven Renilla Luciferase expression

pSV β -Gal for SV40 promoter driven β -galactosidase expression

pCAT3 for SV40 promoter driven chloramphenicol acetyltransferase expression

The corresponding single RNAi vectors (MuliSite GatewayTM Entry vectors (Invitrogen's Gateway technology see appendix B)) all contained an RNAi cassette, consisting of a human U6 promoter driving transcription of an shRNA construct (sh-oligonucleotides see 5.4.1.):

pJG177 RNAi target Firefly Luciferase

pJG178 RNAi target Renilla Luciferase

pJG179, pCM4 to pCM7 RNAi target β -galactosidase

Triple-RNAi-vectors cloned out of the single RNAi vectors (see 5.4.7., appendix A):

- pCM3, pCM8 RNAi targeting Firefly Luciferase, Renilla Luciferase and β -galactosidase
- pJG100 control plasmid, identical to pCM3 and pCM8, but without RNAi constructs

5.2.4.1. Preparation of cells for reporter assays

48h after transfection (see 5.1.2.) the cells were collected by centrifugation for 3 minutes at 110g (800rpm) in a Heraeus Megafuge 1.0, washed three times in PBS, and were either aliquoted and/or cell pellets were processed accordingly for the different reporter assays.

5.2.4.2. Luciferase reporter assay

To simultaneously test two independent luciferase enzymatic activities within one sample we chose the Dual-Luciferase Reporter Assay System of Promega (Madison, WI, USA). The cell pellet was lysed for 15 minutes at room temperature in 1xPLB (Passive Lysis Buffer), immediately followed by measurement on a luminometer (Anthos Lucy 3).

Two 20 μ l aliquots of each sample were pipetted into a 96-well plate suitable for luminometric measurement. The luminometer was programmed to first add 100 μ l LAR II to the lysates and shake the reaction mixture for two seconds, before Firefly Luciferase activity was measured for 10 seconds. Addition of 100 μ l Stop&Glow was again followed by two seconds mixing and 10 seconds measurement of Renilla Luciferase activity.

7.2.4.3. β -Galactosidase reporter assay

In a third reporter assay, activities of β -galactosidase were measured spectrophotometrically. The cells were resuspended in 4°C cold lysis buffer and centrifuged for 10 minutes at 16100g (13.200rpm) at 4°C (Eppendorf Centrifuge 5415D). 45 μ l of the supernatant were mixed with 268 μ l 0.1M sodium phosphate solution, 4 μ l 100x Mg solution and 88 μ l ONPG (o-nitrophenyl β -D-galactopyranoside; Sigma-Aldrich, St. Louis, MO, USA). After 30 minutes of incubation at 37°C, the optical density was measured at 420nm with a Hitachi U-2000 spectrophotometer.

Solutions:	lysis buffer	0.25M Tris/HCl pH 7.5 0.5% Triton X-100
	0.1M sodium phosphate solution	16.4ml 0.5M Na ₂ HPO ₄ 9ml 0.2M NaH ₂ PO ₄

	74.6ml H ₂ O
100x Mg solution	0.1M MgCl ₂ 4.5M β-Mercaptoethanol
1x ONPG	4mg/ml ONPG (Sigma-Aldrich, St.Louis, MO, USA) in 0.1M sodium phosphate solution (pH 7.5)

5.2.4.4. CAT enzyme assay

As an independent reporter system for normalization of transfections in a triple RNAi experiment we used the CAT (Chloramphenicol Acetyltransferase) Enzyme Assay System of Promega (Madison, WI, USA). After 15 minutes of incubation in 1x Reporter Lysis Buffer at room temperature, the samples were placed on ice and vortexed for 10-15 seconds. The lysates were heated to 60°C (Eppendorf Thermomixer compact) for 10 minutes and centrifuged (Eppendorf Centrifuge 5415C) for 2 minutes. Each supernatant was used for two independent reaction mixtures, each containing:

90μl	cell extract
1.5μl	[¹⁴ C] Chloramphenicol (0.1mCi/ml) (Moravek Biochemicals, Brea, CA, USA)
5μl	n-Butyryl CoA
28.5μl	dH ₂ O

The reaction mixture was incubated for 75 minutes at 37°C, briefly spun and mixed with 300μl of mixed Xylenes (Aldrich). After 30 seconds of vortexing, the phases were separated by three minutes of centrifugation at 16000g. The upper, organic, phase was mixed with 100μl of 0.25M Tris/HCl (pH 8.0) by vortexing and again separated by centrifugation. 200μl of the xylene phase were mixed with scintillation fluid (Ready Safe; Beckman Coulter, Fullerton, CA, USA) and radioactivity was measured with a liquid scintillation analyzer (Packard 2000CA).

5.2.4.5. Normalization, Interpretation

Two aliquots of each sample were measured to calculate an average value. To determine the efficiency of RNAi constructs, we correlated reporter enzyme activities of co-transfections of reporter plasmids with either RNAi vectors or control vectors (identical RNAi vectors without an inserted sh-oligonucleotide). The reporter activity of control transfection was set to 100%. Different transfections were normalized by the use of an independent reporter assay (e.g. CAT enzyme assay) and standard deviations were calculated from the differences in RNAi efficiency of repeated transfections.

Solutions:	Lysis buffer	1/5 <u>Phosphate buffer</u> 100mM NaCl 1mM Dithiothreitol (DTT) 1/50 50x Protease inhibitor mix
	Phosphate buffer	0.5M NaH ₂ PO ₄ (pH 7)

5.3.5. Miniprep DNA purification

We purified plasmid DNA from bacterial cultures with the Wizard Plus Miniprep DNA Purification System of Promega (Madison, WI, USA) according to manufacturer's instruction. In brief, 1.5ml of an over night culture were centrifuged 3 minutes at 2300g (5000rpm, Eppendorf Centrifuge 5415D). The pellet was resuspended in 250µl of resuspension solution. The addition of 250µl of cell lysis solution was followed by inverting the tube four times. After addition of 250µl of neutralization solution the lysate was again mixed by inverting the tube. During centrifugation at 15700g (13000rpm), the Minicolumn/syringe barrel assembly was fixed on a vacuum manifold and filled with 1ml of resuspended resin. The supernatant of the lysate was transferred to the column and vacuum was applied until the liquid was sucked out of the column. 2ml of wash solution (95% ethanol) were added and the column was dried by applying vacuum. The Minicolumn was transferred to a microtube and centrifuged for two minutes at full speed (15700g / 13000rpm), to remove residual wash solution. Afterwards the Minicolumn was transferred to a new collection tube, 50µl of ddH₂O were added and after one minute of incubation, the dissolved plasmid DNA was eluted by 20 seconds of centrifugation.

5.3.6. Midiprep DNA purification

To purify bigger amounts of plasmid DNA of bacterial cultures, we used the JETstar Plasmid Midi Kit (Genomed, Löhne, Germany). Therefore, we equilibrated the purification column with 10ml of solution E4 and centrifuged 100ml of over night culture for 3 minutes at 3000g (4000rpm) in a Heraeus Megafuge 1.0R. The bacterial pellet (which can alternatively be stored at -20°C without loss in efficiency) was resuspended in 4ml of RNase containing solution E1. After addition of 4ml of solution E2, the tube was inverted 10 times and incubated for 5 minutes at room temperature. To stop cell lysis, 4ml of neutralizing solution E3 were added and the tube was again inverted 10 times. The lysate was centrifuged for 15 minutes at 3000g (4000rpm) and the supernatant was transferred to the equilibrated column, which flows by gravity. The dry column was washed with 20ml of solution E5, followed by elution of the DNA with 5ml of solution E6. 3.5ml of isopropanol were mixed to the DNA

containing solution, which was centrifuged for 30 minutes at 13400g (9000rpm) and 4°C (pre-cooled HB-4 rotor, Sorvall centrifuge RC5C). The pellet was washed with 5ml of 70% ethanol and centrifuged again, this time for 5 minutes. The opaque DNA pellet was air dried and was resolved in up to 100µl of ddH₂O. The DNA concentration of an 1:100 aqueous dilution was measured spectrophotometrically at 260nm.

5.3.7. DNA restriction digest

reaction mixture: 2µl of recommended 10x reaction buffer
 0.5-1µg DNA (e.g. 5µl miniprep)
 0.3µl of each restriction enzyme
 ddH₂O to a final volume of 20µl

First 10x reaction buffer was diluted in ddH₂O, than the DNA sample was mixed to the solution. Finally the reaction was started by the addition of restriction enzyme, followed by 1-3h of incubation at 37°C.

For preparative digestion of DNA (up to 10µg) it is useful to choose a bigger overall volume (up to 100µl), to incubate for a longer time (e.g. over night) and to use more restriction enzyme (the amount of glycerol should not exceed 10%). Digested DNA was stored at 4°C, for long term storage it was kept on -20°C.

5.3.8. DNA agarose gel electrophoresis

Agarose (0.8% to 2%; Sigma, St. Louis, MO, USA) was suspended in 1x TAE buffer and dissolved by boiling in the microwave. The solution was cooled down to about 60°C and ethidiumbromide (0.01 mg/ml) was added prior to pouring the gel. The gel was overlaid with 1x TAE and the samples were mixed with 1/10 volume of 10x DNA loading buffer, before loaded on the gel together with 1µg of a DNA marker (1Kb Plus, Invitrogen). Gels were run for 1-2h at 70-110V in 1x TAE buffer and DNA bands were detected by UV light (UV Transilluminator, UVP).

Solutions:	1x TAE buffer	40mM Tris acetate pH 8 1mM EDTA pH 8
	10x DNA loading buffer	10mM Na ₃ PO ₄ pH 6.7 50% Glycerol 0.1% Bromphenol blue

5.3.9. Elution of DNA fragments from agarose gel

To elute DNA from agarose gels, we used the QIAquick Gel Extraction Kit (Qiagen, Hilden, Germany). After electrophoresis, the desired band was cut out of the gel and weighed. The gel was dissolved in a threefold of buffer QG (100mg gel = 300µl buffer) by incubation for 10 minutes at 50°C (Eppendorf Thermomixer compact). The sample was applied to a spin column, which was placed in a microtube. The columns were centrifuged at 15700g (14.000rpm) for one minute (Eppendorf Centrifuge 5415D) and the flow-through was discarded. 750µl of buffer PE were added to the column and 2-5 minutes of incubation were followed by a second centrifugation step. Again the flow-through was discarded and the column was centrifuged again to remove residual ethanol from buffer PE. The column was placed into a new tube and incubated for one minute with 30µl of ddH₂O. Afterwards the dissolved DNA was eluted by centrifugation at top speed. The dissolved DNA fragment was stored at -20°C, or for short term storage at 4°C.

5.3.10. Dephosphorylation of DNA fragments

To prevent religation of a once digested vector backbone during ligation with an insert, we performed dephosphorylation of the linearized plasmid.

An aqueous solution of a DNA fragment, not exceeding 5µg of DNA, was mixed with 10µl of CIP buffer (Roche, Basel, Switzerland) and diluted with ddH₂O to 97.5 µl. 2.5 µl of CIP (calf intestinal phosphatase; Roche, Basel, Switzerland) were added, the mixture was vortexed and spun down (Eppendorf Centrifuge 5415D), followed by incubation for 30 minutes at 37°C (Eppendorf Thermomixer compact). Further 2.5µl of CIP were added and the solution was incubated for 45 minutes at 55°C. Afterwards 2.5µl of 20% SDS, 1µl of 0.5M EDTA (pH 8.0) and 0.5µl of proteinase K [20mg/ml] (Invitrogen, Carlsbad, CA, USA) were added and the mixture was again vortexed, spun down and incubated for 30 minutes at 37°C. The solution was diluted with 100µl of ddH₂O and extracted with 200µl of PCI (25x phenol, 24x chloroform, 1x isoamyl alcohol). The aqueous phase was collected and the organic phase was re-extracted with 200µl of ddH₂O. The DNA collected in the aqueous phases was precipitated with ethanol to achieve a higher DNA concentration.

5.3.11. Ethanol precipitation of DNA

To concentrate DNA samples or to clean it from bacterial remnants, we precipitated DNA with ethanol. Therefore, we mixed an aqueous solution of DNA with half the volume of 7.5M ammonium acetate or 1/10 volume of 2.5M sodium acetate. 2.5 volumes of ethanol were

added and the mixture was vortexed vigorously. 15 minutes to 1h of incubation at -20°C were followed by centrifugation at 15700g (13.000rpm) for 10 – 20 minutes (Eppendorf Centrifuge 5415D). The pellet was washed with 70% ethanol, centrifuged for another 10 minutes and dried at room temperature. Finally the DNA was resolved in a small volume of ddH₂O.

5.3.12. DNA ligation

To ligate DNA, we mixed the aqueous solutions of a digested vector-backbone from gel-elution with 2µl of 10x ligase buffer (Roche, Basel, Switzerland). In most cases, a surplus of smaller DNA fragments as annealed oligonucleotides (see 5.4.2), or a gel eluted insert (see 5.3.9) after restriction digest (see 5.3.7), or PCR (see 5.4.4) was added and the volume was adjusted to 19µl with ddH₂O. Finally 1µl of T4 DNA Ligase (Roche, Basel, Switzerland) was added to start the ligation. The reaction was either incubated at room temperature for three hours, at 16°C over night, or at 4°C over the weekend.

5.3.13. Zero Blunt TOPO PCR cloning

As normal ligation did not work on a blunt-end PCR product (see 5.4.4.), we decided to try the Zero Blunt TOPO PCR cloning of Invitrogen (Carlsbad, CA, USA). The reaction mixture consisted of: 4.5µl of PCR product eluted from agarose gel (see 5.3.9.), 1µl of salt solution and 0.5µl of linearized pCR-Blunt II-TOPO vector (with covalently bound and activated topoisomerase I). The reaction was incubated at room temperature for 15 minutes and cooled on ice. Half of the reaction mixture was transformed (see 5.3.2.) into *E.Coli* DB 3.1, the other 3µl to *E.Coli* TOP 10F'.

5.3.14. Poly(A⁺) mRNA isolation

We made use of the mRNA isolation kit from Roche (Basel, Switzerland) to prepare mRNAs from HeLa, HEK 293 and 3T3 F442A cells. The cells were trypsinized, centrifuged and the cell pellet was washed two times in ice cold PBS. 1.5ml of lysis buffer were added to about 10⁷ cells, which were sheared mechanically by passing through a 21 gauge needle (Braun, Melsungen, Germany). Streptavidin magnetic particles were resuspended and 150µl were transferred to a new tube. They were magnetically separated from the storage buffer and washed once in 250µl of lysis buffer, which was entirely removed afterwards. 1.5µl of biotin-labelled oligo (dT)₂₀ probe were pipetted to the lysate and the magnetic particles were resuspended in the mixture. The sample was incubated for 5 minutes at 37°C to immobilize the mRNA via its hybridised biotin-labelled oligonucleotides onto the magnetic particles.

These were magnetically separated and washed three times each with 250µl of washing buffer. After the washing buffer was removed quantitatively, the particles were resuspended in 25µl of RNase-free water. To elute the mRNA from the particles, the sample was incubated for 2 minutes at 65°C, the particles were separated and the supernatant was transferred to a new tube. The mRNA sample was stored on -20°C, for longterm storage on -80°C.

5.3.15. cDNA synthesis

cDNA synthesis was performed with the SuperScript™ III First-Strand Synthesis System for RT-PCR from Invitrogen (Carlsbad, CA, USA). 12µl of poly(A⁺) mRNA (see 5.3.14.) were mixed with 1.5µl of 50µM oligo (dT)₂₀ primer and 1.5µl of 10mM dNTP mix. The sample was incubated at 65°C for five minutes, followed by incubation on ice for at least one minute. In the meantime, a cDNA synthesis mix consisting of 3µl of 10xRT buffer, 6µl of 25mM MgCl₂, 3µl of 0.1M DTT, 1.5µl of RNaseOUT (40 U/µl) and 1.5µl of SuperScript™ III reverse transcriptase (200 U/µl) per sample was prepared. 15µl of cDNA synthesis mix were added to each RNA/primer mixture. The tube was gently mixed and shortly spinned. The reaction was incubated at 50°C for 50 minutes and terminated at 85°C for five minutes. The mixture was cooled on ice and spinned down, followed by addition of 1.5µl of RNaseH and incubation at 37°C for 20 minutes. The cDNA samples were directly used for RT-PCR (see 5.3.16.), the remaining samples were stored at -20°C.

5.3.16. RT-PCR

For expression analyses of LAP2 isoforms in different human and murine tissues, as well as during differentiation of murine embryonic stem cells to cardiomyocytes (cDNAs generated by Martina Stary), cDNAs (see 5.3.15.) generated from poly(A)⁺ mRNAs (see 5.3.14.) were normalized based on GAPDH (human and mouse) and RhoA (mouse) expression levels. 10µl of normalized cDNAs were supplemented with 30pmol of forward and reverse primers specific for LAP2β or GAPDH, or RhoA and ddH₂O to a final volume of 25µl. The sample was heated to 95°C for five minutes, cooled on ice and spinned in an Eppendorf Centrifuge 5415D. Finally puReTaq ready-to-go PCR beads (Amersham Biosciences, Little Calfont, Buckinghamshire, UK) were added and PCR was performed using a Biometra T3 thermocycler system.

The following primers and PCR parameters were used:

Primers:

LAP2 β :

Forward primer:

LAP2com_hm1 5' – GTG GGA ACA ACC AGG AAG CTA TAT GA – 3'

Reverse primer:

LAP br_hm1 5' – CTC CCA CTT CAG CTC TTG TCA ATG – 3'

GAPDH:

Forward primer:

GAPmh1: 5' – CATCACCATCTTCCAGGAGCGA – 3'

Reverse primer:

GAPmh2: 5' – CCTGCTTCACCACCTTCTTGAT – 3'

RhoA:

Forward primer:

Rho1: 5' – GTGGAATTC-GCCTTGCATCTGAGAAGT – 3'

Reverse primer:

Rho2: 5' – CACGAATTC-AATTAACCGCATGAGGCT – 3'

PCR parameters:

2 cycles	95°C	5min
	64°C	1min 10sec
	72°C	4min
2 cycles	95°C	50sec
	62°C	1min
	72°C	3min
32 cycles	95°C	45sec
	60°C	55sec
	72°C	2min 10sec
once	72°C	10min
hold	4°C	

5.4. RNAi cloning strategy

5.4.1. short hairpin oligonucleotides – RNAi constructs

The short hairpin oligonucleotides (sh-oligonucleotides) were designed to form shRNAs after transcription, which are further processed to functional siRNAs by the cell-intrinsic RNAi-machinery. Candidate oligonucleotides for respective target mRNAs were calculated using a software available at ‘www.cshl.edu/public/SCIENCE/hannon.html’. By the use of the BLAST database we excluded sequence homology of our oligonucleotides with others than the target genes. Features of the sh-oligonucleotides:

- Oligonucleotides A encode an antisense, a loop and a sense strand.
- Termination of transcription was mediated by a run of Ts at the end of oligonucleotide A.
- The eight nucleotide loop-structure of the hairpin oligonucleotides (oligonucleotide A: GAAGCTTG) includes a HindIII restriction site.
- Oligonucleotides B were designed complementary to oligonucleotides A with additional asymmetric overhangs (5’ GATC.....CG 3’) to enable unidirectional ligation (see 7.3.12) of the annealed oligonucleotides (see 5.4.2) into a BseRI/BamHI digested vector.
- Some G-U pairings in the RNA hairpin stem were included to stabilize hairpins during propagation in bacteria.

Short hairpin oligonucleotides A and B used in our studies are listed in Table 5-5.

<i>Plasmid name</i>	<i>target (organism)</i>	<i>oligo A/B</i>	<i>sequence (5’-3’)</i>	<i>cDNA coding nt-region</i>
pJG101 pJG111	LAP2 general (h, m)	A	TGAGGTGCTGCAGGTAGAGCTGGAAGCTTGCAGCTCTACC TGCAGCACCTCACTTTTTT	115-137
		B	GATCAAAAAAGTGAGGTGCTGCAGGTAGAGCTGCAAGCTT CCAGCTCTACCTGCAGCACCTCACG	
pJG102 pJG112	LAP2 β , γ , ϵ (h, m, r)	A	TCTGAGAATTCAGTGATTGGCAGAATAGGAAGCTTGCTATT CTGCCGATTACTGAGTTCTCGGACATTTTTT	919-946
		B	GATCAAAAAATGTCCGAGAAGCTCAGTAATCGGCAGAATA GCAAGCTTCCTATTCTGCCAATCACTGAATTCTCAGACG	
pJG103 pJG113	emerin (h)	A	CAGCAAGGTGGTCAGCTCGGTATCCGAAGAAGCTTGTTCCG GATGCCGAGTTGACCCGCTTGTTCGCTTTTTT	20-49

		B	GATCAAAAAAGCGCAACAAGGCGGTCAACTCGGCATCCGA ACAAGCTTCTTCGGATACCGAGCTGACCACCTTGCTGCG	
pJG104 pJG114	LAP2 general (h)	A	GTTGCGAGCCGTGAGGTGCTGCAGGTAGGAAGCTTGCTAC TTGTAGCACTTCACGGCTCGCGACCGGTTTTT	120-147
		B	GATCAAAAAACCGGTGCGGAGCCGTGAAGTGCTACAAGTAG CAAGCTTCTACCTGCAGCACCTCACGGCTCGCAACCG	
pJG105	BAF (h, m, r)	A	GCTCTGCCACGAAGTCTCGGTGCGAAGCTTGGCACCGAGA CTTCGTGGCAGAGCTTTTT	18-40
		B	GATCAAAAAAGTCTGCCACGAAGTCTCGGTGCCAAGCTTC GCACCGAGACTTCGTGGCAGAGCCG	
pJG106 pJG116	LAP2 α (h, m)	A	GAGGACGGGTGGAGATTTACAGGGAAGCTTGCCTGAAATCT CCACCCGTCCTTTTT	663-698
		B	GATCAAAAAAGAGGACGGGTGGAGATTTACAGGCAAGCTTCC CTGAAATCTCCACCCGTCCTCCG	
pJG107	Lco1 (h)	A	ATTGTCTTGCCCAATCAAGTAACACTTGAAGCTTGCAGAGT GTTACTTGGTTGGGTAAGACGATCATTTTTTT	260-287
		B	GATCAAAAAAATGATCGTCTTACCAACCAAGTAACACTC GCAAGCTTCCAAGTGTACTTGATTGGGCAAGACAATCG	
pJG108 pJG118	LAP2 α (h)	A	ACTGATCAATTCTCTTCTGGAAGCTTGCAAGAAGAGAATTGA TCAGTCTTTTTT	1225-1245
		B	GATCAAAAAAGACTGATCAATTCTCTTCTGCAAGCTTCCAG AAGAGAATTGATCAGTCG	
pJG109 pJG119	LAP2 α (h)	A	GCACTGTGTTTCAGGCTGAGAAGATGACGGAAGCTTGCCTC GTCTTCTCAGCCTGAGCATAGTGCTATTTTTTT	878-908
		B	GATCAAAAAAATAGCACTATGCTCAGGCTGAGAAGACGAC GCAAGCTTCCGTATCTTCTCAGCCTGAACACAGTGCCG	
pJG110 pJG120	laminA (h, m)	A	AGTTGCCAGGAGGTAGGAGCGGGTGACGAAGCTTGGTCA TCCGCTTCTGCCTCTGGGCAGCTCCATTTTTT	1925-1953
		B	GATCAAAAAATGGAGCTGCCAGGAGGCAGAAGCGGATG ACCAAGCTTCGTCACCCGCTCCTACCTCTGGGCAACTCG	
pJG177 pCM3	Firefly Luciferase	A	GATTCCAATTCAGCGGGAGCCACCTGATGAAGCTTGATCA GGTGGCTCTGCTGAGTTGGAGTCTATTTTTT	
pCM8		B	GATCAAAAAAATAGACTCCAACCTCAGCAGGAGCCACCTGA TCAAGCTTCATCAGGTGGCTCCCGCTGAATTGGAATCCG	
pJG178 pCM3	Renilla Luciferase	A	ACGTAATGTAGTGATCCAGGAGGCGATGAAGCTTGATCG TCTTCTGGATCACTATAAGTATCTCACTTTTTT	
pCM8		B	GATCAAAAAAGTGAGATACTTATAGTGATCCAGAAGACGA TCAAGCTTCATCGCCTCTGGATCACTACAAGTACCTCG	
pJG179 pCM3	β - galactosidase1	A	CGTTCGACCCAGGCGTTAGGTCAATGCGAAGCTTGGTATT GATCCTAATGCCTGGGTCGAGCGCTGTTTTT	
		B	GATCAAAAAACAGCGCTCGACCCAGGCATTAGGATCAATA CCAAGCTTCGATTGACCCTAACGCCTGGGTCGAACGCG	

Primers:

Element A:

Forward primer:

B4f 5' – GGGGACAAC TTTGTATAGAAAAGTTG - TCACCGAGGGCCTATTTCCCATG - 3'

Reverse primer:

B1r-2 5' – GGGGACTGCTTTTTTGTACAAACTTG - GGTCGGCGCGCCACCCTTG - 3'

Element B:

Forward primer:

B1f 5' – GGGGACAAGTTTGTACAAAAAAGCAGGCTCC - 3'

Reverse primer:

B2r 5' – GGGGACCACTTTGTACAAGAAAGCTGGGTCG - 3'

Element C:

Forward primer:

B2f 5' – GGGGACAGCTTTCTTGTACAAAGTGG - CCTATTTCCCATGATTCCTTC - 3'

Reverse primer:

B3r 5' – GGGGACAAC TTTGTATAATAAAGTTG - GGTCGGCGCGCCACCCTTG - 3'

PCR parameters:

1 cycle	95°C	5min
	64°C	1min
	72°C	3min
2 cycles	95°C	1min
	62°C	1min
	72°C	3min
27 cycles	95°C	40sec
	60°C	45sec
	72°C	2min 32sec
once	72°C	4min
hold	4°C	

The PCR products were used for BP reaction (see 5.4.5.2.) to give three different MultiSite Gateway™ Entry vectors.

5.4.4. PCR to clone a MultiSite Gateway™ destination vector

Our aim was to amplify the Gateway™ – compatible cassette of Invitrogen's pDEST R4-R3 vector (see appendix A) and to ligate it into other plasmids, to obtain different Destination vectors. The PCR product includes recombination sites (*attR4* and *attR3*, see appendix B), a Chloramphenicol resistance gene and the *ccdB* gene, which is useful for negative selection after recombination.

To test the primers, we performed the PCR with puReTaq ready-to-go PCR beads (Amersham Biosciences, Little Calfont, Buckinghamshire, UK). Therefore, we mixed 30pmol of each primer and 100ng of pDEST R4-R3 with ddH₂O to an overall volume of 25µl and added one PCR bead.

The PCR product we used for cloning, was generated by a proof reading DNA polymerase. The 25µl reaction mixture included 2.5µl of 10x Pfu Reaction buffer (Stratagene, La Jolla, CA, USA), 4µl of dNTPs [2.5mM], 30pmol of each primer, 100ng of pDEST R4-R3 and 1µl of Pfu Turbo Hot Start DNA Polymerase (Stratagene, La Jolla, CA, USA).

PCR was performed using a Biometra T3 thermocycler system. The following primers and PCR parameters were used:

Primers:

Forward primer:

RFM1 5' – GCGATATCTACGCCAAGCTATCAAC – 3'

Reverse primer:

RFM2 5' – CGGATATCAACGACGGCCAGTGAAT – 3'

<u>PCR parameters:</u>	1 cycle	95°C	5min
		56°C	1min
		72°C	10min
	1 cycle	95°C	1min
		56°C	1min
		72°C	10min
	28 cycles	95°C	50sec
		58°C	1min
		72°C	10min
		72°C	15min
	once	72°C	15min
	hold	4°C	

As the primers have non-base-pairing overhangs coding for EcoRV restriction sites, we performed the first two PCR cycles with a lower annealing temperature.

5.4.5. GatewayTM recombination reactions (Invitrogen, Carlsbad, CA, USA)

For information on the GatewayTM system, see appendix B.

5.4.5.1. LR recombination reaction

We used the LR recombination reaction to shuttle the functional RNAi cassettes from pSHAG (pJG101 – pJG110) to GatewayTM compatible pTracer (pJG111 – pJG120) (see 5.4.6.).

The reaction mixture included 3µl of 5x LR Clonase reaction buffer, 1µl of pSHAG Entry clone, 1µl of pTracer Destination vector and buffer TE (pH 8) (see 5.4.2.) to a total volume of

13µl. Finally LR Clonase was thawed on ice for two minutes, vortexed twice and spun briefly. The enzyme was stored at –80°C immediately after 2µl were added to the reaction. The reaction was mixed briefly by vortexing two times, followed by short spinning. Then it was incubated for 1-3 hours at room temperature. Afterwards 1.5µl of proteinase K [2µg/µl] were added and the recombination reaction was terminated at 37°C for 10 minutes. 10µl of the solution were transformed into competent *E.Coli* DH5α (see 5.3.1.).

5.4.5.2. BP recombination reaction

In our case the BP recombination reaction was used to shuttle PCR products (see 5.4.3.) into Donor vectors to clone MultiSite Gateway™ Entry vectors (see 5.4.7.). Element A was transferred to pDONR P4-P1R, forming pMU6-A. Element B was recombined with pDONR 221, to form pMU6-B and Element C was shuttled into pDONR P2R-P3, to form pMU6-C.

The reaction mixture included 4µl of buffer TE (pH 8) (see 5.4.2.), 3µl of 5x BP Clonase reaction buffer, 5µl of PCR product (Element A, B, or C, see 5.4.3.), 1µl of corresponding Donor vector (pDONR P4-P1R, pDONR 221, or pDONR P2R-P3, each [1µg/µl]; vector maps see appendix A) and finally 2µl of BP Clonase (procedure see LR Clonase 5.4.5.1.). The whole reaction was mixed briefly by vortexing two times, before it was incubated for 2.5 hours at room temperature. Afterwards 1.5µl of proteinase K [2µg/µl] were added and the reaction was incubated at 37°C for 10 minutes. 10µl of the recombination reaction were transformed into competent *E.Coli* DH5α (see 5.3.1.).

5.4.5.3. MultiSite Gateway™ LR reaction

The MultiSite Gateway™ LR reaction was used to shuttle three RNAi-cassettes from three different Entry vectors into one Destination vector (pDEST R4-R3). As Entry vectors we used:

pMU6-A, pMU6-B and pMU6-C to clone pJG100

pJG177, pJG178 and pJG179 to clone pCM3

pJG177, pJG178 and pCM4 to clone pCM8

The reaction mixture contained: about 20-25fmol of each plasmid (60ng pDEST R4-R3, 45ng of each Entry vector), 4µl of 5x LR Clonase™ Plus Reaction Buffer and buffer TE (pH 8) (see 5.4.2.) to 16µl. The LR Clonase™ Plus was thawed on ice for 2 minutes, vortexed twice and spun briefly. The enzyme was stored at –80°C immediately after 4µl were added to the reaction. The reaction was mixed briefly by vortexing two times, followed by short spinning. Then it was incubated for 16-20 hours at room temperature. Afterwards 2µl of proteinase K

[2µg/µl] were added and the recombination reaction was terminated at 37°C for 10 minutes. 10µl of the solution were transformed into competent *E.Coli* DH5α (see 5.3.1.).

5.4.6. Cloning strategy for single target RNAi vectors

The sh-oligonucleotides (see 5.4.1.) were annealed (see 5.4.2.) and ligated (see 5.3.12.) into a BseR1/BamH1 digested pSHAG vector (obtained from G. Hannon, CSHL; plasmids pJG101 to pJG110, see Table 5-5 or appendix A). This vector has a bacterial origin of replication and encodes a kanamycin resistance for bacterial amplification and selection. As the cloning site for sh-oligonucleotides is located directly behind a human RNA polymerase III U6 promoter, the pSHAG vector is also suitable for transient transfection of human cells.

The human U6 promoter and the restriction sites for BseRI and BamHI are surrounded by GatewayTM (Invitrogen) recombination sites (*attL* sites) to easily shuttle the RNAi-cassette between different gateway compatible vectors (see appendix B). The GatewayTM compatible pTracer plasmid was selected as destination vector for this transfer (see 5.4.5.1.), leading to plasmids pJG111 to pJG121 (see Table 5-5 or appendix A). The pTracer vector is suitable for transient and stable transfection in eukaryotic cells (see 5.1.2., 5.1.3.), as it enables double-selection on a co-expressed CMV driven GFP-Blasticidin chimera. Furthermore the pTracer vector encodes a bacterial origin of replication and an ampicillin resistance for bacterial amplification and selection. The GFP-Blasticidin chimera can also be used for bacterial selection, as it is also EM7 driven.

5.4.7. The Triple-RNAi-Vector approach

The aim was to design three MultiSite GatewayTM Entry vectors (see appendix B), each encoding an RNAi-cassettes (see 5.4.6.), which then could be shuttled into a Destination vector, forming a Triple-RNAi-Vector.

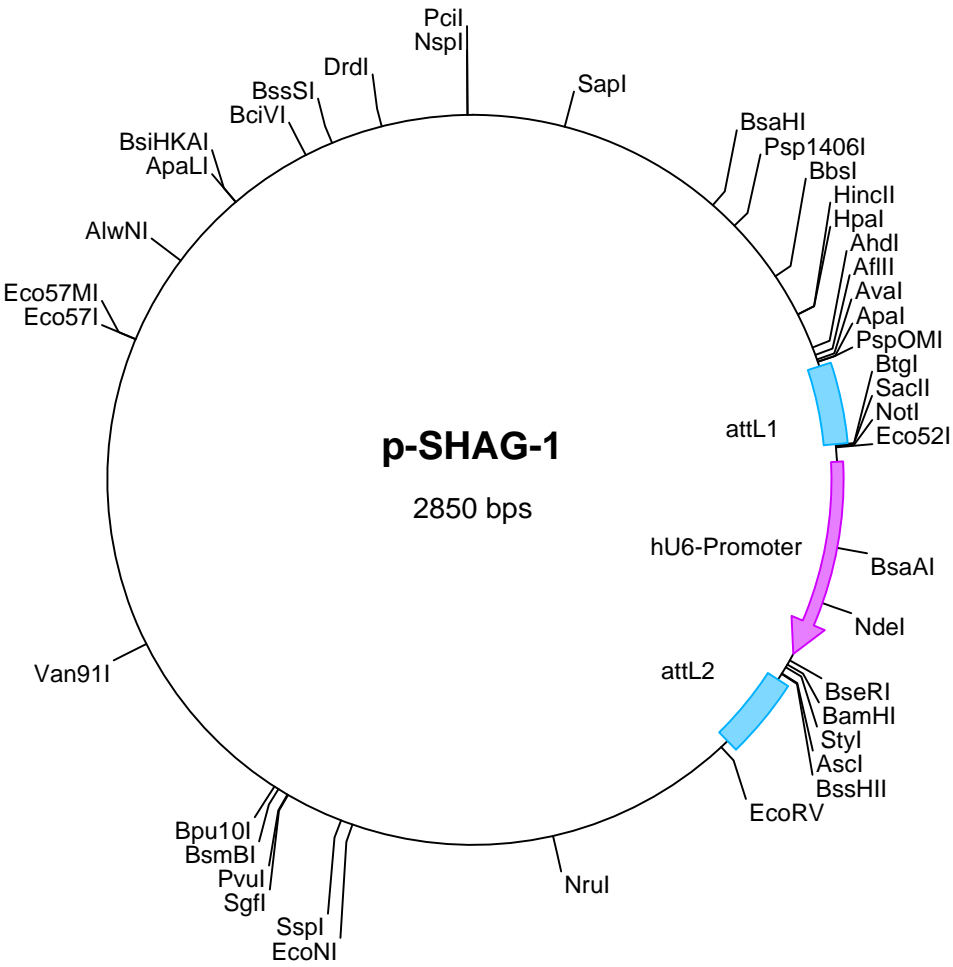
First we designed three pairs of primers according to Invitrogen's manual, to amplify three RNAi-cassettes out of pSHAG with suitable recombination sites for MultiSite GatewayTM reactions (see 5.4.3.). The three PCR products were transferred to Donor vectors by separate BP recombination reactions (see 5.4.5.2.). The resulting Entry vectors pMU6-A, pMU6-B and pMU6-C were sequenced with M13 forward and M13 reverse primers by VBC-Genomics, to confirm the integrity of the recombination sites. Afterwards MultiSite GatewayTM LR reaction (see 5.4.5.3.) was tested and control vector pJG100 was cloned. RNAi constructs (see 5.4.1.), targeting exogenous reporter proteins (Firefly Luciferase, Renilla Luciferase and β-galactosidase), were ligated (see 5.3.12.) into the pMU6 plasmids, leading to plasmids

pJG177, pJG178, pJG179, pCM4, pCM5, pCM6 and pCM7. These constructs were tested in co-transfection experiments. Finally two more MultiSite GatewayTM LR reactions were performed to obtain pCM3 and pCM8 (see 5.4.5.3.) The functionality of the system was tested by co-transfection experiments.

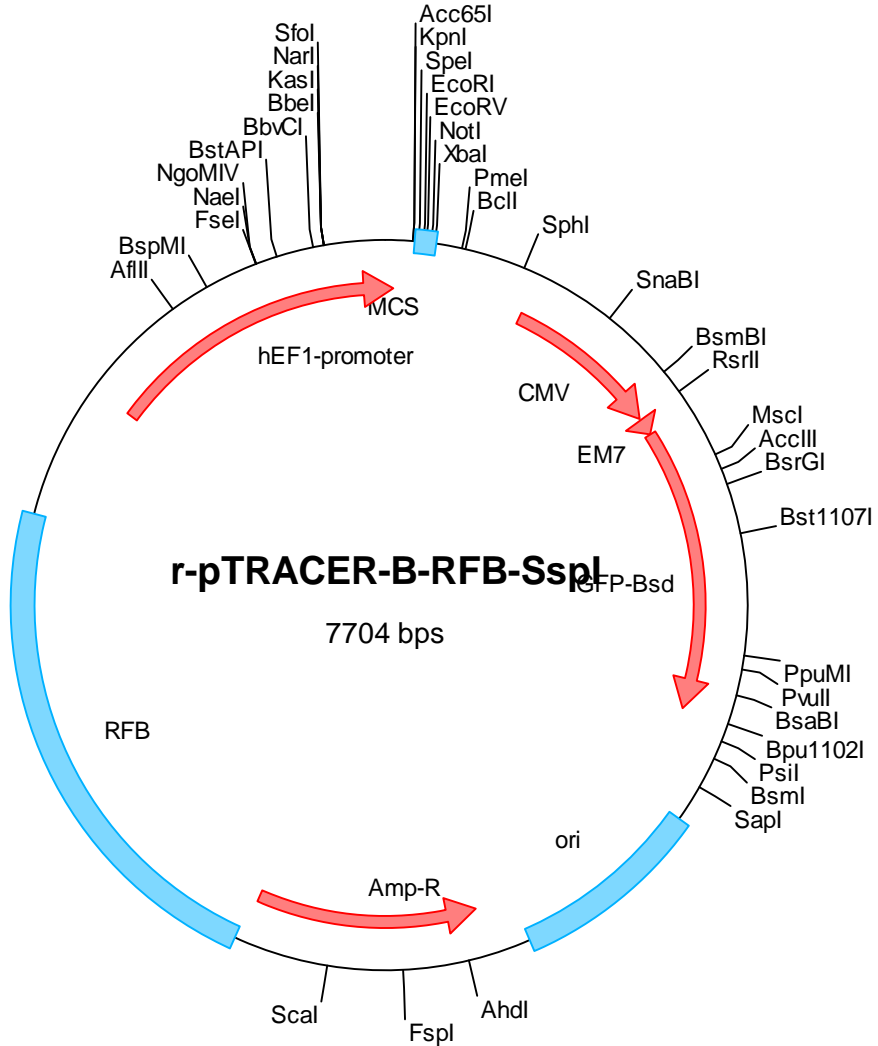
6. APPENDIX

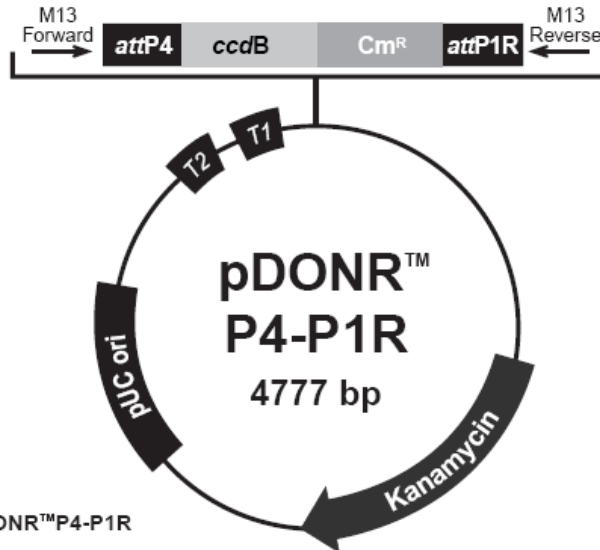
6.1. Appendix A

Vector maps of Gateway™ and reporter plasmids



Gateway™ compatible pTracer

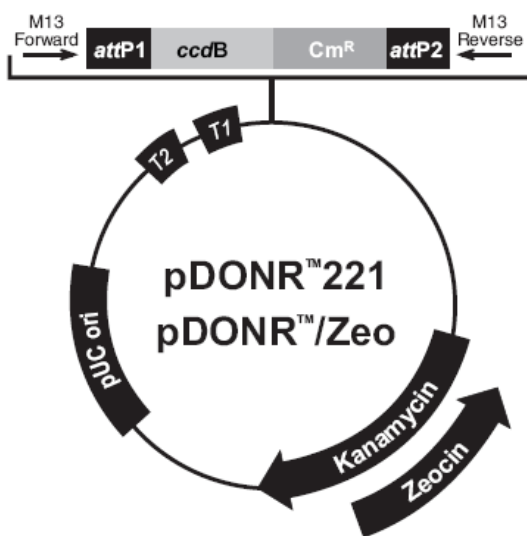




**Comments for pDONR™P4-P1R
4777 nucleotides**

rrnB T2 transcription termination sequence: bases 268-295 (c)
rrnB T1 transcription termination sequence: bases 427-470 (c)
M13 Forward (-20) priming site: bases 537-552
attP4 recombination site: bases 593-824 (c)
ccdB gene: bases 1181-1486 (c)
Chloramphenicol resistance gene: bases 1828-2487 (c)
attP1R recombination site: bases 2748-2979 (c)
M13 Reverse priming site: bases 3042-3058
Kanamycin resistance gene: bases 3171-3980
pUC origin: bases 4101-4774
(c) = complementary strand

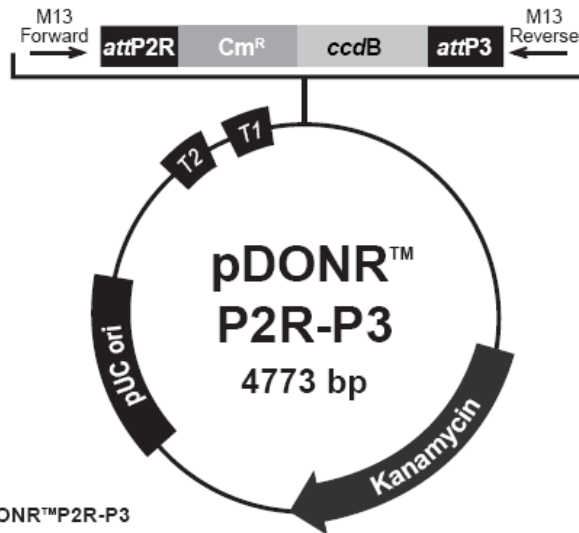




Comments for:

	pDONR™221 4762 nucleotides	pDONR™/Zeo 4291 nucleotides
<i>rrnB</i> T2 transcription termination sequence (c):	268-295	268-295
<i>rrnB</i> T1 transcription termination sequence (c):	427-470	427-470
M13 Forward (-20) priming site:	537-552	537-552
<i>attP1</i> :	570-801	570-801
<i>ccdB</i> gene (c):	1197-1502	1197-1502
Chloramphenicol resistance gene (c):	1847-2506	1847-2506
<i>attP2</i> (c):	2754-2985	2754-2985
T7 Promoter/priming site (c):	3000-3019	3003-3022
M13 Reverse priming site:	3027-3043	3027-3043
Kanamycin resistance gene:	3156-3965	---
EM7 promoter (c):	---	3486-3552
Zeocin resistance gene (c):	---	3111-3485
pUC origin:	4086-4759	3615-4288





**Comments for pDONR™P2R-P3
4773 nucleotides**

rrnB T2 transcription termination sequence: bases 268-295 (c)

rrnB T1 transcription termination sequence: bases 427-470 (c)

M13 Forward (-20) priming site: bases 537-552

attP2R recombination site: bases 591-822

Chloramphenicol resistance gene: bases 1083-1742

ccdB gene: bases 2084-2389

attP3 recombination site: bases 2746-2977

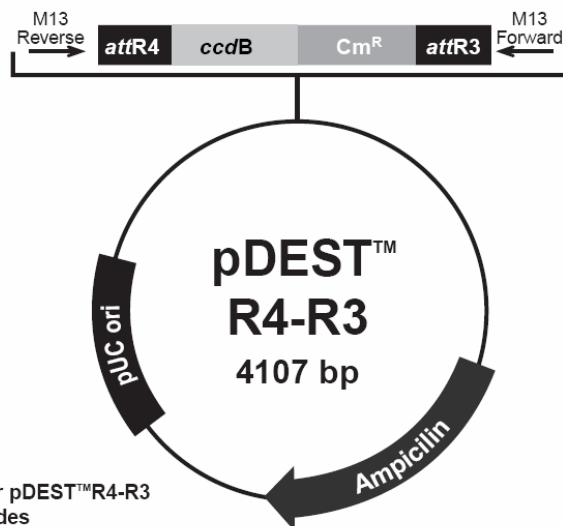
M13 Reverse priming site: bases 3038-3054

Kanamycin resistance gene: bases 3167-3976

pUC origin: bases 4097-4770

(c) = complementary strand



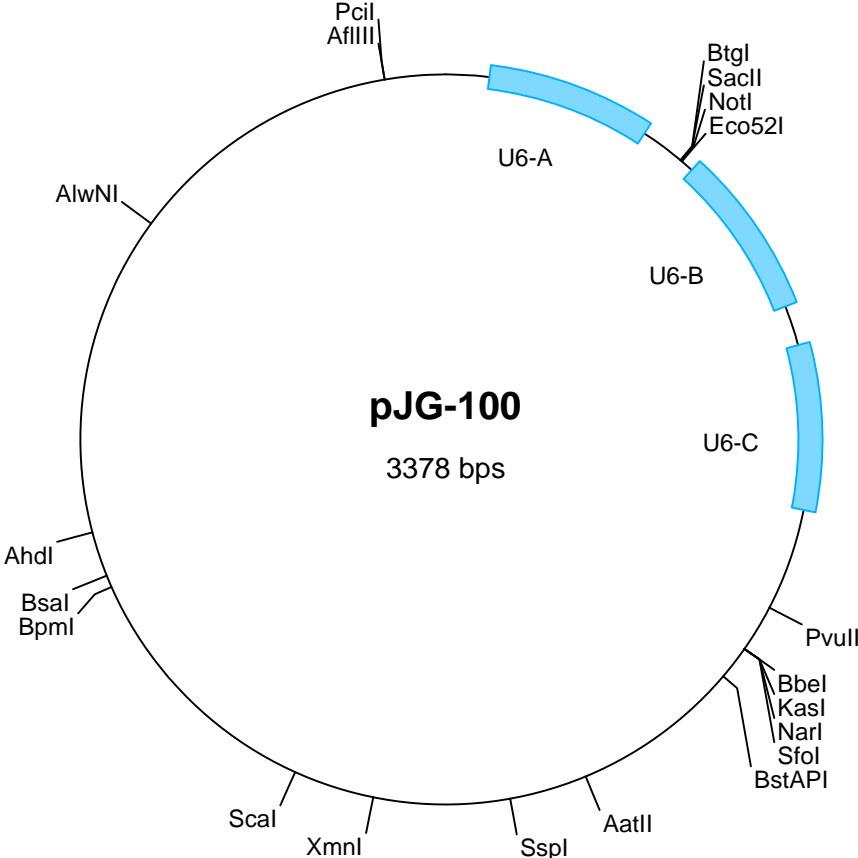


**Comments for pDEST™R4-R3
4107 nucleotides**

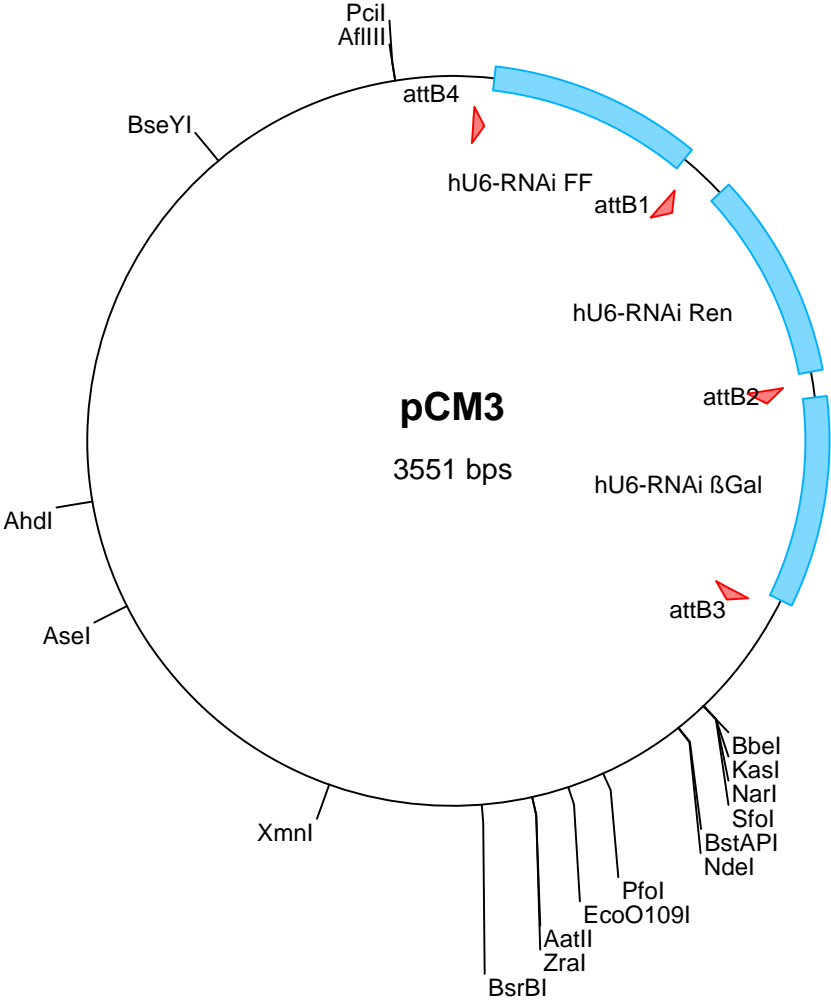
- M13 Reverse priming site: bases 1-17
- attR4 recombination site: bases 37-161
- ccdB gene: bases 201-506 (c)
- Chloramphenicol resistance gene: bases 848-1507 (c)
- attR3 recombination site: bases 1616-1740 (c)
- M13 Forward (-20) priming site: bases 1749-1764 (c)
- bla promoter: bases 2244-2342
- Ampicillin (*bla*) resistance gene: bases 2343-3203
- pUC origin: bases 3348-4021
- (c) = complementary strand



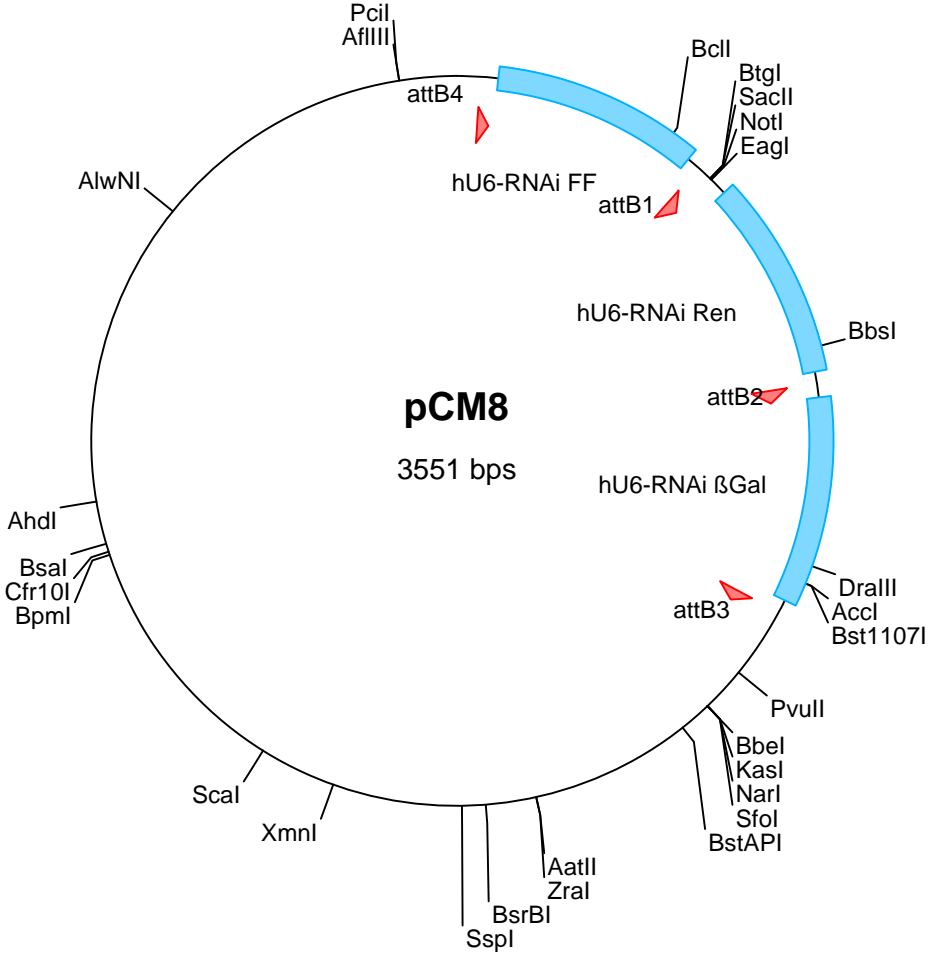
Triple-RNAi-Vector control vector (three promoters, but no RNAi constructs)



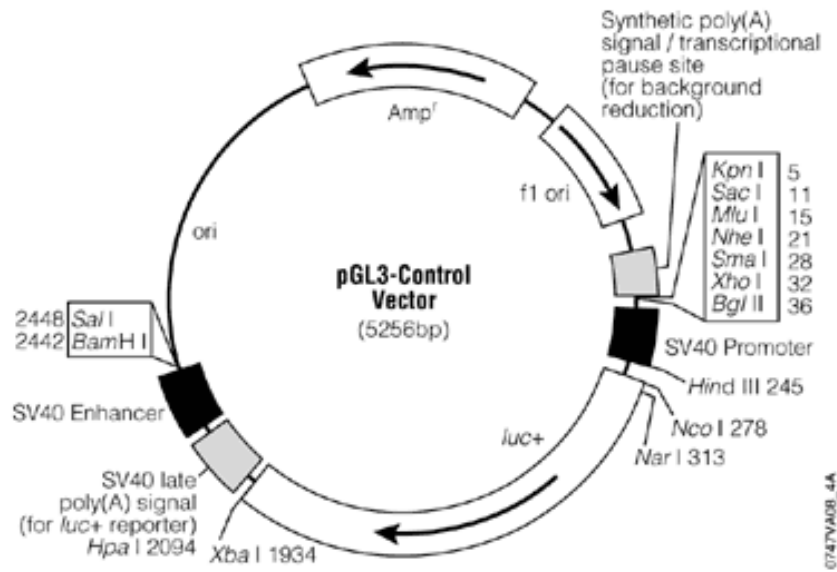
Triple-RNAi-Vector to target Firefly Luciferase, Renilla Luciferase and β -galactosidase



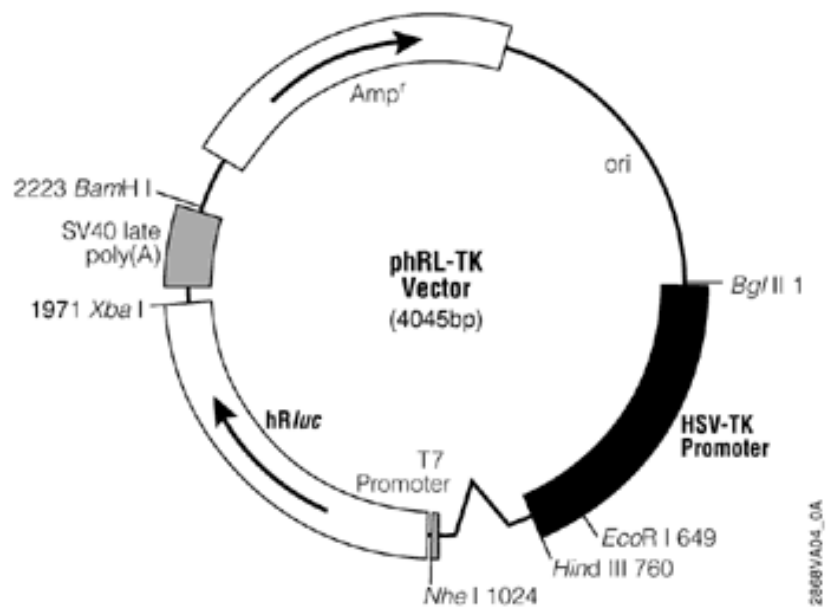
Triple-RNAi-Vector to target Firefly Luciferase, Renilla Luciferase and β -galactosidase



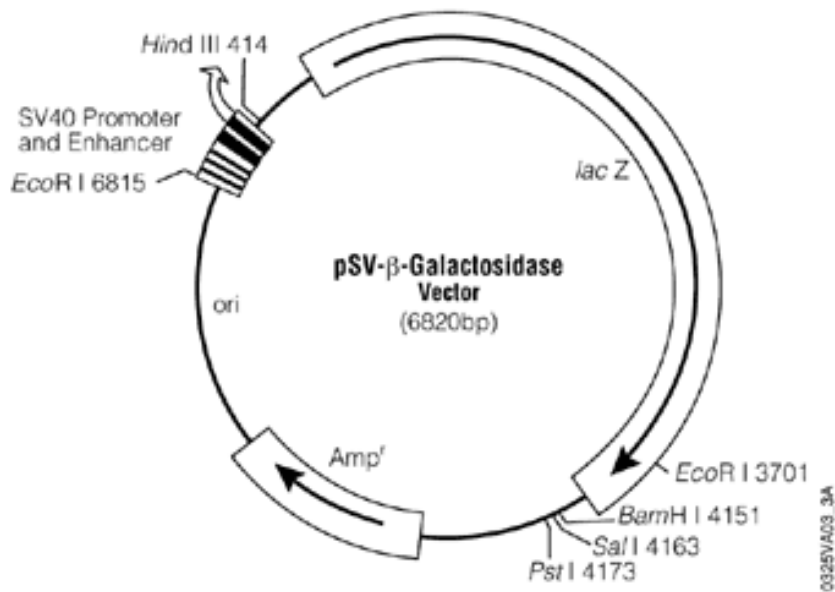
pGL3 for SV40 driven Firefly Luciferase expression (Promega)



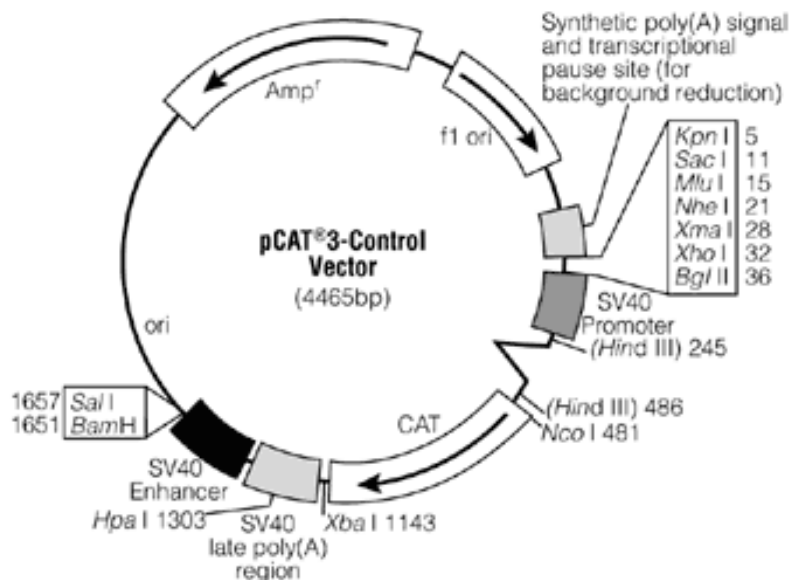
phRL for Thymidine kinase driven Renilla Luciferase expression (Promega)



pSVβ-Gal for SV40 driven β-galactosidase expression (Promega)



pCAT3 for SV40 driven chloramphenicol acetyltransferase expression (Promega)



6.2. Appendix B

6.2.1. The Gateway™ Technology

The Gateway™ system is a universal cloning method based on the site-specific integration of bacteriophage lambda into the *E. coli* chromosome (Landy, 1989). The system had been adapted to improve cloning specificity and efficiency (Bushman et al., 1985). A Clonase enzyme mix mediates the recombination between specific attachment sites (*att*) of the interacting DNA molecules. The recombination is conservative, which means that there is no gain or loss of nucleotides. Originally lambda integration occurred between *attP* sites (lambda chromosome) and *attB* sites (*E. coli* chromosome) and gave rise to *attL* and *attR* sites.

The proposed cloning strategy starts with the gene of interest in an *attB* flanked expression vector, or by amplifying the gene together with the recombination sites by PCR. The gene of interest can then easily be shuttled into a donor vector, resulting in an entry clone by BP reaction (see Figure 6-1 (A)). The *ccdB* gene initially encoded by the donor vector and after the BP reaction by the by-product, can be used for negative selection. The *ccdB* protein interferes with *E. coli* DNA gyrase (Bernard and Couturier, 1992) and thereby inhibits growth of most *E. coli* strains. In succession, the gene of interest can easily be shuttled into a destination vector of choice by an LR reaction to give an expression clone (see Figure 6-1 (B)). In this reaction, the *attL* and *attR* sites recombine to *attB* and *attP* sites.

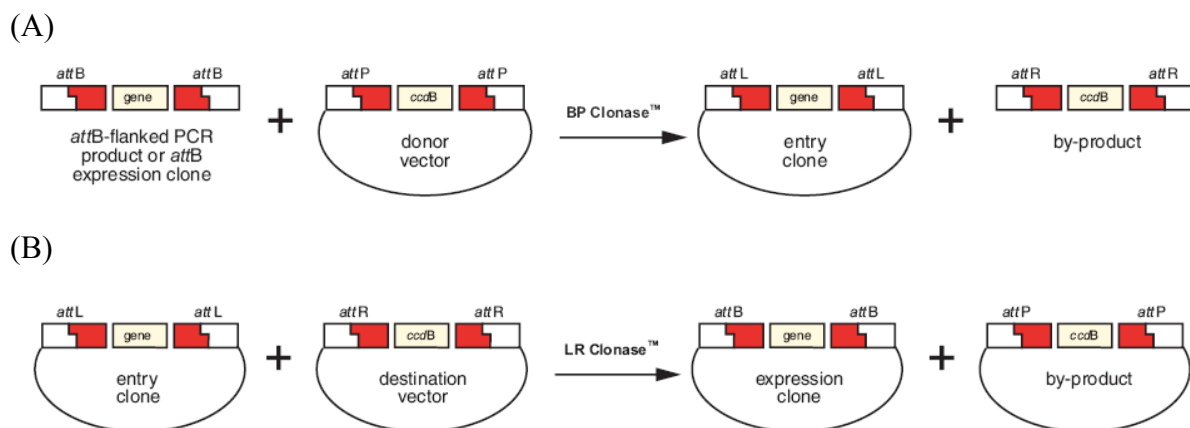


Figure 6-1: Schematic view of Gateway™ mediated recombination. (A) BP Clonase shuttles a gene of interest, flanked by *attB* sites, which can be amplified by PCR, or encoded by an Expression clone, into a Donor vector (*attP* sites). The BP reaction results in an Entry Clone encoding the gene, flanked by *attL* sites and a by-product (*attR* sites). (B) LR reaction mediated by LR Clonase between an Entry Clone (*attL* sites) encoding the gene of interest and a Destination vector (*attR* sites) results in an Expression Clone (*attB* sites) carrying the gene and a by-product (*attP* sites). Modified from Gateway™ Technology manual (Invitrogen).

6.2.2. The MultiSite Gateway™ Technology

This system is a further development of the Gateway™ system. It offers rapid and efficient construction of an expression clone encoding three fragments of choice (e.g. promoter, gene of interest and termination sequence, or in our case three RNAi-cassettes) in a defined order and orientation. Therefore the *att* sites have been further modified to enable simultaneous, recombination of three fragments. Instead of two *att* sites in the standard Gateway™ system, the MultiSite Gateway™ Technology uses four different *att* sites. The *att* sites thereby remain highly specific (e.g. *attB1* only recombines with *attP1*, resulting in *attL1* and *attR1*).

Three steps to create a MultiSite Gateway™ Expression clone:

- 1) First, the three genes of interest must be separately amplified by PCR and specific *attB* primers, to obtain three PCR products, flanked by *attB4* – 5' element - *attB1*, *attB1* – central element - *attB2* and *attB2* – 3' element – *attB3*.
- 2) To create Entry Clones, the PCR products are shuttled into Donor vectors (pDONR™P4-P1R, pDONR™221, pDONR™P2R-P3) by three separate BP recombination reactions. These are normal BP reactions, like in the standard Gateway™ system, except the recombination between *attB1* of the 5' element and P1R of pDONR™P4-P1R, which leads to an *attR1* site (similar for the reaction of the *attB2* site of the 3' element and the P2R recombination site of pDONR™P2R-P3). The three Entry Clones are schematically shown in the upper part of Fig. B-2.
- 3) Finally, a single MultiSite Gateway™ LR recombination reaction between the three Entry Clones and one Destination vector has to be performed to obtain an Expression Clone encoding all three genes of interest in a defined order and orientation (see Figure 6-2).

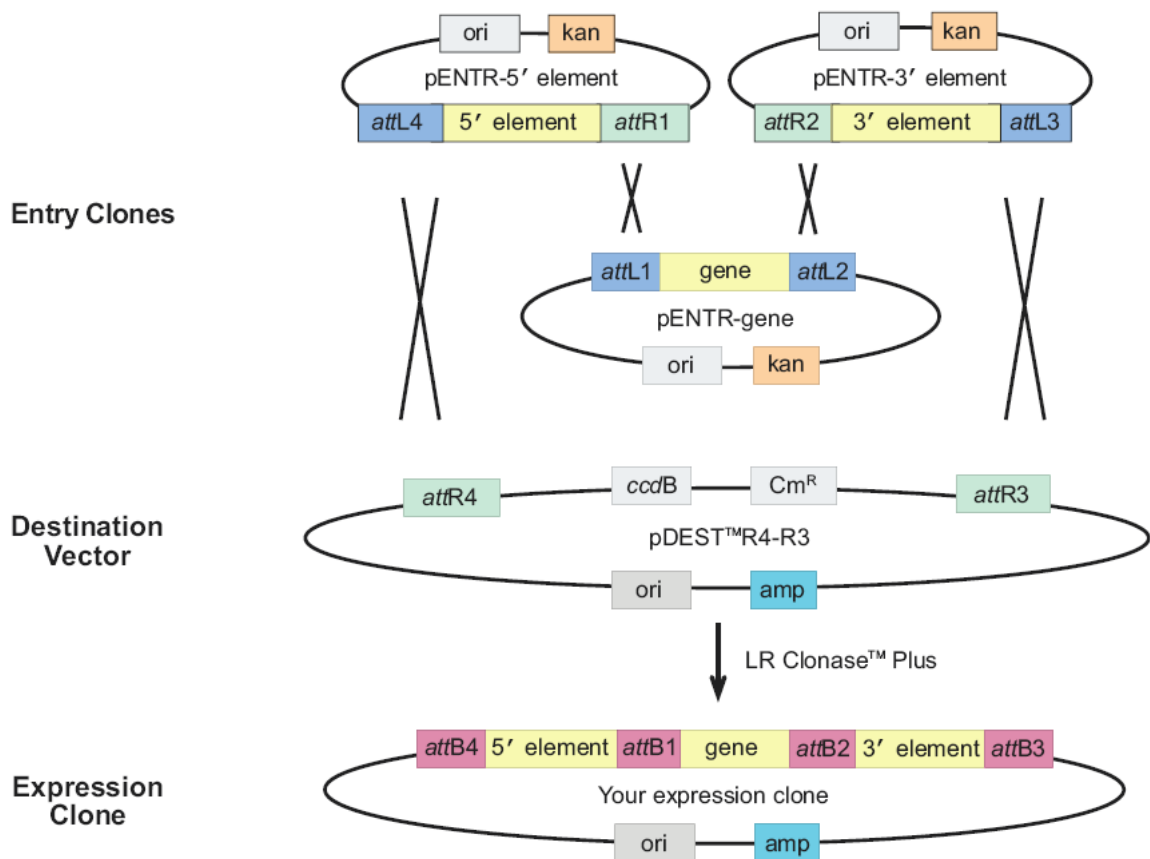


Figure 6-2: Schematic view of a MultiSite Gateway™ LR recombination reaction. Three Entry Clones, each encoding a DNA sequence of interest flanked by specific *att* sites and a Destination vector recombine to give an Expression Clone, encoding the three DNA sequences in a defined order and orientation. Modified from MultiSite Gateway™ Technology manual (Invitrogen).

7. REFERENCES

- Aebi, U., Cohn, J., Buhle, L. and Gerace, L.** (1986). The nuclear lamina is a meshwork of intermediate-type filaments. *Nature* **323**, 560-4.
- Arts, G. J., Langemeijer, E., Tissingh, R., Ma, L., Pavliska, H., Dokic, K., Dooijes, R., Mesic, E., Clasen, R., Michiels, F. et al.** (2003). Adenoviral vectors expressing siRNAs for discovery and validation of gene function. *Genome Res* **13**, 2325-32.
- Banerjee, D. and Slack, F.** (2002). Control of developmental timing by small temporal RNAs: a paradigm for RNA-mediated regulation of gene expression. *Bioessays* **24**, 119-29.
- Bartel, B. and Bartel, D. P.** (2003). MicroRNAs: at the root of plant development? *Plant Physiol* **132**, 709-17.
- Beaudouin, J., Gerlich, D., Daigle, N., Eils, R. and Ellenberg, J.** (2002). Nuclear envelope breakdown proceeds by microtubule-induced tearing of the lamina. *Cell* **108**, 83-96.
- Bernard, P., and Couturier, M.** (1992). Cell killing by the F plasmid CcdB protein involves poisoning of DNA-topoisomerase II complexes. *J Mol Biol* **226**, 735-745.
- Bernstein, E., Caudy, A. A., Hammond, S. M. and Hannon, G. J.** (2001). Role for a bidentate ribonuclease in the initiation step of RNA interference. *Nature* **409**, 363-6.
- Billy, E., Brondani, V., Zhang, H., Muller, U. and Filipowicz, W.** (2001). Specific interference with gene expression induced by long, double-stranded RNA in mouse embryonal teratocarcinoma cell lines. *Proc Natl Acad Sci U S A* **98**, 14428-33.
- Bohnsack, M. T., Czaplinski, K. and Gorlich, D.** (2004). Exportin 5 is a RanGTP-dependent dsRNA-binding protein that mediates nuclear export of pre-miRNAs. *Rna* **10**, 185-91.
- Boutet, S., Vazquez, F., Liu, J., Beclin, C., Fagard, M., Gratias, A., Morel, J. B., Crete, P., Chen, X. and Vaucheret, H.** (2003). Arabidopsis HEN1: a genetic link between endogenous miRNA controlling development and siRNA controlling transgene silencing and virus resistance. *Curr Biol* **13**, 843-8.
- Boyle, S., Gilchrist, S., Bridger, J. M., Mahy, N. L., Ellis, J. A. and Bickmore, W. A.** (2001). The spatial organization of human chromosomes within the nuclei of normal and emerin-mutant cells. *Hum Mol Genet* **10**, 211-9.
- Bridger, J. M., Kill, I. R., O'Farrell, M. and Hutchison, C. J.** (1993). Internal lamin structures within G1 nuclei of human dermal fibroblasts. *J Cell Sci* **104 (Pt 2)**, 297-306.

- Brummelkamp, T. R., Bernards, R. and Agami, R.** (2002). A system for stable expression of short interfering RNAs in mammalian cells. *Science* **296**, 550-3.
- Burke, B. and Ellenberg, J.** (2002). Remodelling the walls of the nucleus. *Nat Rev Mol Cell Biol* **3**, 487-97.
- Bushman, W., Thompson, J. F., Vargas, L. and Landy, A.** (1985). Control of directionality in lambda site specific recombination. *Science* **230**, 906-11.
- Cai, M., Huang, Y., Ghirlando, R., Wilson, K. L., Craigie, R. and Clore, G. M.** (2001). Solution structure of the constant region of nuclear envelope protein LAP2 reveals two LEM-domain structures: one binds BAF and the other binds DNA. *Embo J* **20**, 4399-407.
- Caplen, N. J., Parrish, S., Imani, F., Fire, A. and Morgan, R. A.** (2001). Specific inhibition of gene expression by small double-stranded RNAs in invertebrate and vertebrate systems. *Proc Natl Acad Sci U S A* **98**, 9742-7.
- Carrington, J. C. and Ambros, V.** (2003). Role of microRNAs in plant and animal development. *Science* **301**, 336-8.
- Chellappan, S. P., Hiebert, S., Mudryj, M., Horowitz, J. M. and Nevins, J. R.** (1991). The E2F transcription factor is a cellular target for the RB protein. *Cell* **65**, 1053-61.
- Chen, Y., Stamatoyannopoulos, G. and Song, C. Z.** (2003). Down-regulation of CXCR4 by inducible small interfering RNA inhibits breast cancer cell invasion in vitro. *Cancer Res* **63**, 4801-4.
- Classon, M. and Harlow, E.** (2002). The retinoblastoma tumour suppressor in development and cancer. *Nat Rev Cancer* **2**, 910-7.
- Cohen, M., Lee, K. K., Wilson, K. L. and Gruenbaum, Y.** (2001). Transcriptional repression, apoptosis, human disease and the functional evolution of the nuclear lamina. *Trends Biochem Sci* **26**, 41-7.
- Collas, P. and Robl, J. M.** (1990). Factors affecting the efficiency of nuclear transplantation in the rabbit embryo. *Biol Reprod* **43**, 877-84.
- Czuderna, F., Santel, A., Hinz, M., Fechtner, M., Durieux, B., Fisch, G., Leenders, F., Arnold, W., Giese, K., Klippel, A. et al.** (2003). Inducible shRNA expression for application in a prostate cancer mouse model. *Nucleic Acids Res* **31**, e127.
- De Sandre-Giovannoli, A., Bernard, R., Cau, P., Navarro, C., Amiel, J., Boccaccio, I., Lyonnet, S., Stewart, C. L., Munnich, A., Le Merrer, M. et al.** (2003). Lamin a truncation in Hutchinson-Gilford progeria. *Science* **300**, 2055.

- Dechat, T., Gajewski, A., Korbei, B., Gerlich, D., Daigle, N., Haraguchi, T., Furukawa, K., Ellenberg, J. and Foisner, R.** (2004). LAP2alpha and BAF transiently localize to telomeres and specific regions on chromatin during nuclear assembly. *J Cell Sci* **117**, 6117-28.
- Dechat, T., Gotzmann, J., Stockinger, A., Harris, C. A., Talle, M. A., Siekierka, J. J. and Foisner, R.** (1998). Detergent-salt resistance of LAP2alpha in interphase nuclei and phosphorylation-dependent association with chromosomes early in nuclear assembly implies functions in nuclear structure dynamics. *Embo J* **17**, 4887-902.
- Dechat, T., Korbei, B., Vaughan, O. A., Vlcek, S., Hutchison, C. J. and Foisner, R.** (2000a). Lamina-associated polypeptide 2alpha binds intranuclear A-type lamins. *J Cell Sci* **113 Pt 19**, 3473-84.
- Dechat, T., Vlcek, S. and Foisner, R.** (2000b). Review: lamina-associated polypeptide 2 isoforms and related proteins in cell cycle-dependent nuclear structure dynamics. *J Struct Biol* **129**, 335-45.
- Denli, A. M. and Hannon, G. J.** (2003). RNAi: an ever-growing puzzle. *Trends Biochem Sci* **28**, 196-201.
- Dorner D., Vlcek S., Foeger N., Gajewski A., Makolm C., Gotzmann J., Hutchison C.J. and Foisner R.** (2006). Lamina-associated polypeptide 2 α regulates cell cycle progression and differentiation via the retinoblastoma-E2F pathway. *J Cell Biol.*, **173**, 83-93.
- Drummond, S., Ferrigno, P., Lyon, C., Murphy, J., Goldberg, M., Allen, T., Smythe, C. and Hutchison, C. J.** (1999). Temporal differences in the appearance of NEP-B78 and an LBR-like protein during *Xenopus* nuclear envelope reassembly reflect the ordered recruitment of functionally discrete vesicle types. *J Cell Biol* **144**, 225-40.
- Dyxhoorn, D. M., Novina, C. D. and Sharp, P. A.** (2003). Killing the messenger: short RNAs that silence gene expression. *Nat Rev Mol Cell Biol* **4**, 457-67.
- Elbashir, S. M., Harborth, J., Lendeckel, W., Yalcin, A., Weber, K. and Tuschl, T.** (2001a). Duplexes of 21-nucleotide RNAs mediate RNA interference in cultured mammalian cells. *Nature* **411**, 494-8.
- Elbashir, S. M., Lendeckel, W. and Tuschl, T.** (2001b). RNA interference is mediated by 21- and 22-nucleotide RNAs. *Genes Dev* **15**, 188-200.
- Elbashir, S. M., Martinez, J., Patkaniowska, A., Lendeckel, W. and Tuschl, T.** (2001c). Functional anatomy of siRNAs for mediating efficient RNAi in *Drosophila melanogaster* embryo lysate. *Embo J* **20**, 6877-88.

- Ellenberg, J., Siggia, E. D., Moreira, J. E., Smith, C. L., Presley, J. F., Worman, H. J. and Lippincott-Schwartz, J.** (1997). Nuclear membrane dynamics and reassembly in living cells: targeting of an inner nuclear membrane protein in interphase and mitosis. *J Cell Biol* **138**, 1193-206.
- Eriksson, M., Brown, W. T., Gordon, L. B., Glynn, M. W., Singer, J., Scott, L., Erdos, M. R., Robbins, C. M., Moses, T. Y., Berglund, P. et al.** (2003). Recurrent de novo point mutations in lamin A cause Hutchinson-Gilford progeria syndrome. *Nature* **423**, 293-8.
- Evans, D. E., Bryant, J. A. and Hutchison, C.** (2004). The nuclear envelope: a comparative overview. *Symp Soc Exp Biol*, 1-8.
- Fire, A., Xu, S., Montgomery, M. K., Kostas, S. A., Driver, S. E. and Mello, C. C.** (1998). Potent and specific genetic interference by double-stranded RNA in *Caenorhabditis elegans*. *Nature* **391**, 806-11.
- Foisner, R.** (2001). Inner nuclear membrane proteins and the nuclear lamina. *J Cell Sci* **114**, 3791-2.
- Foisner, R.** (2003). Cell cycle dynamics of the nuclear envelope. *ScientificWorldJournal* **3**, 1-20.
- Foisner, R. and Gerace, L.** (1993). Integral membrane proteins of the nuclear envelope interact with lamins and chromosomes, and binding is modulated by mitotic phosphorylation. *Cell* **73**, 1267-79.
- Fukagawa, T., Nogami, M., Yoshikawa, M., Ikeno, M., Okazaki, T., Takami, Y., Nakayama, T. and Oshimura, M.** (2004). Dicer is essential for formation of the heterochromatin structure in vertebrate cells. *Nat Cell Biol* **6**, 784-91.
- Furukawa, K.** (1999). LAP2 binding protein 1 (L2BP1/BAF) is a candidate mediator of LAP2-chromatin interaction. *J Cell Sci* **112 (Pt 15)**, 2485-92.
- Furukawa, K., Pante, N., Aebi, U. and Gerace, L.** (1995). Cloning of a cDNA for lamina-associated polypeptide 2 (LAP2) and identification of regions that specify targeting to the nuclear envelope. *Embo J* **14**, 1626-36.
- Gajewski, A., Csaszar, E., and Foisner, R.** (2004). A phosphorylation cluster in the chromatin-binding region regulates chromosome association of LAP2alpha. *J Biol Chem* **279**, 35813-35821.
- Georgatos, S. D., Pyrpasopoulou, A. and Theodoropoulos, P. A.** (1997). Nuclear envelope breakdown in mammalian cells involves stepwise lamina disassembly and

- microtubule-drive deformation of the nuclear membrane. *J Cell Sci* **110** (Pt 17), 2129-40.
- Gil, J. and Esteban, M.** (2000). Induction of apoptosis by the dsRNA-dependent protein kinase (PKR): mechanism of action. *Apoptosis* **5**, 107-14.
- Goldman, A. E., Moir, R. D., Montag-Lowy, M., Stewart, M. and Goldman, R. D.** (1992). Pathway of incorporation of microinjected lamin A into the nuclear envelope. *J Cell Biol* **119**, 725-35.
- Goldman, R. D., Gruenbaum, Y., Moir, R. D., Shumaker, D. K. and Spann, T. P.** (2002). Nuclear lamins: building blocks of nuclear architecture. *Genes Dev* **16**, 533-47.
- Gotzmann, J. and Foisner, R.** (1999). Lamins and lamin-binding proteins in functional chromatin organization. *Crit Rev Eukaryot Gene Expr* **9**, 257-65.
- Gotzmann, J. and Foisner, R.** (2005). A-type lamin complexes and regenerative potential: a step towards understanding laminopathic diseases? *Histochem Cell Biol*, 1-9.
- Gotzmann, J. and Gerner, C.** (2000). A method to produce Ponceau replicas from blots: application for Western analysis. *Electrophoresis* **21**, 523-5.
- Grishok, A., Tabara, H. and Mello, C. C.** (2000). Genetic requirements for inheritance of RNAi in *C. elegans*. *Science* **287**, 2494-7.
- Gruenbaum, Y., Goldman, R. D., Meyuhas, R., Mills, E., Margalit, A., Fridkin, A., Dayani, Y., Prokocimer, M. and Enosh, A.** (2003). The nuclear lamina and its functions in the nucleus. *Int Rev Cytol* **226**, 1-62.
- Gruenbaum, Y., Margalit, A., Goldman, R. D., Shumaker, D. K. and Wilson, K. L.** (2005). The nuclear lamina comes of age. *Nat Rev Mol Cell Biol* **6**, 21-31.
- Guo, S. and Kemphues, K. J.** (1995). par-1, a gene required for establishing polarity in *C. elegans* embryos, encodes a putative Ser/Thr kinase that is asymmetrically distributed. *Cell* **81**, 611-20.
- Gupta, S., Schoer, R. A., Egan, J. E., Hannon, G. J. and Mittal, V.** (2004). Inducible, reversible, and stable RNA interference in mammalian cells. *Proc Natl Acad Sci U S A* **101**, 1927-32.
- Hamilton, A., Voinnet, O., Chappell, L. and Baulcombe, D.** (2002). Two classes of short interfering RNA in RNA silencing. *Embo J* **21**, 4671-9.
- Hamilton, A. J. and Baulcombe, D. C.** (1999). A species of small antisense RNA in posttranscriptional gene silencing in plants. *Science* **286**, 950-2.

- Hammond, S. M., Bernstein, E., Beach, D. and Hannon, G. J.** (2000). An RNA-directed nuclease mediates post-transcriptional gene silencing in *Drosophila* cells. *Nature* **404**, 293-6.
- Hammond, S. M., Boettcher, S., Caudy, A. A., Kobayashi, R. and Hannon, G. J.** (2001). Argonaute2, a link between genetic and biochemical analyses of RNAi. *Science* **293**, 1146-50.
- Hannon, G. J.** (2002). RNA interference. *Nature* **418**, 244-51.
- Hannon, G. J. and Rossi, J. J.** (2004). Unlocking the potential of the human genome with RNA interference. *Nature* **431**, 371-8.
- Haraguchi, T., Koujin, T., Segura-Totten, M., Lee, K. K., Matsuoka, Y., Yoneda, Y., Wilson, K. L. and Hiraoka, Y.** (2001). BAF is required for emerin assembly into the reforming nuclear envelope. *J Cell Sci* **114**, 4575-85.
- Heald, R. and McKeon, F.** (1990). Mutations of phosphorylation sites in lamin A that prevent nuclear lamina disassembly in mitosis. *Cell* **61**, 579-89.
- Herrmann, H. and Foisner, R.** (2003). Intermediate filaments: novel assembly models and exciting new functions for nuclear lamins. *Cell Mol Life Sci* **60**, 1607-12.
- Hofemeister, H., Weber, K. and Stick, R.** (2000). Association of prenylated proteins with the plasma membrane and the inner nuclear membrane is mediated by the same membrane-targeting motifs. *Mol Biol Cell* **11**, 3233-46.
- Holmer, L. and Worman, H. J.** (2001). Inner nuclear membrane proteins: functions and targeting. *Cell Mol Life Sci* **58**, 1741-7.
- Hozak, P., Sasseville, A. M., Raymond, Y. and Cook, P. R.** (1995). Lamin proteins form an internal nucleoskeleton as well as a peripheral lamina in human cells. *J Cell Sci* **108** (Pt 2), 635-44.
- Hunter, C. and Poethig, R. S.** (2003). miSSING LINKS: miRNAs and plant development. *Curr Opin Genet Dev* **13**, 372-8.
- Hutchison, C. J., Alvarez-Reyes, M. and Vaughan, O. A.** (2001). Lamins in disease: why do ubiquitously expressed nuclear envelope proteins give rise to tissue-specific disease phenotypes? *J Cell Sci* **114**, 9-19.
- Hutchison, C. J. and Worman, H. J.** (2004). A-type lamins: guardians of the soma? *Nat Cell Biol* **6**, 1062-7.
- Jagatheesan, G., Thanumalayan, S., Muralikrishna, B., Rangaraj, N., Karande, A. A. and Parnaik, V. K.** (1999). Colocalization of intranuclear lamin foci with RNA splicing factors. *J Cell Sci* **112** (Pt 24), 4651-61.

- Jazag, A., Kanai, F., Ijichi, H., Tateishi, K., Ikenoue, T., Tanaka, Y., Ohta, M., Imamura, J., Guleng, B., Asaoka, Y. et al.** (2005). Single small-interfering RNA expression vector for silencing multiple transforming growth factor-beta pathway components. *Nucleic Acids Res* **33**, e131.
- Johnson, B. R., Nitta, R. T., Frock, R. L., Mounkes, L., Barbie, D. A., Stewart, C. L., Harlow, E. and Kennedy, B. K.** (2004). A-type lamins regulate retinoblastoma protein function by promoting subnuclear localization and preventing proteasomal degradation. *Proc Natl Acad Sci U S A* **101**, 9677-82.
- Kaelin, W. G., Jr.** (1999). Functions of the retinoblastoma protein. *Bioessays* **21**, 950-8.
- Kasschau, K. D., Xie, Z., Allen, E., Llave, C., Chapman, E. J., Krizan, K. A. and Carrington, J. C.** (2003). P1/HC-Pro, a viral suppressor of RNA silencing, interferes with Arabidopsis development and miRNA uncton. *Dev Cell* **4**, 205-17.
- Kawasaki, H. and Taira, K.** (2004). Induction of DNA methylation and gene silencing by short interfering RNAs in human cells. *Nature* **431**, 211-7.
- Kennerdell, J. R. and Carthew, R. W.** (2000). Heritable gene silencing in Drosophila using double-stranded RNA. *Nat Biotechnol* **18**, 896-8.
- Ketting, R. F., Fischer, S. E., Bernstein, E., Sijen, T., Hannon, G. J. and Plasterk, R. H.** (2001). Dicer functions in RNA interference and in synthesis of small RNA involved in developmental timing in *C. elegans*. *Genes Dev* **15**, 2654-9.
- Ketting, R. F., Haverkamp, T. H., van Luenen, H. G. and Plasterk, R. H.** (1999). Mut-7 of *C. elegans*, required for transposon silencing and RNA interference, is a homolog of Werner syndrome helicase and RNaseD. *Cell* **99**, 133-41.
- Laemmli, U. K.** (1970). Cleavage of structural proteins during the assembly of the head of bacteriophage T4. *Nature* **227**, 680-5.
- Lamond, A. I. and Earnshaw, W. C.** (1998). Structure and function in the nucleus. *Science* **280**, 547-53.
- Landy, A.** (1989). Dynamic, structural, and regulatory aspects of lambda site-specific recombination. *Annu Rev Biochem* **58**, 913-49.
- Laronne, A., Rotkopf, S., Hellman, A., Gruenbaum, Y., Porter, A. C. and Brandeis, M.** (2003). Synchronization of interphase events depends neither on mitosis nor on cdk1. *Mol Biol Cell* **14**, 3730-40.
- Lee, N. S., Dohjima, T., Bauer, G., Li, H., Li, M. J., Ehsani, A., Salvaterra, P. and Rossi, J.** (2002a). Expression of small interfering RNAs targeted against HIV-1 rev transcripts in human cells. *Nat Biotechnol* **20**, 500-5.

- Lee, Y., Ahn, C., Han, J., Choi, H., Kim, J., Yim, J., Lee, J., Provost, P., Radmark, O., Kim, S. et al.** (2003). The nuclear RNase III Drosha initiates microRNA processing. *Nature* **425**, 415-9.
- Lee, Y., Jeon, K., Lee, J. T., Kim, S. and Kim, V. N.** (2002b). MicroRNA maturation: stepwise processing and subcellular localization. *Embo J* **21**, 4663-70.
- Li, H., Li, W. X. and Ding, S. W.** (2002). Induction and suppression of RNA silencing by an animal virus. *Science* **296**, 1319-21.
- Lim, L. P., Glasner, M. E., Yekta, S., Burge, C. B. and Bartel, D. P.** (2003). Vertebrate microRNA genes. *Science* **299**, 1540.
- Lin, F., Blake, D. L., Callebaut, I., Skerjanc, I. S., Holmer, L., McBurney, M. W., Paulin-Levasseur, M. and Worman, H. J.** (2000). MAN1, an inner nuclear membrane protein that shares the LEM domain with lamina-associated polypeptide 2 and emerin. *J Biol Chem* **275**, 4840-7.
- Lipardi, C., Wei, Q. and Paterson, B. M.** (2001). RNAi as random degradative PCR: siRNA primers convert mRNA into dsRNAs that are degraded to generate new siRNAs. *Cell* **107**, 297-307.
- Llave, C., Xie, Z., Kasschau, K. D. and Carrington, J. C.** (2002). Cleavage of Scarecrow-like mRNA targets directed by a class of Arabidopsis miRNA. *Science* **297**, 2053-6.
- Loewinger, L. and McKeon, F.** (1988). Mutations in the nuclear lamin proteins resulting in their aberrant assembly in the cytoplasm. *Embo J* **7**, 2301-9.
- Lund, E., Guttinger, S., Calado, A., Dahlberg, J. E. and Kutay, U.** (2004). Nuclear export of microRNA precursors. *Science* **303**, 95-8.
- Lutz, R. J., Trujillo, M. A., Denham, K. S., Wenger, L. and Sinensky, M.** (1992). Nucleoplasmic localization of prelamin A: implications for prenylation-dependent lamin A assembly into the nuclear lamina. *Proc Natl Acad Sci U S A* **89**, 3000-4.
- Mallory, A. C., Reinhart, B. J., Bartel, D., Vance, V. B. and Bowman, L. H.** (2002). A viral suppressor of RNA silencing differentially regulates the accumulation of short interfering RNAs and micro-RNAs in tobacco. *Proc Natl Acad Sci U S A* **99**, 15228-33.
- Mancini, M. A., Shan, B., Nickerson, J. A., Penman, S. and Lee, W. H.** (1994). The retinoblastoma gene product is a cell cycle-dependent, nuclear matrix-associated protein. *Proc Natl Acad Sci U S A* **91**, 418-22.
- Margalit, A., Vlcek, S., Gruenbaum, Y. and Foisner, R.** (2005). Breaking and making of the nuclear envelope. *J Cell Biochem* **95**, 454-65.

- Markiewicz, E., Dechat, T., Foisner, R., Quinlan, R. A. and Hutchison, C. J.** (2002). Lamin A/C binding protein LAP2alpha is required for nuclear anchorage of retinoblastoma protein. *Mol Biol Cell* **13**, 4401-13.
- Martienssen, R. A. and Colot, V.** (2001). DNA methylation and epigenetic inheritance in plants and filamentous fungi. *Science* **293**, 1070-4.
- Martins, S., Eikvar, S., Furukawa, K. and Collas, P.** (2003). HA95 and LAP2 beta mediate a novel chromatin-nuclear envelope interaction implicated in initiation of DNA replication. *J Cell Biol* **160**, 177-88.
- Matsukura, S., Jones, P. A. and Takai, D.** (2003). Establishment of conditional vectors for hairpin siRNA knockdowns. *Nucleic Acids Res* **31**, e77.
- Mattout-Drubezki, A. and Gruenbaum, Y.** (2003). Dynamic interactions of nuclear lamina proteins with chromatin and transcriptional machinery. *Cell Mol Life Sci* **60**, 2053-63.
- Matzke, M. A. and Birchler, J. A.** (2005). RNAi-mediated pathways in the nucleus. *Nat Rev Genet* **6**, 24-35.
- McManus, M. T. and Sharp, P. A.** (2002). Gene silencing in mammals by small interfering RNAs. *Nat Rev Genet* **3**, 737-47.
- Meister, G. and Tuschl, T.** (2004). Mechanisms of gene silencing by double-stranded RNA. *Nature* **431**, 343-9.
- Mette, M. F., Aufsatz, W., van der Winden, J., Matzke, M. A. and Matzke, A. J.** (2000). Transcriptional silencing and promoter methylation triggered by double-stranded RNA. *Embo J* **19**, 5194-201.
- Mittal, V.** (2004). Improving the efficiency of RNA interference in mammals. *Nat Rev Genet* **5**, 355-65.
- Miyagishi, M. and Taira, K.** (2002). U6 promoter-driven siRNAs with four uridine 3' overhangs efficiently suppress targeted gene expression in mammalian cells. *Nat Biotechnol* **20**, 497-500.
- Mlotshwa, S., Voinnet, O., Mette, M. F., Matzke, M., Vaucheret, H., Ding, S. W., Pruss, G. and Vance, V. B.** (2002). RNA silencing and the mobile silencing signal. *Plant Cell* **14 Suppl**, S289-301.
- Mochizuki, K., Fine, N. A., Fujisawa, T. and Gorovsky, M. A.** (2002). Analysis of a piwi-related gene implicates small RNAs in genome rearrangement in tetrahymena. *Cell* **110**, 689-99.
- Moir, R. D., Spann, T. P. and Goldman, R. D.** (1995). The dynamic properties and possible functions of nuclear lamins. *Int Rev Cytol* **162B**, 141-82.

- Morris, K. V., Chan, S. W., Jacobsen, S. E. and Looney, D. J.** (2004). Small interfering RNA-induced transcriptional gene silencing in human cells. *Science* **305**, 1289-92.
- Mourrain, P., Beclin, C., Elmayer, T., Feuerbach, F., Godon, C., Morel, J. B., Jouette, D., Lacombe, A. M., Nikic, S., Picault, N. et al.** (2000). Arabidopsis SGS2 and SGS3 genes are required for posttranscriptional gene silencing and natural virus resistance. *Cell* **101**, 533-42.
- Naldini, L., Blomer, U., Gallay, P., Ory, D., Mulligan, R., Gage, F. H., Verma, I. M. and Trono, D.** (1996). In vivo gene delivery and stable transduction of nondividing cells by a lentiviral vector. *Science* **272**, 263-7.
- Napoli, C., Lemieux, C. and Jorgensen, R.** (1990). Introduction of a Chimeric Chalcone Synthase Gene into Petunia Results in Reversible Co-Suppression of Homologous Genes in trans. *Plant Cell* **2**, 279-289.
- Navarro, C. L., De Sandre-Giovannoli, A., Bernard, R., Boccaccio, I., Boyer, A., Genevieve, D., Hadj-Rabia, S., Gaudy-Marqueste, C., Smitt, H. S., Vabres, P. et al.** (2004). Lamin A and ZMPSTE24 (FACE-1) defects cause nuclear disorganization and identify restrictive dermopathy as a lethal neonatal laminopathy. *Hum Mol Genet* **13**, 2493-503.
- Nili, E., Cojocaru, G. S., Kalma, Y., Ginsberg, D., Copeland, N. G., Gilbert, D. J., Jenkins, N. A., Berger, R., Shaklai, S., Amariglio, N. et al.** (2001). Nuclear membrane protein LAP2beta mediates transcriptional repression alone and together with its binding partner GCL (germ-cell-less). *J Cell Sci* **114**, 3297-307.
- Nykanen, A., Haley, B. and Zamore, P. D.** (2001). ATP requirements and small interfering RNA structure in the RNA interference pathway. *Cell* **107**, 309-21.
- Olsen, P. H. and Ambros, V.** (1999). The lin-4 regulatory RNA controls developmental timing in *Caenorhabditis elegans* by blocking LIN-14 protein synthesis after the initiation of translation. *Dev Biol* **216**, 671-80.
- Ozaki, T., Saijo, M., Murakami, K., Enomoto, H., Taya, Y. and Sakiyama, S.** (1994). Complex formation between lamin A and the retinoblastoma gene product: identification of the domain on lamin A required for its interaction. *Oncogene* **9**, 2649-53.
- Paddison, P. J., Caudy, A. A., Bernstein, E., Hannon, G. J. and Conklin, D. S.** (2002). Short hairpin RNAs (shRNAs) induce sequence-specific silencing in mammalian cells. *Genes Dev* **16**, 948-58.

- Paddison, P. J. and Hannon, G. J.** (2002). RNA interference: the new somatic cell genetics? *Cancer Cell* **2**, 17-23.
- Palauqui, J. C., Elmayan, T., Pollien, J. M. and Vaucheret, H.** (1997). Systemic acquired silencing: transgene-specific post-transcriptional silencing is transmitted by grafting from silenced stocks to non-silenced scions. *Embo J* **16**, 4738-45.
- Pasquinelli, A. E., Reinhart, B. J., Slack, F., Martindale, M. Q., Kuroda, M. I., Maller, B., Hayward, D. C., Ball, E. E., Degnan, B., Muller, P. et al.** (2000). Conservation of the sequence and temporal expression of let-7 heterochronic regulatory RNA. *Nature* **408**, 86-9.
- Pasquinelli, A. E. and Ruvkun, G.** (2002). Control of developmental timing by microRNAs and their targets. *Annu Rev Cell Dev Biol* **18**, 495-513.
- Pham, J. W., Pellino, J. L., Lee, Y. S., Carthew, R. W. and Sontheimer, E. J.** (2004). A Dicer-2-dependent 80s complex cleaves targeted mRNAs during RNAi in *Drosophila*. *Cell* **117**, 83-94.
- Qin, X. F., An, D. S., Chen, I. S. and Baltimore, D.** (2003). Inhibiting HIV-1 infection in human T cells by lentiviral-mediated delivery of small interfering RNA against CCR5. *Proc Natl Acad Sci U S A* **100**, 183-8.
- Rao, L., Perez, D. and White, E.** (1996). Lamin proteolysis facilitates nuclear events during apoptosis. *J Cell Biol* **135**, 1441-55.
- Roignant, J. Y., Carre, C., Mugat, B., Szymczak, D., Lepesant, J. A. and Antoniewski, C.** (2003). Absence of transitive and systemic pathways allows cell-specific and isoform-specific RNAi in *Drosophila*. *Rna* **9**, 299-308.
- Romig, H., Fackelmayer, F. O., Renz, A., Ramsperger, U. and Richter, A.** (1992). Characterization of SAF-A, a novel nuclear DNA binding protein from HeLa cells with high affinity for nuclear matrix/scaffold attachment DNA elements. *Embo J* **11**, 3431-40.
- Rubinson, D. A., Dillon, C. P., Kwiatkowski, A. V., Sievers, C., Yang, L., Kopinja, J., Rooney, D. L., Ihrig, M. M., McManus, M. T., Gertler, F. B. et al.** (2003). A lentivirus-based system to functionally silence genes in primary mammalian cells, stem cells and transgenic mice by RNA interference. *Nat Genet* **33**, 401-6.
- Ruchaud, S., Korfali, N., Villa, P., Kottke, T. J., Dingwall, C., Kaufmann, S. H. and Earnshaw, W. C.** (2002). Caspase-6 gene disruption reveals a requirement for lamin A cleavage in apoptotic chromatin condensation. *Embo J* **21**, 1967-77.

- Ruiz, M. T., Voinnet, O. and Baulcombe, D. C.** (1998). Initiation and maintenance of virus-induced gene silencing. *Plant Cell* **10**, 937-46.
- Salina, D., Bodoor, K., Eckley, D. M., Schroer, T. A., Rattner, J. B. and Burke, B.** (2002). Cytoplasmic dynein as a facilitator of nuclear envelope breakdown. *Cell* **108**, 97-107.
- Schuck, S., Manninen, A., Honsho, M., Fullekrug, J. and Simons, K.** (2004). Generation of single and double knockdowns in polarized epithelial cells by retrovirus-mediated RNA interference. *Proc Natl Acad Sci U S A* **101**, 4912-7.
- Shen, C., Buck, A. K., Liu, X., Winkler, M. and Reske, S. N.** (2003). Gene silencing by adenovirus-delivered siRNA. *FEBS Lett* **539**, 111-4.
- Shimi, T., Koujin, T., Segura-Totten, M., Wilson, K. L., Haraguchi, T. and Hiraoka, Y.** (2004). Dynamic interaction between BAF and emerin revealed by FRAP, FLIP, and FRET analyses in living HeLa cells. *J Struct Biol* **147**, 31-41.
- Shinagawa, T. and Ishii, S.** (2003). Generation of Ski-knockdown mice by expressing a long double-strand RNA from an RNA polymerase II promoter. *Genes Dev* **17**, 1340-5.
- Shumaker, D. K., Kuczmarski, E. R. and Goldman, R. D.** (2003). The nucleoskeleton: lamins and actin are major players in essential nuclear functions. *Curr Opin Cell Biol* **15**, 358-66.
- Shumaker, D. K., Lee, K. K., Tanhehco, Y. C., Craigie, R. and Wilson, K. L.** (2001). LAP2 binds to BAF.DNA complexes: requirement for the LEM domain and modulation by variable regions. *Embo J* **20**, 1754-64.
- Sijen, T., Fleenor, J., Simmer, F., Thijssen, K. L., Parrish, S., Timmons, L., Plasterk, R. H. and Fire, A.** (2001). On the role of RNA amplification in dsRNA-triggered gene silencing. *Cell* **107**, 465-76.
- Siolas, D., Lerner, C., Burchard, J., Ge, W., Linsley, P. S., Paddison, P. J., Hannon, G. J. and Cleary, M. A.** (2005). Synthetic shRNAs as potent RNAi triggers. *Nat Biotechnol* **23**, 227-31.
- Song, J. J., Smith, S. K., Hannon, G. J. and Joshua-Tor, L.** (2004). Crystal structure of Argonaute and its implications for RISC slicer activity. *Science* **305**, 1434-7.
- Stark, G. R., Kerr, I. M., Williams, B. R., Silverman, R. H. and Schreiber, R. D.** (1998). How cells respond to interferons. *Annu Rev Biochem* **67**, 227-64.
- Stein, P., Svoboda, P., Anger, M. and Schultz, R. M.** (2003). RNAi: mammalian oocytes do it without RNA-dependent RNA polymerase. *Rna* **9**, 187-92.

- Stewart, S. A., Dykxhoorn, D. M., Palliser, D., Mizuno, H., Yu, E. Y., An, D. S., Sabatini, D. M., Chen, I. S., Hahn, W. C., Sharp, P. A. et al.** (2003). Lentivirus-delivered stable gene silencing by RNAi in primary cells. *Rna* **9**, 493-501.
- Stuurman, N., Heins, S. and Aebi, U.** (1998). Nuclear lamins: their structure, assembly, and interactions. *J Struct Biol* **122**, 42-66.
- Sui, G., Soohoo, C., Affar el, B., Gay, F., Shi, Y. and Forrester, W. C.** (2002). A DNA vector-based RNAi technology to suppress gene expression in mammalian cells. *Proc Natl Acad Sci U S A* **99**, 5515-20.
- Tabara, H., Sarkissian, M., Kelly, W. G., Fleenor, J., Grishok, A., Timmons, L., Fire, A. and Mello, C. C.** (1999). The rde-1 gene, RNA interference, and transposon silencing in *C. elegans*. *Cell* **99**, 123-32.
- Taddei, A., Hediger, F., Neumann, F. R. and Gasser, S. M.** (2004). The function of nuclear architecture: a genetic approach. *Annu Rev Genet* **38**, 305-45.
- Tahbaz, N., Kolb, F. A., Zhang, H., Jaronczyk, K., Filipowicz, W. and Hobman, T. C.** (2004). Characterization of the interactions between mammalian PAZ PIWI domain proteins and Dicer. *EMBO Rep* **5**, 189-94.
- Tavernarakis, N., Wang, S. L., Dorovkov, M., Ryazanov, A. and Driscoll, M.** (2000). Heritable and inducible genetic interference by double-stranded RNA encoded by transgenes. *Nat Genet* **24**, 180-3.
- Taylor, M. R., Slavov, D., Gajewski, A., Vlcek, S., Ku, L., Fain, P. R., Carniel, E., Di Lenarda, A., Sinagra, G., Boucek, M. M., et al.** (2005). Thymopoietin (lamina-associated polypeptide 2) gene mutation associated with dilated cardiomyopathy. *Hum Mutat* **26**, 566-574.
- Timmons, L. and Fire, A.** (1998). Specific interference by ingested dsRNA. *Nature* **395**, 854.
- van de Wetering, M., Oving, I., Muncan, V., Pon Fong, M. T., Brantjes, H., van Leenen, D., Holstege, F. C., Brummelkamp, T. R., Agami, R. and Clevers, H.** (2003). Specific inhibition of gene expression using a stably integrated, inducible small-interfering-RNA vector. *EMBO Rep* **4**, 609-15.
- van der Krol, A. R., Mur, L. A., de Lange, P., Mol, J. N. and Stuitje, A. R.** (1990). Inhibition of flower pigmentation by antisense CHS genes: promoter and minimal sequence requirements for the antisense effect. *Plant Mol Biol* **14**, 457-66.

- Verdel, A., Jia, S., Gerber, S., Sugiyama, T., Gygi, S., Grewal, S. I. and Moazed, D.** (2004). RNAi-mediated targeting of heterochromatin by the RITS complex. *Science* **303**, 672-6.
- Vigers, G. P. and Lohka, M. J.** (1992). Regulation of nuclear envelope precursor functions during cell division. *J Cell Sci* **102** (Pt 2), 273-84.
- Vlcek, S., Dechat, T. and Foisner, R.** (2001). Nuclear envelope and nuclear matrix: interactions and dynamics. *Cell Mol Life Sci* **58**, 1758-65.
- Vlcek, S., Just, H., Dechat, T. and Foisner, R.** (1999). Functional diversity of LAP2alpha and LAP2beta in postmitotic chromosome association is caused by an alpha-specific nuclear targeting domain. *Embo J* **18**, 6370-84.
- Vlcek, S., Korbei, B. and Foisner, R.** (2002). Distinct functions of the unique C terminus of LAP2alpha in cell proliferation and nuclear assembly. *J Biol Chem* **277**, 18898-907.
- Voinnet, O., Vain, P., Angell, S. and Baulcombe, D. C.** (1998). Systemic spread of sequence-specific transgene RNA degradation in plants is initiated by localized introduction of ectopic promoterless DNA. *Cell* **95**, 177-87.
- Volpe, T. A., Kidner, C., Hall, I. M., Teng, G., Grewal, S. I. and Martienssen, R. A.** (2002). Regulation of heterochromatic silencing and histone H3 lysine-9 methylation by RNAi. *Science* **297**, 1833-7.
- Wassenegger, M., Heimes, S., Riedel, L. and Sanger, H. L.** (1994). RNA-directed de novo methylation of genomic sequences in plants. *Cell* **76**, 567-76.
- Wilson, K. L.** (2000). The nuclear envelope, muscular dystrophy and gene expression. *Trends Cell Biol* **10**, 125-9.
- Wilson, K. L., Zastrow, M. S. and Lee, K. K.** (2001). Lamins and disease: insights into nuclear infrastructure. *Cell* **104**, 647-50.
- Winston, W. M., Molodowitch, C. and Hunter, C. P.** (2002). Systemic RNAi in *C. elegans* requires the putative transmembrane protein SID-1. *Science* **295**, 2456-9.
- Wiznerowicz, M. and Trono, D.** (2003). Conditional suppression of cellular genes: lentivirus vector-mediated drug-inducible RNA interference. *J Virol* **77**, 8957-61.
- Xia, H., Mao, Q., Paulson, H. L. and Davidson, B. L.** (2002). siRNA-mediated gene silencing in vitro and in vivo. *Nat Biotechnol* **20**, 1006-10.
- Yang, L., Guan, T. and Gerace, L.** (1997). Integral membrane proteins of the nuclear envelope are dispersed throughout the endoplasmic reticulum during mitosis. *J Cell Biol* **137**, 1199-210.

- Ye, Q., Barton, R. M. and Worman, H. J.** (1998). Nuclear lamin-binding proteins. *Subcell Biochem* **31**, 587-610.
- Yi, R., Qin, Y., Macara, I. G. and Cullen, B. R.** (2003). Exportin-5 mediates the nuclear export of pre-microRNAs and short hairpin RNAs. *Genes Dev* **17**, 3011-6.
- Yu, J. Y., Taylor, J., DeRuiter, S. L., Vojtek, A. B. and Turner, D. L.** (2003). Simultaneous inhibition of GSK3alpha and GSK3beta using hairpin siRNA expression vectors. *Mol Ther* **7**, 228-36.
- Zamore, P. D.** (2002). Ancient pathways programmed by small RNAs. *Science* **296**, 1265-9.
- Zamore, P. D., Tuschl, T., Sharp, P. A. and Bartel, D. P.** (2000). RNAi: double-stranded RNA directs the ATP-dependent cleavage of mRNA at 21 to 23 nucleotide intervals. *Cell* **101**, 25-33.

8. Curriculum vitae

Christian Makolm



Geburtsdatum: 23. April 1976
Geburtsort: Hollabrunn, NÖ
Nationalität: Österreich
Adresse: Piaristengasse 34/12A
1080 Wien
Telefon: 0699/12217548
e-mail: Christian.Makolm@gmx.at

Ausbildung

06/2009 voraussichtlicher Studienabschluss Chemie
10/2002 – 04/2004 Diplomarbeit (New RNAi Vector Application & Functional LAP2 α Analysis)
Abteilung für Molekulare Zellbiologie (Prof. Foisner)
Department für Medizinische Biochemie, Medizinische Universität Wien
02/2001 – 06/2001 Projektmitarbeit (organisch-chemische Synthese)
Université de Provence Aix-Marseille
seit 09/1994 Studium der Chemie, Universität Wien
06/1994 Matura am Bundesrealgymnasium Stockerau

Beruf, (studienbegleitende Tätigkeiten)

ab 07/2009 Offiziersausbildung, Berufsfeuerwehr Wien
11/2008 – 07/2009 Bildungskarenz
03/2006 – 11/2008 technischer Mitarbeiter in Research & Development
Bender MedSystems GmbH
10/2005 – 04/2006 AustroMars (wissenschaftliches Isolationsexperiment)
für die Crew qualifiziert und ausgebildet,
CapCom (Kommunikationsschnittstelle) im Kontrollzentrum
08/2002 Baxter AG (Experimental Virology, Biosafety Level 3)
07 – 08/2001 Institute of Molecular Pathology
07 – 09/2000 Baxter AG (Molecular Cell Biology)
07 – 08/1999 Baxter AG (Lyophilization)
10/1998 – 05/1999 Sports Experts (Verkäufer)
08 / 1998 Österreichisches Institut für Hämoderivate (Feinfraktionierung I)
07/1998 Sports Experts (Verkäufer)
07 – 08/1997 Immuno AG (Inlandsversand)

Weitere Qualifikationen

Sprachen:	Englisch fließend Französisch Grundkenntnisse
Software:	MS-Office, Adobe Photoshop, Adobe Illustrator, Corel Draw, Clone Manager Suite, EndNote, Zeiss LSM, fachspezifische Internet Datenbanken, Unix Grundwissen
Stipendien:	SOKRATES/ERASMUS Mobilitätsstipendium (2001) Top Stipendium des Landes Niederösterreich (2004)
Sonstiges:	Führerschein B, Ersthelfer (inkl. Frühdefibrillation)

Publikationen

Dorner D., Vlcek S., Foeger N., Gajewski A., Makolm C., Gotzmann J., Hutchison C.J. and Foisner R. (2006). Lamina-associated polypeptide 2 α regulates cell cycle progression and differentiation via the retinoblastoma-E2F pathway. *J. Cell Biol.*, 173, 83-93.

Posterpräsentation:

Makolm C., Foisner R., and Gotzmann J. Targeting the Nuclear Envelope by RNA-Interference Joint Annual Meeting of ÖGBM/ÖGGGT/ÖGBT/ANGT 2003, (Graz, Austria)

Poster:

Dorner D., Makolm C., Gotzmann J., Hutchison C.J. and Foisner R.
LAP2 α regulates pRb-mediated cell cycle exit and differentiation, Fabisch-Symposium 'Functional Organization of the Nuclear Envelope in Health and Disease' (Berlin, Deutschland)

Kongresse, Workshops

Joint Annual Meeting of ÖGBM/ÖGGGT/ÖGBT/ANGT 2003, (Graz, Austria)

Joint Annual Meeting of ÖGBM/ÖGGGT/ÖGBT/ANGT 2004, (Wien, Austria)

6th International Cytokine Conference (Wien, 2006)

„Mars 2030 - AustroMars Science Workshop“ (Salzburg, 2006)

„Introduction to Flow Cytometry“, (OEGFZ, Wien 2007)

„Joint Annual Meeting of Immunology of the Austrian and German Societies“ (ÖGAI, DGFI, Wien 2008)

Hobbys

Handball Leistungssport (1993 – 2005), Klettern, Bergsteigen, Kochen